

# **Holocene vegetation and environmental changes with a focus on peat ecosystems in southwestern and northeastern Amazonia**

Dissertation

for the award of the degree

“Doctor of Philosophy” (Ph.D. Division of Mathematics and Natural Science)

of the Georg-August-University of Göttingen

within the doctoral program Biodiversity, Ecology and Evolution

submitted by

**Bowen Wang**

from China

Göttingen, 2024

Thesis committee

Prof. Dr. Hermann Behling

(Department of Palynology and Climate Dynamics, University of Göttingen)

Prof. Dr. Holger Kreft

(Department of Biodiversity, Macroecology and Biogeography, University of Göttingen)

Dr. Kartika Anggi Hapsari

(College of Life and Environmental Sciences, University of Exeter)

Members of the Examination Board

Reviewer: Prof. Dr. Hermann Behling

(Department of Palynology and Climate Dynamics, University of Göttingen)

Second reviewer: Prof. Dr. Holger Kreft

(Department of Biodiversity, Macroecology and Biogeography, University of Göttingen)

Further members of the Examination Board:

Dr. Kartika Anggi Hapsari

(College of Life and Environmental Sciences, University of Exeter)

Prof. Dr. Erwin Bergmeier

(Department of Vegetation and Phytodiversity Analysis, University of Göttingen)

Prof. Dr. Daniela Sauer

(Department of Physical Geography, University of Göttingen)

Prof. Dr. Elisabeth Dietze

(Department of Physical Geography, University of Göttingen)

Date of oral examination: 06.02.2024

*I dedicate it to my parents Jincun Wang and Liping Zhu,  
and my PhD supervisor Prof. Dr. Hermann Behling.*

# Content

<b>SUMMARY.....</b>	<b>VI</b>
<b>CHAPTER 1.....</b>	<b>1</b>
1.1 INTRODUCTION.....	1
1.2 RESEARCH QUESTIONS.....	5
1.3 STUDY AREA.....	5
1.3.1 <i>Madre de Dios region in southwestern Amazonia</i> .....	5
1.3.2 <i>Lagoa da Fazenda region in northeastern Amazonia</i> .....	7
1.4 METHODOLOGY.....	8
1.4.1 <i>Core sampling and chronology</i> .....	8
1.4.2 <i>Pollen and spore analysis</i> .....	8
1.4.3 <i>Loss-on-ignition (LOI) analysis</i> .....	9
1.4.4 <i>Organic carbon (C) analysis</i> .....	9
1.4.5 <i>Macro-charcoal analysis</i> .....	10
1.4.6 <i>Chemical composition analysis by X-ray fluorescence (XRF)</i> .....	11
1.4.7 <i>Mineralogical identification by X-Ray Diffraction (XRD)</i> .....	11
1.4.8 <i>Mineral identification by Scanning Electron Microscope (SEM) with Energy Dispersive Spectroscopy (EDS)</i> .....	12
REFERENCE.....	12
<b>CHAPTER 2.....</b>	<b>16</b>
ABSTRACT.....	17
2.1 INTRODUCTION.....	18
2.2 STUDY AREA.....	19
2.3 METHODS.....	21
2.3.1 <i>Core sampling and chronology</i> .....	21
2.3.2 <i>Pollen analysis</i> .....	21
2.3.3 <i>Loss-on-ignition (LOI) analysis and carbon content analysis</i> .....	22
2.4 RESULTS.....	22
2.4.1 <i>Stratigraphy and chronology</i> .....	22
2.4.2 <i>Pollen data</i> .....	24
2.4.3 <i>LOI and carbon data</i> .....	25
2.5 INTERPRETATION AND DISCUSSION.....	30
2.5.1 <i>Late Holocene vegetation and environment as well as the development and dynamics of the aguajal</i> .....	30

2.5.2	<i>Factors influencing changes in vegetation, peat, and carbon accumulation</i>	34
2.5.3	<i>Comparison with aguajales in northern Peru</i>	37
2.6	SUMMARY AND CONCLUSION	39
	AUTHOR CONTRIBUTIONS	39
	ACKNOWLEDGMENTS	39
	REFERENCES	40
<b>CHAPTER 3</b>		<b>44</b>
	ABSTRACT	45
	KEYWORDS	45
3.1	INTRODUCTION	46
3.2	STUDY AREA	47
3.3	METHODS	49
3.3.1	<i>Core sampling and chronology</i>	49
3.3.2	<i>Pollen and charcoal analysis</i>	49
3.3.3	<i>Loss-On-Ignition (LOI) analysis</i>	50
3.3.4	<i>X-Ray Fluorescence (XRF)</i>	50
3.4	RESULTS	51
3.4.1	<i>Stratigraphy and chronology</i>	51
3.4.2	<i>Pollen and charcoal data</i>	52
3.4.3	<i>LOI data</i>	56
3.4.4	<i>XRF data</i>	56
3.5	INTERPRETATION AND DISCUSSION	57
3.5.1	<i>Late Holocene environmental reconstruction</i>	57
3.5.2	<i>Further interpretation of the drivers of the changes in the palm swamp</i>	60
3.5.3	<i>Comparison of the pollen records of the palm swamp and oxbow lake</i>	62
3.5.4	<i>Comparison with other records in Peru</i>	63
3.6	SUMMARY AND CONCLUSION	65
	ACKNOWLEDGMENTS	66
	REFERENCES	66
<b>CHAPTER 4</b>		<b>70</b>
	ABSTRACT	71
	KEYWORDS	71
4.1	INTRODUCTION	72
4.2	STUDY AREA	72
4.3	METHODS	74

4.3.1	<i>Core sampling and chronology</i> .....	74
4.3.2	<i>Pollen and spore analysis</i> .....	75
4.3.3	<i>Macro-charcoal analysis</i> .....	75
4.3.4	<i>Loss-On-Ignition (LOI) and organic C analysis</i> .....	75
4.3.5	<i>Chemical composition analysis by portable X-ray Fluorescence (pXRF)</i> .....	76
4.3.6	<i>Mineralogical identification by X-ray diffraction (XRD)</i> .....	76
4.3.7	<i>Mineral identification by Scanning Electron Microscope (SEM) with Energy Dispersive Spectroscopy (EDS)</i> .....	76
4.4	RESULTS.....	77
4.4.1	<i>Stratigraphy and chronology</i> .....	77
4.4.2	<i>Pollen and macro-charcoal data</i> .....	78
4.4.3	<i>LOI and organic C data</i> .....	80
4.4.4	<i>Chemical composition by pXRF</i> .....	81
4.4.5	<i>Mineralogical composition by XRD</i> .....	82
4.4.6	<i>Mineral phases after SEM/EDS</i> .....	82
4.5	INTERPRETATION AND DISCUSSION.....	89
4.5.1	<i>Late Holocene environmental reconstruction</i> .....	89
4.5.2	<i>Comparison with other records</i> .....	94
4.6	SUMMARY AND CONCLUSION.....	95
	ACKNOWLEDGEMENTS.....	96
	REFERENCES.....	96
<b>CHAPTER 5</b>	<b>SYNTHESIS</b> .....	<b>101</b>
5.1	OVERVIEW OF THE AMAZONIAN CLIMATE IN THE HOLOCENE.....	101
5.2	PEAT ECOSYSTEMS IN WESTERN AMAZONIA.....	110
5.2.1	<i>Summary of the Madre de Dios studies</i> .....	110
5.2.2	<i>Comparison with other studies in western Amazonia</i> .....	111
5.3	PEAT ECOSYSTEMS IN EASTERN AMAZONIA.....	112
5.3.1	<i>Summary of the Lagoa da Fazenda study</i> .....	112
5.3.2	<i>Comparison with other studies in eastern Amazonia</i> .....	113
5.4	SUMMARY OF PEAT ECOSYSTEMS IN AMAZONIA AND OUTLOOK.....	114
	REFERENCE.....	114
	<b>ACKNOWLEDGEMENTS</b> .....	<b>117</b>

## Summary

Amazon rainforests are well-known for playing a significant role in the climate, hydrological cycle, and biodiversity on earth. Recent investigations found that Amazonia may contain the largest peat carbon (C) stock in the tropics. Easily to be degraded, Amazonia peat ecosystems are potentially to be a large C source which impacts the global climate. Thus, it is important to understand what drives the development of Amazonia peat ecosystems, and if the drivers are local or regional. In this study, we used the multiproxy method to investigate peat ecosystems in southwestern Amazonia (southern Peru) and northeastern Amazonia (northern Brazil) where the knowledge of peat ecosystems is little known. In the Madre de Dios region in southern Peru, we investigated a *Mauritia* palm swamp (*aguajal*) using an *aguajal* core and an oxbow lake core. Indicated by the *aguajal* record, the studied *aguajal* developed from open water since ca. 1380 cal yr BP, then became a marsh since ca. 820 cal yr BP, and then formed a dense *aguajal* since ca. 640 cal yr BP and more open *aguajal* since ca. 300 cal yr BP. Peat and C stayed at high accumulation rates since their start in ca. 820 cal yr BP, but the rates became lower since ca. 520 cal yr BP. The oxbow lake record revealed that the initial open water may develop from a cutting off from the Madre de Dios River at ca. 1760 cal yr BP, and the lower peat and C accumulation rates since ca. 520 cal yr BP were probably caused by regional less wet climate. In the Caxiana region in northern Brazil, a peat record named Lagoa da Fazenda, from a net of former small river valleys was studied. The results show that since ca. 7000 cal yr BP, the local inundated forest started to form with the onset of peat and C accumulation, caused by Atlantic sea level rise blocking the rivers. The study site was influenced by flooding since ca. 2600 cal yr BP and by strong local human activities since ca. 260 cal yr BP. Through the investigations and comparison with other available studies, we found that the processes of peat ecosystems are diverse whether in vegetation successions or peat and C accumulation rates. The diversity is caused by various conditions in different regions. For example, we found that the peat ecosystem closer to the sea is more influenced by Atlantic sea level, but it is driven by river dynamics in more inland areas. Regional human activities may play an important role in peat ecosystem development by changing regional climate or causing flooding (by causing soil erosion). This study helps to further understand the mechanism of tropical peat ecosystems and make conversation plans.

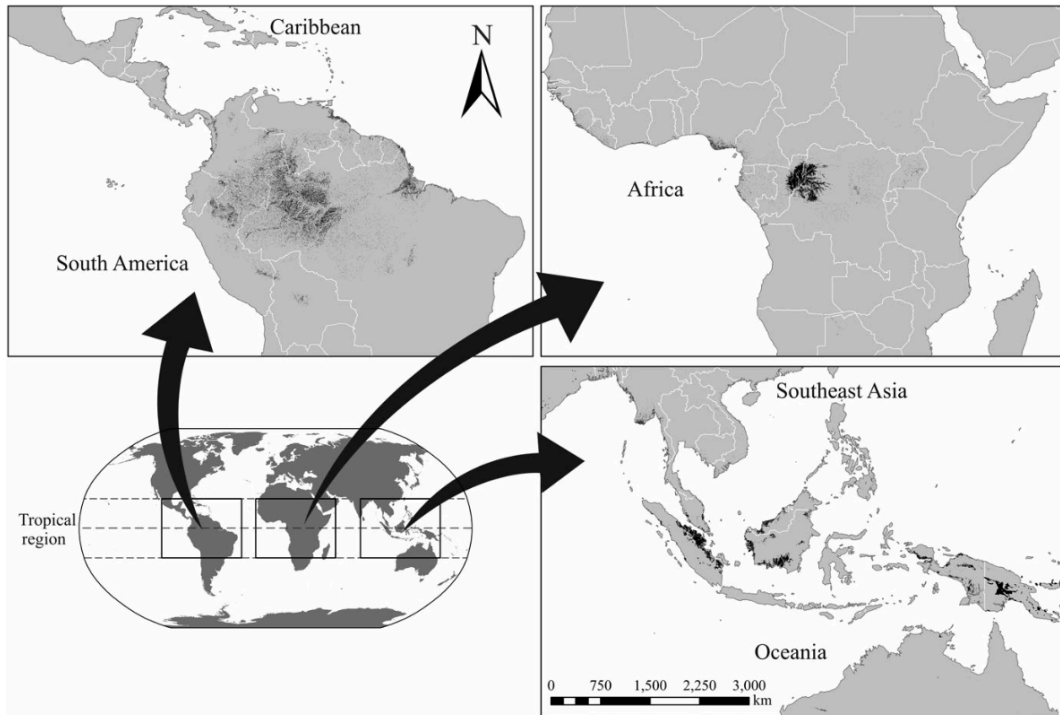
# Chapter 1

## 1.1 Introduction

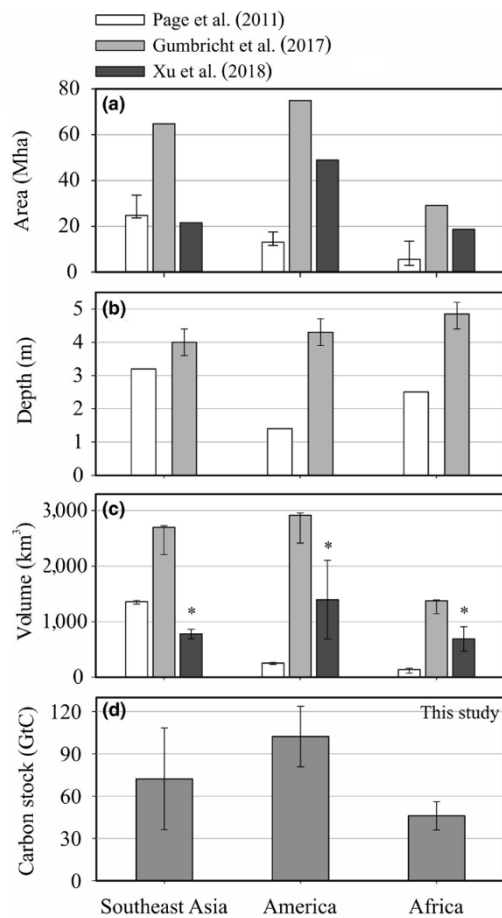
The Amazon rainforest is the largest rainforest ecosystem on earth, with an area of ca. 6,700,000 km<sup>2</sup> (Mittermeier et al., 2003), representing ca. 50% of the global tropical rainforest area. Such a large area of the Amazon rainforest exerts intense evapotranspiration, by which the water that plants absorb is converted to water vapor and transferred into the atmosphere. In this process, the Amazon rainforest can pump latent heat from the atmosphere, cooling the surface of the Amazonia. Influenced by the insolation contrast between the tropics and the higher latitudes, the surface air in the tropics is heated, expanded, and vertically moves to the upper troposphere, while the air in the higher latitudes is cooled, shrunk, and drops to the surface. The upper tropospheric air pressure in the tropics is greater than in the higher latitudes, while the surface air pressure in the tropics is lower than that. The contrast of air pressure between the tropics and the higher latitudes forms the atmospheric circulation on earth. Through atmospheric circulation, the participation of the Amazon rainforest in heat and moisture influences the higher latitudes (NOAA, 2023; Roberts, 2009). This is the main reason that the Amazon rainforest plays a crucial role in the global climate. Furthermore, the Amazon rainforest has ca. 40,000 species of plants, ca. 1300 species of birds, 425 species of mammals, 371 species of reptiles, and 427 species of amphibians (Mittermeier et al., 2003). The extraordinary biodiversity demonstrates the significance of the Amazon rainforest to global biodiversity conservation.

As a huge natural organic carbon (C) stock in the soil, peat ecosystems in the Amazon rainforest rightfully get attention. South America (mainly Amazonia), Southeast Asia, and Africa are the three main peat C stocks in the tropics (Fig. 1.1). According to the new statistics, Amazonia potentially is the largest peat and C stock in the tropics, rather than Southeast Asia (Ribeiro et al., 2020, Fig. 1.2). For example, Gumbrecht et al. (2017) estimated that tropical America contains 750,000 km<sup>2</sup> of peatland area and ca. 3120 km<sup>3</sup> of peat volume, which is higher than ca. 650,000 km<sup>2</sup> and ca. 2730 km<sup>3</sup> in Asia and ca. 290,000 km<sup>2</sup> and ca. 1410 km<sup>3</sup> in Africa. Ribeiro et al. (2020) calculated that tropical America contains 90–120 gigatons (Gt) C stock, which is larger than Southeast Asia and Africa (Fig. 1.2).





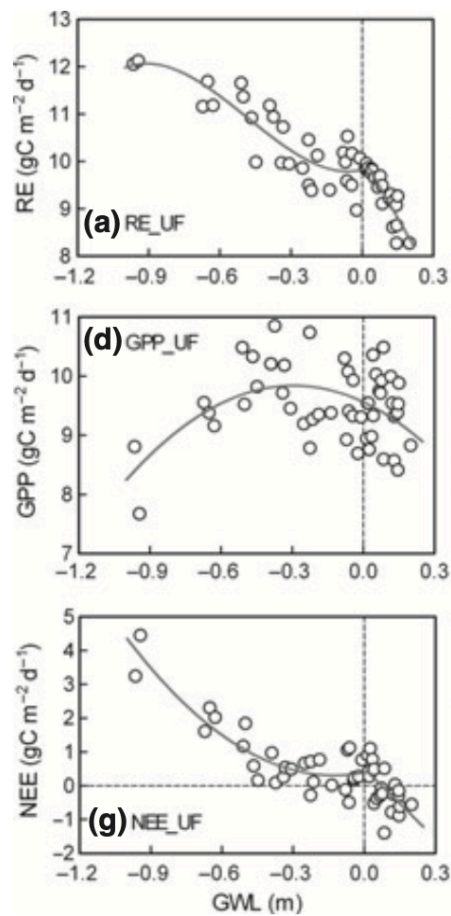
**Fig. 1.1** Tropical peatlands distribution (Ribeiro et al., 2020, data is from Xu et al., 2018)



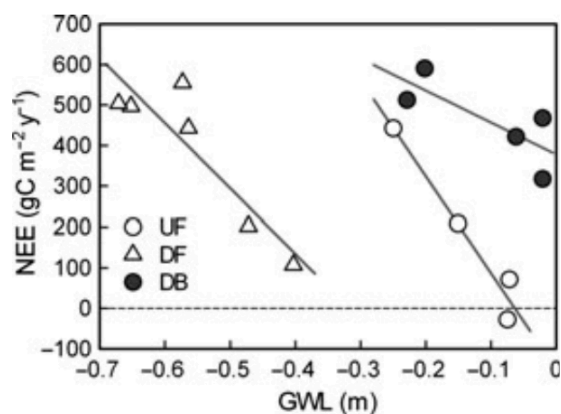
**Fig. 1.2** Estimated peat area, depth, volume, and carbon stock (Ribeiro et al., 2020)

However, peat ecosystems are easily degraded, changing from a C sink into a C source influenced by some factors. Different from temperate regions, Amazonian peat ecosystems as an important component of tropical peat ecosystems have their special mechanism of peat formation and vegetation coverage, but it is incompletely known. The basic logic of peat formation is net peat C accumulation, which is the joint result of gross primary production that accumulates the organic material (OM) and ecosystem respiration (sum of plants respiration and peat decay) that releases OM. When OM accumulates over 45% of the sedimentation, peat forms in the tropics (Wüst et al., 2003). It is now known that the tropical peat formation is mainly controlled by the water table. For example, Hirano et al. (2012) investigated Indonesian swamps and found that the peat only formed when the water table is higher than ca. 0.1–0.3 m (monthly mean; Fig. 1.3) or ca. -0.05 (annual mean; Fig. 1.4), and the annual CO<sub>2</sub> emissions on ecosystem scale increase 79–238 g C m<sup>-2</sup> per 0.1 m lowering of the water table. This linear relationship between the CO<sub>2</sub> exchanges and the water table is probably because of the enhancement of oxidative peat decomposition when the water table became lower. By influencing the depth and stability of the water table, lateral river migration and climate changes control peat C accumulation. To a lesser extent, vegetation coverage can impact peat C accumulation by influencing the available oxygen concentration in the water-logged soil. For example, *Mauritia* and other palms in neotropical swamps have pneumatophores, which can transfer oxygen to the water-logged soil (De Granville, 1974). Furthermore, peat ecosystems can be eroded by river flooding and human activities.

Available Holocene palaeoecological studies of peat ecosystems in Amazonia focus on the northwestern region especially in northern Peru (e.g., Kelly et al., 2017, 2020; Läähteenoja et al., 2012; Roucoux et al., 2013; Swindle et al., 2018), but almost nothing is known in southwestern and northeastern Amazonia. To further explore processes of peat and organic C accumulation and vegetation dynamics and their influencing factors in Amazonia, we studied peat ecosystems in the Madre de Dios region in southeastern Peru (southwestern Amazonia) and Lagoa da Fazenda region in northern Brazil (northeastern Amazonia). Based on chronology constructed by <sup>14</sup>C radiocarbon dating, we used Loss-On-Ignition (LOI) analysis to study peat formation and accumulation rate, organic C analysis to explore organic C accumulation rate, and pollen and spore analysis to investigate vegetation dynamics. Combined with geochemical analysis and macro-charcoal analysis, we can further explore the influencing factors of the above dynamics.



**Fig. 1.3** Responses of monthly mean respiration (RE), gross primary production (GPP), and CO<sub>2</sub> exchange (NEE) on ecosystem scale to changes of groundwater level for the intact peat swamp forest with little drainage (UF) in Indonesia (Hirano et al., 2012).



**Fig. 1.4** Relationship between annual NEE and annual mean groundwater level in a intact peat swamp forest with little drainage (UF), a drained swamp forest (DF), and a drained burnt swamp forest (DB), respectively. (Hirano et al., 2012)

## 1.2 Research questions

The main research questions of this study include:

1. When and how did peat ecosystems develop including vegetation dynamics as well as peat and organic C accumulation in the southwestern and northeastern Amazonia?
2. What drives the development of the peat ecosystems?
3. Are processes of the peat ecosystem development local or regional?

## 1.3 Study area

### 1.3.1 Madre de Dios region in southwestern Amazonia

Madre de Dios is a river that descends from the Andes and then meanders to the southeast at an elevation of ca. 350 m a.s.l. in southern Peru in southwestern Amazonia. Madre de Dios River is white water that carries a heavy suspension load with high concentrations of calcium and has a circumneutral pH (Thieme et al., 2007; Pitman, 2010; Puhakka et al. 1992). The river itself and its floodplains are limited by the old river terraces, which are locally called *terra firme* elevated 10 to 30 m above the floodplains. Areas of *terra firme* are not flooded. Numerous perennial seepages from the *terra firme* converge at the intersection of the impervious foundation (called Ipururu basement) and the *terra firme* forming peatlands (Householder et al., 2012). The peatlands are generally dominated by *Mauritia*, which is locally called *aguajal*. Thousands of *aguajales* are distributed in the Madre de Dios River region (Chapter 2 Fig. 2.1). *Aguajales* normally do not receive water or sediment influx from the river, except during periods of high flooding or river course changes. Therefore, *aguajales* generally are nutrient-poor with a relatively stable water table, typically varying less than 50 cm. The documented maximum depth of *aguajales* is up to 9 m, which shows the potential of the *aguajales* to be a large peat carbon (C) stock.

To explore environmental changes in the *aguajales*, we took two sediment cores from an *aguajal* in the Madre de Dios region to be a representative. One core is from the central part of the *aguajal* where grows dense palms of *Mauritia*. The other core is from an oxbow lake, which is in the eastern part of the *aguajal*. The *aguajal* core can show the basic condition of the *aguajal*, the oxbow lake core can represent the environmental changes on a more regional scale. As the Madre de Dios region is near the Los Amigos River, the *aguajal* core is named Los Amigos *Aguajal* (12.56°S, 70.12°W, LAA), and the oxbow lake core is named Los Amigos Lake (12.56°S, 70.11°W, LAL).

### A. Climate

The Madre de Dios region has a mildly seasonal tropical climate (Pitman, 2010; Terborgh, 1983). The mean annual temperature is 24.1°C with maxima up to 39°C (Pitman, 2010). Episodic cold Antarctic air influx from polar air masses may cause significant cooling down to 8°C during the period of May to August, locally called “Friajes”. The mean annual rainfall of the area is 2700–3000 mm. More than 80% of rainfall falls between October and May.

### B. Modern vegetation

In the Madre de Dios region, the vegetation coverage is determined by the different geomorphologic conditions, which mainly include *aguajal*, floodplain, and *terra firme*. *Aguajales* are dominated by *Mauritia*, which is a single-stemmed, long-lived, and dioecious palm tree. *Mauritia* can grow up to 30–40 m in height and 60 cm in stem diameter with an average canopy cover of up to 75% (Virapongse et al., 2017).

Rull (1998) introduced the basic information and ecological characteristics of *Mauritia*. *Mauritia* is an old element of the Neotropical flora, its earliest pollen record can be extended back to near the boundary of the Cretaceous and Tertiary about 65 million years before the present. Nowadays, *Mauritia* palms are widely distributed in Amazonia, which is mostly restricted to its lowlands, especially in Orinoco basins, between 10°N–10°S latitudes. *Mauritia* grows in different ecosystems ranging from coastal swamps to inland gallery forests at elevations up to ca. 1000 m. Among ecosystems that *Mauritia* grows, the most frequent ecosystems are the pure stands of *Mauritia flexuosa* or it is a component in mixed forests. It generally requires a tropical warm and humid climate with more than 1000 mm of annual precipitation and permanently flooded soils. These ecosystems are locally called *morichales* in Colombia and Venezuela, *veredas* or *buritizales* in Brazil, and *aguajales* in Peru.

In alluvial soils (sand, silt and clay) along the Madre de Dios River, floodplain forests grow. Influenced by flooding events, floodplain forests are rich in nutrients and growing fast, but often cannot develop into old-grown and diverse forests (Balslev et al., 2016). Moraceae, Arecaceae, Meliaceae and Rubiaceae are frequent families in floodplain forests (Nebel et al., 2001).

In well-drained soils on the old terrace of the Madre de Dios River, *terra firme* forests grow. Without the influence of river flooding, *terra firme* forests can be old-grown and more diverse than floodplain forests. Species frequently recorded in *terra firme* forests are *Geonoma deversa* and *G. macrostachys* (both Arecaceae), *Hevea guianensis* (Moraceae) and *Mabea* (Euphorbiaceae), which are typical Amazonian forest trees (Balslev et al., 2016).

### 1.3.2 Lagoa da Fazenda region in northeastern Amazonia

Lagoa da Fazenda (LF) is a swamp, which is an abandoned river from the Baía de Caxiuanã in northern Brazil. The studied sediment core is from the LF (1°46'51" S, 51°25'19" W, 3 m above sea level). Baía de Caxiuanã is a 40 km long and 8–15 km wide inland bay lying on a relatively flat plain between the Xingu River and the Pacajá River, located ca. 350 km west of Belém City (Pará State). Nowadays, Baía de Caxiuanã has no connections with the Amazon River, but has a small east-flowing stream via Baía de Portel, Baía do Melgaço, and Rio Pará to the Atlantic Ocean. Caxiuanã National Forest Reserve is on the west bank of the Baía de Caxiuanã. This reserve is covered by Amazonian rainforests, which developed on deep latosols and spodosols (areas with white sand) derived from cretaceous sedimentary rocks from the Alter do Chão Formation and Quaternary sedimentary rocks of the Barreiras Formation. The research station “Estação Científica Ferreira Penna” (ECFPn, 1°44'07" S, 51°27'47" W, ca. 7 km northwest of the coring site) is also located in this reserve. Some records show that the water level at ECFPn is influenced by low and high tides, ranging between 17 and 21 cm, with an average of 33 cm from December 1995 to April 1996 (Hida et al., 1997).

#### A. Climate

The climate in the Lagoa da Fazenda region is typically tropical climate, which is warm, and humid without marked dry periods (Nimer, 1989). The climate station Breves is ca. 100 km east of the coring site. Recorded mean annual precipitation is about 2500 mm (1969–1980). The mean annual temperature is about 26°C, ranging from 22.2 to 32.9°C (Moraes et al., 1997).

#### B. Modern vegetation

Around 85% of the Lagoa da Fazenda area is covered by unflooded upland forests called *terra firme*, and most of the rest area is covered by inundated forests called *várzea* and *igapó*, which are both highly diverse. A plant investigation shows that 2452 plant species with diameter breast height >10 cm were recorded on studied plots (13 hectares) at the ECFPn (Lisboa et al., 1997; Ferreira et al., 1997). It also shows that the most common tree families and species of *terra firme* forests are *Rinorea guianensis* (Violaceae), *Tetragastris panamensis* (Burseraceae), *Lecythis idatimon*, *Eschweilera coriacea* and *E. grandiflora* (Lecythidaceae), and *Vouacapua americana* (Caesalpinaceae), Melastomataceae, and Moraceae. Characteristic species of *várzea* forest are *Virola surinamensis* (Myristicaceae), *Pachira aquatica* (Bombacaceae), *Euterpe oleracea* and *Mauritia flexuosa* (Arecaceae). Furthermore, small areas of savanna-like vegetation dominated by herbaceous plants (e.g., Cyperaceae, Poaceae)

probably formed by inundation or human activity, are also found in this region.

### C. *Human activities*

Evidenced by several archaeological sites with black soils (*terra preta*) along the shore of the Baía de Caxiuanã, humans have lived in the Lagoa da Fazenda region since the Pre-Columbian era (Kern and Costa, 1997). Thermoluminescence-dated ceramic fragments are not older than 720 yr BP (Kern, 1996). However, The Rio Curuá record (ca. 7 km distance to the LF coring site) shows a marked frequent occurrence of fires in the study region, suggesting the increased human presence since ca. 2500 cal yr BP (Behling and Costa, 2000).

## 1.4 Methodology

### 1.4.1 Core sampling and chronology

The studied sediment cores (LAA, LAL, LF) were collected using a Russian Corer with 50 cm long sections. The stratigraphy of each studied core was characterized by visualization according to physical attributes (Aaby and Berglund, 1986).

For each studied core, a few samples with organic material of peat, clay, mud, charcoal, or wood were taken for Accelerator Mass Spectrometry (AMS) radiocarbon dating. Almost all samples were dated in the Poznań Radiocarbon Laboratory, Poland. The dates calibrated by the SHCal13.14C (Hogg et al., 2013) and 0 cm (-48 cal yr BP) were used to construct an age-depth model by the Bacon script (Blaauw and Christen, 2011) using software R.

### 1.4.2 Pollen and spore analysis

Pollen and spores from deposits can generally be identified to family, often to genus, and sometimes to species level. Identifying and counting the high number of different pollen and spore taxa allows us to analyze past plant diversity dynamics. For example, pollen and spore assemblages from a peatland core generally can reflect the local vegetation of the peatland, while a lake core influenced by fluvial dynamics can reflect a more regional scale. The pollen-vegetation relationship also should be considered, which can be found in modern pollen-rain studies (e.g., Gosling et al., 2009).

For the lab work of pollen and spore analysis, pollen samples were generally taken in about 10–20 cm intervals along each core in this study, which specifically depended on the period represented by an interval. For each pollen sample, the volume is about 0.5 or 1 cm<sup>3</sup>. Before the processing, one tablet of exotic *Lycopodium* spores (20,846±1546 or 9666±212) was added to each sample for calculation of pollen concentration (grains

cm<sup>-3</sup>) and pollen accumulation rate (grains cm<sup>-2</sup> yr<sup>-1</sup>). All samples were prepared using standard pollen analytical techniques and acetolysis and mounted with glycerin (Faegri and Iversen, 1989). The large reference collection of the Department of Palynology and Climate Dynamics and available literature were used for pollen and spore identification and counting (e.g. Roubik and Moreno, 1991; Colinvaux et al., 1999). A minimum of 300 pollen grains will be counted for each pollen sample. TILIA software of version 2.6.1 was used to calculate and plot the pollen and spore diagram. The pollen and spore taxa presented in the diagram are percentages of the pollen sum which only includes terrestrial pollen. All the taxa were grouped into broad life forms, such as palms, trees and shrubs, herbs, aquatics, and pteridophyta. CONISS module of the software was used for the cluster analysis of the terrestrial pollen taxa (Grimm, 1987).

### 1.4.3 Loss-on-ignition (LOI) analysis

LOI analysis is used to determine the proportion of organic material (OM) in the sediment for each core in this study. Based on the proportion of OM, the sediment can be classified as “peat” (LOI>45%), “muck” (35%<LOI<45%), “organic-rich soil sediment” (20%<LOI<35%), “mineral soil or sediment with organic material” (LOI<20%). The classification is according to Wüst et al. (2003).

LOI analysis was performed according to Heiri et al. (2001). Samples for LOI were taken at the same depth as the pollen samples. The volume of each LOI sample is 0.5 or 1 cm<sup>3</sup>. The OM content (the result of LOI) of each sample was calculated by the percentage of the difference between the weight after 24 hours of drying at 105°C ( $W_{dry}$ ) and the weight after 4 hours of combustion at 550°C ( $W_c$ ) in  $W_{dry}$ :

$$\text{LOI OM content (\%)} = \frac{W_{dry} - W_c}{W_{dry}} * 100$$

Combined with the chronology (section 3.1), the sediment/peat accumulation rate for each sample can be calculated by the difference of depth ( $D_{depth}$  (cm)) divided by the difference of calibrated age ( $D_{age}$  (yr)) between every two samples:

$$\text{Sediment or peat accumulation rate (cm/yr)} = \frac{D_{depth}}{D_{age}}$$

### 1.4.4 Organic carbon (C) analysis

Organic C analysis is used to determine the organic C content in the sediment, which is carried out on the LAA and LF core in this study. Samples for organic C analysis were taken at the same depth as the pollen samples. The volumes for C samples range from 0.5 to 6 cm<sup>3</sup>, which depends on the organic C content in the sediment (quality of



material is required in the later test). All samples were dried at 70 °C for 24 hours and weighed ( $W_{\text{dry}}$  (g)), and then were finely ground in an agate mortar. Each ground dry sample was weighed ( $W_{\text{dry and ground}}$  (g)). Then, the percentage of C content ( $C_{\text{total}}$  (%)) and the percentage of Nitrogen (N) content ( $N_{\text{total}}$  (%)) in the material of each ground dry sample were tested by Elementar Vario EL III. After that, each sample was burnt at 600°C for 5 hours and weighed ( $W_{\text{burn}}$  (g)). The percentage of inorganic C content in each burnt sample ( $C_{\text{burn}}$  (%)) was tested by Elementar Vario EL III. This test requires that the mass of each burnt sample is at least 20 mg. The percentage of organic C content in each sample ( $C_{\text{org}}$  (%)) was calculated by:

$$C_{\text{org}} (\%) = C_{\text{total}}(\%) - C_{\text{burn}}(\%) * \frac{W_{\text{burn}}}{W_{\text{dry and ground}}}$$

The ratio of organic C to total N for each sample is calculated by:

$$\frac{C}{N} = \frac{C_{\text{org}}(\%)}{N_{\text{total}}(\%)}$$

Combined with the chronology (section 3.1) and the sediment/peat accumulation rate, the organic C accumulation rate for each sample can be calculated by the sediment/peat accumulation rate multiplied by organic C content in unit volume. Bulk density, which is calculated by  $W_{\text{dry}}$  divided by the volume of the originally taken sample ( $V_{\text{sample}}$  (cm<sup>3</sup>)), multiplied by  $C_{\text{org}}$  (%) is organic C content in unit volume. The calculation can be shown as the following formula:

$$\begin{aligned} & \text{Organic C accumulation rate (g/m}^2\text{/yr)} \\ & = \text{Sediment or peat accumulation rate (cm/yr)} * \frac{W_{\text{dry}}(\text{g})}{V_{\text{sample}}(\text{cm}^3)} * C_{\text{org}} (\%) * 10000 \end{aligned}$$

#### 1.4.5 Macro-charcoal analysis

Macro-charcoal analysis was carried out on LAL and LF cores. For macro-charcoal (>125 µm) counting, we took samples at the same depth as pollen and spore analysis for the LAL core, but took samples of 1 cm<sup>3</sup> in 1–2 cm for the LF core. Charcoal samples were prepared according to Stevenson and Haberle (2005). Firstly, all samples were dispersed in 5–10 ml 10% KOH for 24h. After that, we used 6% hydrogen peroxide (H<sub>2</sub>O<sub>2</sub>) to remove organic material and left overnight. At last, all samples were wet sieved using a 125 µm sieve. Charcoal identification literature was used such as Clark and Royall (1995), Jensen et al. (2007) and Umbanhowar Jr and Mcgrath (1998). Macro-charcoal accumulation rate can be calculated by the amount of counted macro-charcoal particles in each sample ( $C_{\text{charcoal}}$ ) divided by the years represented by the

sample (yr):

$$\text{Macrocharcoal accumulation rate (particles/yr)} = \frac{C_{\text{charcoal}}}{\text{yr}}$$

Macro-charcoal accumulation rate can reflect the frequency and intensity of past fires in local. Combined with other paleo-data, we can explore if fire events were driven by natural and/or anthropogenic factors.

#### **1.4.6 Chemical composition analysis by X-ray fluorescence (XRF)**

XRF is generally carried out on lake sediments for chemical composition analysis, which is on LAL and LF core in this study.

For the LAL core, non-destructive XRF scanning was performed with an Itrax Core scanner (Cox Analytical Systems) at the University of Bremen, Institute of Geography in Germany. The LAL core was scanned at a resolution of 5 mm using a Mo X-ray tube (30 kV, 18 mA) with a dwell time of 0.5 s per step. To improve the signal-to-noise ratio, four consecutive spectra were later combined and reprocessed with the scanning software (Q-spec, Cox Analytical Systems) to achieve a spatial resolution of 2 mm with a dwell time of 40 s. Raw element data (integrated peak areas as total counts) were normalized by the coherent scatter radiation (coh) to minimize matrix effects. Si/coh, K/och, Ti/coh, Ca/coh, and ratios of Ca/Ti, Fe/Mn were provided.

For the LF core, in total 11 samples (depth in 395–390 cm, 330–325 cm, 280–275 cm, 230–225 cm, 180–175 cm, 130–125 cm, 94–89 cm, 70–65 cm, 45–40 cm, 30–25 cm, and 10–5 cm) were taken for semiquantitative chemical composition analysis by portable XRF, which were performed in the Institute of Geosciences of the Federal University of Pará. The analyzed elements are represented by their respective oxides ( $\text{Al}_2\text{O}_3$ ,  $\text{SiO}_2$ ,  $\text{TiO}_2$ ,  $\text{Fe}_2\text{O}_3$ ,  $\text{MgO}$ ,  $\text{P}_2\text{O}_5$ ,  $\text{K}_2\text{O}$ ,  $\text{CaO}$ ) or itself such as Sulfur (S), which were determined directly on the pressed natural dried samples. Furthermore, pXRF also allow to test LOI for 11 samples.

#### **1.4.7 Mineralogical identification by X-Ray Diffraction (XRD)**

XRD analysis was carried out on the LF core for mineralogical identification, using the 11 samples same as pXRF analysis (section 3.6). XRD analysis was performed by a Bruker D2 Phaser X-ray diffractometer equipped with a Cu anode and a Ni- $k\beta$  filter, at the Federal University of Pará, Brazil. We used the powder method. The diffractometer was set in the  $\theta$ - $\theta$  Bragg-Brentano geometry with a Linear Lynxeye detector. Each sample was ground in an agate mortar and measured in reflection mode from  $5^\circ$  to  $70^\circ$   $2\theta$  range with  $0.02^\circ$  step size and 38.4 s per step counting time. The mineral characterizations were performed using the software High Score Plus 5.0, with the aid

of the database of the Powder Diffraction Files from the International Center for Diffraction Data.

#### **1.4.8 Mineral identification by Scanning Electron Microscope (SEM) with Energy Dispersive Spectroscopy (EDS)**

In addition to XRD analysis, SEM/EDS allow to identify other minerals obtaining images and do semi-quantitative (spot and chemical mapping) chemical analysis of the identified minerals. The SEM/EDS analysis was carried out on five samples of the 11 samples of XRF and XRD analysis for LF core (sections 3.6 and 3.7), which includes 395–390 cm, 230–225 cm, 130–125 cm, 30–25 cm, and 10–5 cm. In this SEM/EDS analysis, the Hitachi TM3000 Scanning Electron Microscope coupled to a Swift ED300 Energy Dispersive Spectrometer was used, with voltage acceleration from 5 to 15 kV and with SDD detector (161 eV Cu-K $\alpha$ ) at the Institute of Geosciences of the Federal University of Pará. The analysis was performed under a low vacuum without metallization.

### **Reference**

- Aaby, B., Berglund, B. E. 1986. Characterization of peat and lake deposits. In Berglund, B.E., (Editor), *Handbook of Holocene palaeoecology and palaeohydrology*. Chichester & New York, J. Wiley & Sons, p. 231-246.
- Balslev, H., Laumark, P., Pedersen, D., Grández, C., 2016. Tropical rainforest palm communities in Madre de Dios in Amazonian Peru. *Revista peruana de biología* 23, 3–12.
- Behling, H., Costa, M.L., 2000. Holocene environmental changes from the Rio Curuá record in the Caxiuanã region, eastern Amazon Basin. *Quaternary Research* 53, 369-377.
- Blaauw, M., Christen, J.A., 2011. Flexible paleoclimate age-depth models using an autoregressive gamma process. *Bayesian Analysis* 6, 457–474.
- Clark, J. S., Royall, P. D., 1995. Particle-size evidence for source areas of charcoal accumulation in late Holocene sediments of eastern North American lakes. *Quaternary Research* 43, 80-89.
- Colinvaux, P., De Oliveira, P.E., Moreno Patiño, J.E., 1999. *Amazon: Pollen Manual and Atlas*. Harwood Academic Publishers, Amsterdam.
- De Granville, J.J., 1974. Aperçu sur la structure des pneumatophores de deux espèces des sols hydromorphes en Guyane. *Mauritia flexuosa* L. et *Euterpe oleracea* Max-t. (Palmae). Généralisation au système respiratoire racinaire d'autres palmiers, *ORSTOM. Ser. Biol.* 23, 3-22.
- Faegri, K., Iversen, J., 1989. *Textbook of Pollen Analysis*, fourth ed. Wiley, Chichester, pp. 67-89.

- Ferreira, L. V., Almeida, S. S., and Rosário, C. S., 1997. As áreas de inundação. In “Caxiuanã” (P. L. B. Lisboa, Coord.), pp. 195–211. Museu Paraense Emílio Goeldi, Belém.
- Gosling, W.D., Mayle, F.E., Tate, N.J., Killeen, T.J., 2009. Differentiation between Neotropical rainforest, dry forest, and savannah ecosystems by their modern pollen spectra and implications for the fossil pollen record. *Review of Palaeobotany and Palynology* 153, 70-85.
- Grimm, E.C., 1987. CONISS: a FORTRAN 77 program for stratigraphically constrained cluster analysis by the method of incremental sum of squares. *Computers & geosciences* 13, 13-35.
- Gumbrecht, T., Roman-Cuesta, R.M., Verchot, L., Herold, M., Wittmann, F., Householder, E., Herold, N., Murdiyarsa, D., 2017. An expert system model for mapping tropical wetlands and peatlands reveals South America as the largest contributor. *Global Change Biology* 23, 3581-3599.
- Heiri, O., Lotter, A.F., Lemcke, G., 2001. Loss on ignition as a method for estimating organic and carbonate content in sediments: reproducibility and comparability of results. *Journal of paleolimnology* 25, 101-110.
- Hida, N., Maia, J. G., Hiraoka, M., Shimmi, O., and Mizutani, N., 1997. Notes on annual and daily water level changes at Breves and Caxiuanã, Amazon estuary. In “Caxiuanã” (P. L. B. Lisboa, Coord.), pp. 97–107. Museu Paraense Emílio Goeldi, Belém.
- Hirano, T., Segah, H., Kusin, K., Limin, S., Takahashi, H., Osaki, M., 2012. Effects of disturbances on the carbon balance of tropical peat swamp forests. *Global Change Biology* 18, 3410–3422.
- Householder, J.E., Janovec, J.P., Tobler, M.W., Page, S., Lähteenoja, O., 2012. Peatlands of the Madre de Dios River of Peru: distribution, geomorphology, and habitat diversity. *Wetlands* 32, 359–368.
- Jensen, K., Lynch, E. A., Calcote, R., Hotchkiss, S. C., 2007. Interpretation of charcoal morphotypes in sediments from Ferry Lake, Wisconsin, USA: do different plant fuel sources produce distinctive charcoal morphotypes? *The Holocene* 17, 907-915.
- Kelly, T.J., Lawson, I.T., Roucoux, K.H., Baker, T.R., Jones, T.D., Sanderson, N.K., 2017. The vegetation history of an Amazonian domed peatland. *Palaeogeography, Palaeoclimatology, Palaeoecology* 468, 129–141.
- Kelly, T.J., Lawson, I.T., Roucoux, K.H., Baker, T.R., Coronado, E.N.H., 2020. Patterns and drivers of development in a west Amazonian peatland during the late Holocene. *Quaternary Science Reviews* 230, 106168.
- Kern, D.C., 1996. “Geoquímica e Pedogeogeuímica de Sítios Arqueológicos com Terra Preta na Floresta Nacional de Caxiuanã (Portel-Pará).” Unpublished Ph.D. dissertation, Universidade Federal do Pará, Pará.
- Kern, D., Costa, M.L. 1997. Composição Química de Solos Antropogênicos Desenvolvidos em Latossolo Amarelo Derivado de Lateritos. *Geociências*

- (UNESP). 16: 157-175.
- Lähteenoja, O., Reategui, Y.R., Rasänen, M., Torres, D.D.C., Oinonen, M., Page, S., 2012. The large Amazonian peatland carbon sink in the subsiding Pastaza–Marañon foreland basin, Peru. *Global Change Biology* 18, 164–178.
- Lisboa, P. L. B., Silva, A. S. L., and Almeida, S. S., 1997. Florística e estrutura dos Ambientes. In “Caxiuanã” (P. L. B. Lisboa, Coord.), pp. 163–193. Museu Paraense Emílio Goeldi, Belém.
- Mittermeier, R.A., Mittermeier, C.G., Brooks, T.M., Pilgrim, J.D., Konstant, W.R., Da Fonseca, G.A., Kormos, C., 2003. Wilderness and biodiversity conservation. *Proceedings of the National Academy of Sciences* 100, 10309–10313.
- Moraes, J. C., Costa, J. P. R., Rocha, E. J. P., and Silva, I. M., 1997. Estudos hidrometeorológicos na Baía do Rio Caxiuanã. In “Caxiuanã” (P. L. B. Lisboa, Coord.), pp. 85–95. Museu Paraense Emílio Goeldi, Belém.
- Nebel, G., Kvist, L.P., Vanclay, J.K., Christensen, H., Freitas, L., Ruíz, J., 2001. Structure and floristic composition of flood plain forests in the Peruvian Amazon: I. Overstorey. *Forest ecology and Management* 150, 27–57.
- Nimer, E., 1989. “Climatologia do Brasil.” Fundação Instituto Brasileiro de Geografia e Estatística, Rio de Janeiro.
- NOAA., 2023. Global Atmospheric Circulations. <https://www.noaa.gov/jetstream/global/global-atmospheric-circulations>.
- Pitman, N.C., 2010. An overview of the Los Amigos watershed, Madre de Dios, southeastern Peru. Washington, DC: Draft report for Amazon Conservation Association.
- Puhakka, M., Kalliola, R., Rajasilta, M., Salo, J., 1992. River types, site evolution and successional vegetation patterns in Peruvian Amazonia. *Journal of Biogeography* 19, 651–665.
- Ribeiro, K., Pacheco, F.S., Ferreira, J.W., de Sousa-Neto, E.R., Hastie, A., Krieger Filho, G. C., Alvalá, P.C., Forti, M.C., Ometto, J. P., 2020. Tropical peatlands and their contribution to the global carbon cycle and climate change. *Global Change Biology* 27, 489-505.
- Roberts, J. M., 2009. The role of forests in the hydrological cycle. *Forests and forest plants* 3, 42-76.
- Roubik, D.W., Moreno, J.E., 1991. Pollen and Spores of Barro Colorado Island, vol. 36. Missouri Botanical Garden, the United States.
- Roucoux, K. H., Lawson, I. T., Jones, T. D., Baker, T. R., Coronado, E. H., Gosling, W. D., Lähteenoja, O., 2013. Vegetation development in an Amazonian peatland. *Palaeogeography, Palaeoclimatology, Palaeoecology* 374, 242-255.
- Rull, V., 1998. Biogeographical and evolutionary considerations of *Mauritia* (Arecaceae), based on palynological evidence. *Review of Palaeobotany and Palynology* 100, 109-122.
- Stevenson, J., Haberle, S., 2005. Macro Charcoal Analysis: A Modified Technique

Used by the Department of Archaeology and Natural History. Australian National University, Canberra.

- Swindles, G.T., Morris, P.J., Whitney, B., Galloway, J.M., Gałka, M., Gallego-Sala, A., Macumber, A.L., Mullan, D., Smith, M.W., Amesbury, M.J., Roland, T.P., Sanei, H., Patterson, R. T., Sanderson, N., Parry, L., Charman D.J., Lopez, O., Valderamma, E., Watson, E.J., Ivanovic, R.F., Valdes, P.J., Turner, T.E., Lähteenoja, O., 2018. Ecosystem state shifts during long-term development of an Amazonian peatland. *Global Change Biology* 24, 738–757.
- Thieme, M., Lehner, B., Abell, R., Hamilton, S.K., Kellndorfer, J., Powell, G., Riveros, J.C., 2007. Freshwater conservation planning in data-poor areas: an example from a remote Amazonian basin (Madre de Dios River, Peru and Bolivia). *Biological Conservation* 135, 484–501.
- Umbanhowar Jr, C.E., Mcgrath, M.J., 1998. Experimental production and analysis of microscopic charcoal from wood, leaves and grasses. *The Holocene* 8, 341-346.
- Virapongse, A., Endress, B.A., Gilmore, M.P., Horn, C., Romulo, C., 2017. Ecology, livelihoods, and management of the *Mauritia flexuosa* palm in South America. *Global ecology and conservation* 10, 70–92.
- Wüst, R.A., Bustin, R.M., Lavkulich, L.M., 2003. New classification systems for tropical organic-rich deposits based on studies of the Tasek Bera Basin, Malaysia. *Catena* 53,133–163.
- Xu, J., Morris, P. J., Liu, J., Holden, J., 2018. PEATMAP: Refining estimates of global peatland distribution based on a meta-analysis. *Catena* 160, 134-140.

# Chapter 2

## Late Holocene peatland palm swamp (*aguajal*) development, carbon deposition and environment changes in the Madre de Dios region, southeastern Peru

<sup>a</sup> Bowen Wang, <sup>a</sup> Kartika Anggi Hapsari, <sup>b</sup> Viviana Horna, <sup>b,c</sup> Zimmermann Reiner, <sup>a</sup> Hermann Behling.

*a University of Goettingen, Department of Palynology and Climate Dynamics, Untere Karaspüle 2, 37073 Goettingen, Germany*

*b University of Bayreuth, Ecological Botanical Gardens ÖBG, 95444 Bayreuth, Germany*

*c University of Hohenheim, Forest Ecology and Remote Sensing Group, Molecular Botany 190a, 70599 Stuttgart, Germany*

Corresponding author: Bowen Wang [bowen.wang@biologie.uni-goettingen.de](mailto:bowen.wang@biologie.uni-goettingen.de)

Palaeogeography, Palaeoclimatology, Palaeoecology (2022) 594, 110955.

## Abstract

Tropical peatlands are an important carbon reservoir; however, they are vulnerable to climate change, fire events, and human disturbances, and may become a significant carbon source if degraded. In this paper, we investigated the late Holocene record of vegetation change, peatland evolution, and C accumulation based on analysis of a sediment core through a *Mauritia* palm dominated swamp (locally called “*aguajal*”) in the Madre de Dios region in southern Peru to better understand tropical peatland dynamics. Sedimentation commenced within shallow water, ponded on an impervious substrate, perhaps within an abandoned river channel or oxbow lake (1380–820 cal yr BP) located adjacent to a steep escarpment with *terra firme* (upland) rainforest above and lateral to floodplain forests. This was followed by the development of marsh (820–640 cal yr BP). A closed-canopy *Mauritia flexuosa*-dominated palm swamp was subsequently established (640–300 cal yr BP) which later changed into an open canopy and mixed-species *Mauritia* palm swamp (300 cal yr BP to present). Two major changes in peat and C accumulation rates were observed: (1) onset of peat and C accumulation at 820 cal yr BP and (2) decrease of peat and C accumulation after 520 cal yr BP. Comparisons of our results with palaeoecological records from *aguajales* in northern Peru suggest that the dynamics were different in this region. The peat and C accumulation rates in our study core in southern Peru were ca. 4 mm yr<sup>-1</sup> and ca. 200 g m<sup>-2</sup> yr<sup>-1</sup> faster, similar to a few sites in northern Peru. *Aguajales* in Madre de Dios region in southern Peru are an important carbon sink. Analyzing the dynamics of *aguajales* which are a kind of typical peatlands in Amazonia and comparing among different sites allows exploration and prediction of regional peatlands’ development under the potential future impact of natural changes.

### Keywords

Late Holocene; peatland development; *aguajal*; vegetation dynamic; carbon storage; southern Peru



## 2.1 Introduction

Peatlands cover around 3% of the global land area but hold equivalent to about half of the carbon (C) that is currently stored as CO<sub>2</sub> in the atmosphere (Dise, 2009). While most peatlands are located in the boreal and subarctic regions of the Northern Hemisphere (Dise, 2009), tropical peatlands are also important and cover ca. 440,000 km<sup>2</sup> and comprise 11% of global peatlands (Page et al., 2011). After Southeast Asia, South America has the second-largest tropical peatlands with ca. 110,000 km<sup>2</sup> which is equivalent to 24% of all tropical peatlands (Page et al., 2011). Peru is the country with abundant peatlands in South America, which covers around 74,644 km<sup>2</sup> peat area and holds 449 Gm<sup>3</sup> peat volume (Gumbricht et al., 2017). Peru represents 4% and 6% of the total tropical peatland area and volume (Gumbricht et al., 2017). Peatlands are vulnerable to (global) climate warming, droughts, falling water tables, and fires as well as destruction by human activities such as conversion to plantations or gold mining activities (Dise, 2009; Hapsari et al., 2017; Page et al., 2011). Today, Peruvian peatlands are at risk of being degraded by hydroelectric projects, road construction, gas and oil exploration, and agricultural activities (Roucoux et al., 2017; Lahteenoja et al., 2009a, 2012; Malhi et al., 2008). Peatland degradation has the potential to transform these areas from being a carbon sink into a source (Dise, 2009; Lahteenoja et al., 2012).

Previous studies have shown that the Pastaza-Maraon foreland basin (PMFB) in northern Peru contains the most extensive and C-dense peatlands of Amazonia (Draper et al., 2014; Lahteenoja et al., 2012), which covers an area of 35,600 ± 2,133 km<sup>2</sup> and contains 3.14 (0.44–8.15) Gt C (Draper et al., 2014). Previous palaeoecological and palynological studies in PMFB in northern Peru explored the development and vegetation dynamics of peatlands and their response to past climate changes (Kelly et al., 2017; Roucoux et al., 2013; Swindles et al., 2018). However, little is known about the peatlands in southern Peru. There, most peatlands are located along the meander belt of the Madre de Dios River and its affluents, estimated to cover around 300 km<sup>2</sup> (Householder et al., 2012). The typical *Mauritia flexuosa* palm swamp peatlands (locally called “aguajales”) is dominated by *Mauritia flexuosa*, a single-stemmed, long-lived, and dioecious palm. This species can grow up to 30–40 m and 60 cm of stem diameter, with an average canopy cover of up to 75% (Virapongse et al., 2017); observations suggest that individuals may reach more than one hundred years of age. We conducted multi-proxy palaeoecological studies on a peatland in the Madre de Dios region to explore the developmental history of an *aguajal*. This study addresses the following questions:

What were the past vegetation and environmental dynamics in the Madre de Dios floodplain region?

Since when and how did the peatland develop into an *aguajal* swamp? How did the peat and carbon accumulation change over time?

What factors may have influenced the peatland dynamics?

Are the successions of vegetation dynamics and peat and carbon accumulation rates in the Madre de Dios comparable to the peatlands in north Peru?

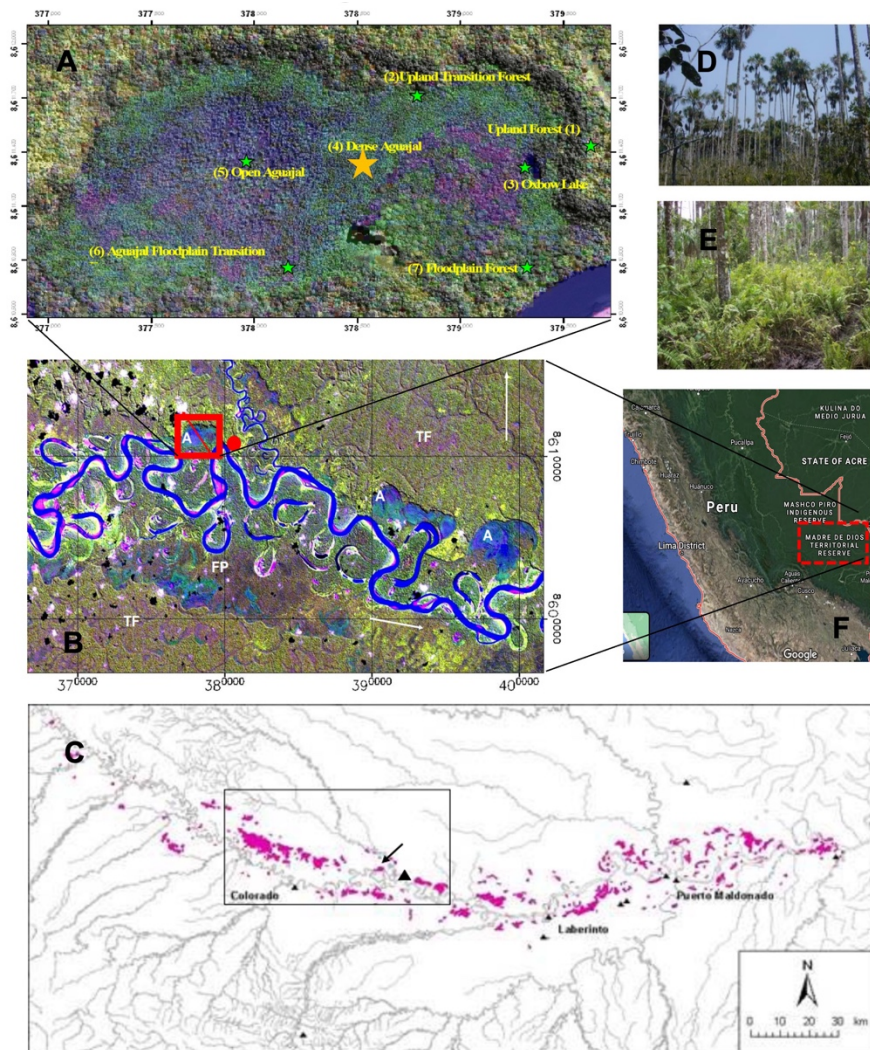
## 2.2 Study area

The studied *aguajal* is located on the floodplain of the Rio Madre de Dios in the south-eastern Peruvian Amazonia (Fig. 2.1). It is named after the nearby Los Amigos River which drains the eastern *terra firme* region and enters the Madre de Dios a few kilometers downstream of the *aguajal* from the east. The Madre de Dios River descends from the Andes and then meanders to the southeast at an elevation of 350 m a.s.l. near the study site. The Madre de Dios is a white water river and carries a heavy suspension load with high concentrations of calcium and has a circumneutral pH (Thieme et al., 2007; Puhakka et al. 1992). Seasonal flooding from the river influences the floodplains. Heavy rainfalls in the Andes may cause river level changes of several meters within a few hours and floodplain forest areas may get inundated and be disturbed by water flow and sedimentation. In contrast, areas with *aguajales* receive normally little to no water or sediment influx from the river. Only during unusual high floods or changes in the main river course sediment-rich water may intrude in *aguajal* areas. The waters of *aguajales* are clear with a slightly brown color and acidic (Thieme et al., 2007). Old river terraces constitute the uplands which are collectively known as “*terra firme*”. These areas are never flooded, rainwater seepage from these areas may contribute to the lateral influx of nutrient-poor water to *aguajales* which are located nearby. The *terra firme* terraces of the Madre de Dios are elevated 10 to 30 m above the floodplain and are limited by steep escarpments to the East (Balslev et al., 2016).

The tropical climate of the Madre de Dios region shows a moderate seasonality. The mean annual rainfall of the area is 2700–3000 mm with more than 80% falling between October and May (Centro de Investigación y Capacitación Rio Los Amigos (CICRA) station). The mean annual temperature is ca. 24°C with maxima up to 39°C (CICRA station, unpublished data). Episodic cold Antarctic air influx from the southeast may cause significant cooling down to 8°C, locally called “*friaje*”.

The vegetation in the study region is determined by the geomorphologic diversity of site conditions (Fig. 2.1b). *Aguajales* are nutrient-poor swamps with a relatively stable

water table, typically varying less than 50 cm, with an organic layer of a few decimetres up to >8 m depth. Besides *Mauritia flexuosa* that is the dominant species, frequent plant species at the border of the studied *aguajal* include *Protium*, *Guatteria*, *Tococa guianensis*, *Eugenia*, *Ceiba*, *Symphonia*, *Ouratea*, *Luehea*, *Zanthoxylum* (report from Eva-Maria Sadowski, unpublished). In contrast to *aguajales*, floodplain forests grow over alluvial soils (sand, silt, and clay) along the river. Floodplain forests are strongly disturbed by river dynamics such as flooding, of which age may not be as old as *terra firme* forests (Balslev et al., 2016). Moraceae, Arecaceae, Meliaceae, and Rubiaceae are frequent families in floodplain forests (Nebel et al., 2001). *Terra firme* forests grow on well-drained soils and are somewhat more diverse than the floodplains. Some species frequently occur in *terra firme* forests surrounding the study *aguajal* are *Geonoma deversa* and *G. macrostachys*, *Hevea guianensis*, *Ischnosiphon*, *Protium* (report from Eva-Maria Sadowski, unpublished).



**Fig. 2.1** Map of Madre de Dios region. A) Landsat TM image of the research swamp. The yellow star is the core position. The green stars with yellow legend illustrate the different types of ecosystems in the study site. B) Landsat image (Landsat ETM+ scene Path 3, Row 96; 23.5.2000; Bands 7/4/2, Projection: UTM 19S, WGS-84) of the middle course of the Madre de Dios showing peatland palm swamps (aguajales, short for A) along the north banks in the vicinity of the Rio de Los Amigos research station CICRA (redpoint). The small river entering from the top is the Rio de Los Amigos. The location of the proposed aguajal is indicated by a red rectangle with a line cutting across from northwest to southeast. The floodplain (FP) and peatland palm swamps are on both sides sharply limited by steep escarpments with terra firme forests (TF). C) This image was taken from Atrium, 2007; it shows the distribution of *Mauritia flexuosa* (Arecaceae) palm swamps and associated wetlands along the Madre de Dios River in southern Peru (Arrow: Palm swamp study site; Black triangle: Rio de Los Amigos research station (CICRA)). D) Open *Mauritia flexuosa* palm swamp (the green star of (5) in figure 1A); E) Medium dense aguajal with ferns in the understory in the coring aguajal; F) The position of Madre de Dios region in Peru.

## 2.3 Methods

### 2.3.1 Core sampling and chronology

The 800 cm-long sediment core from the Los Amigos *Aguajal* (LAA, Madre de Dios region, 12.56°S, 70.12°W) was collected in the geometrical center of that peatland palm swamp (Fig. 2.1) using a Russian Peat Corer (Jowsey, 1966). The core stratigraphy is described following Wüst et al. (2003) classification (refer to the LOI section) and visually inspect for the sediment including color, presence of plant material, and clay. Four 2 cm<sup>3</sup> bulk organic material samples (Table 2.2) were taken from the LAA core for Accelerator Mass Spectroscopy (AMS) radiocarbon dating and sent to the Poznań Radiocarbon Laboratory, Poland. The age-depth model was constructed using the R package *clam* (Blaauw, 2010) and calibrated using the SHCal13.14C southern hemisphere calibration curve (Hogg et al., 2013).

### 2.3.2 Pollen analysis

For pollen analysis, 1 cm<sup>3</sup> samples were taken at 20-cm intervals along the LAA core. Prior to processing, one tablet of exotic *Lycopodium* spores was added to each sample for calculation of pollen concentration (grains cm<sup>-3</sup>) and pollen accumulation rate (grains cm<sup>-2</sup> yr<sup>-1</sup>). All samples were prepared using standard pollen analytical techniques and acetolysis (Faegri and Iversen, 1989). Sample residues were mounted in a glycerine gelatine medium. Identification of pollen grains and spores was carried out using the reference collection of the Department of Palynology and Climate Dynamics at the University of Göttingen and available literature (e.g. Roubik and

Moreno, 1991; Colinvaux et al., 1999). A minimum of 300 pollen grains (except the sample at 495 cm counting with 251 grains) was counted for the total pollen sum of each sample, aquatic taxa and fern spores were excluded. Pollen and spore data are presented in pollen diagrams as percentages of the total pollen sum. All pollen taxa were grouped into broad life forms including palms, trees and shrubs, herbs, aquatics, and Pteridophyta, and a separate group for the taxa which occur in the Andes. The software TILIA of version 2.6.1 was used to calculate and plot the pollen diagrams. CONISS module of the software was used for the cluster analysis of terrestrial pollen taxa (Grimm, 1987).

### **2.3.3 Loss-on-ignition (LOI) analysis and carbon content analysis**

The sequential loss-on-ignition analysis is a common and widely used method to estimate the organic material (OM) content of sediments, which was carried out according to Heiri et al. (2001) in this study. 1 cm<sup>3</sup> samples were taken at 20-cm intervals. All samples were firstly dried at 105°C for 24 h and then combusted at 550°C for 4 h. The LOI organic material content (%) of each sample was calculated as the percentage of the difference between the weight after drying at 105°C ( $W_{dry}$ ) and the weight after combustion at 550°C ( $W_c$ ) in  $W_{dry}$ .

In total 78 samples for carbon content analysis were taken along the LAA core. Each sample of 0.5 cm<sup>3</sup> was taken at a 10-cm interval. Firstly, the samples were dried at 60°C for 48 h and finely ground. Then each sample was weighed (1–2 mg for samples with high organic material and 5–10 mg for samples with low organic material). Afterward, each sample was treated with 200µL 1 mol/l HCl to remove carbonates and was dried for 24h at 40°C prior to the determination of organic carbon content ( $C_{org}$ ) using high-temperature oxidation in a Euro EA3000 elemental analyzer at the Leibnitz Centre for Tropical Marine Ecology in Bremen.

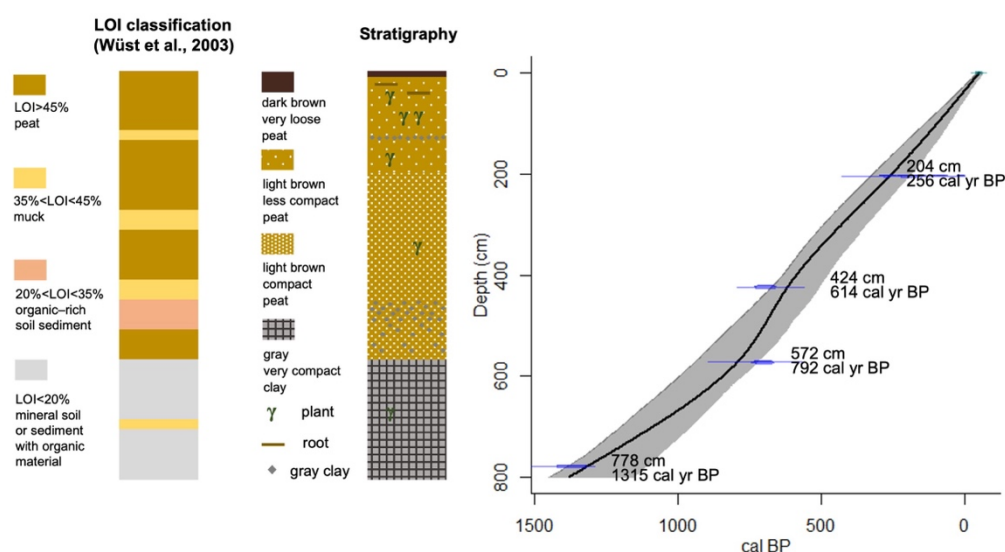
## **2.4 Results**

### **2.4.1 Stratigraphy and chronology**

The 800-cm-long LAA core from Madre de Dios consists mainly of dark brown decomposed peat with plant material (0–13 cm depth), light brown decomposed peat with plants (13–125 cm and 137–200 cm), light brown decomposed peat with a few plants (200–443 cm), light brown decomposed peat with clay (443–573 cm) and clay (125–137 cm and 573–800 cm depth) (Fig. 2.2, Table 2.1).

The four AMS radiocarbon dates are 205±30, 800±30, 825±30, 1545±30 yr BP at the depth of 204, 424, 572, 778 cm, respectively. The age-depth model (Fig. 2.2), which

was established based on the dating result, shows that the core sediment record spanning 1380 years, OM and C started to accumulate at 820 cal yr BP.



**Fig. 2.2** Stratigraphy, loss-on-ignition (LOI)-classification (based on LOI result of LAA core and Wüst et al. (2003)), and age-depth model of the Los Amigos *Aguajal* (LAA) core.

Depth (cm)	Description
0–13	dark brown decomposed peat, with plant remains, very loose
13–200	light brown decomposed peat, with plant remains, not very compact until 50 cm with roots and fine roots ( <i>Mauritia</i> ) 70–100 cm with more plant remains 125–137 cm with grey clay
200–443	light brown decomposed peat, with a few plants remains, compact
443–573	light brown decomposed peat with clay, compact, 450–483 cm with more grey clay
573–800	grey clay with a few very fine plants remains, very compact

**Table 2.1** Stratigraphy of the LAA core

Depth (cm)	Lab. Code	Radiocarbon dates ( <sup>14</sup> C yr BP)	Calibrated age (cal yr BP)
204	Poz-122518	205±30	256
424	Poz-121536	800±30	614
572	Poz-119332	825±30	792
778	Poz-119191	1545±30	1315

**Table 2.2** Radiocarbon dates of the LAA core

## 2.4.2 Pollen data

A total of 119 pollen and spore taxa were identified in the LAA core, including 21 unknown pollen and spore types. Important taxa are shown in the pollen diagram (Fig. 2.4a). The taxa that the maximum percentage throughout the core is lower than 2% (except Rhamnaceae/*Rhamnus* occupies 5.3% at the depth of 550 cm) are not shown in Fig. 2.4a, which can be seen in the full pollen diagram (Appendix I). The record was divided into four palynological zones (LAA-I to LAA-IV) based on the constrained cluster analysis on terrestrial pollen percentages, using CONISS (Grimm, 1987). Ranges of pollen concentration and accumulation rate are 15,000–87,000 grains cm<sup>-3</sup> and 5,000–33,000 grains cm<sup>-2</sup> yr<sup>-1</sup> in zone LAA-I, which are lower than 15,000–288,000 grains cm<sup>-3</sup> and 14,000–19,100 grains cm<sup>-2</sup> yr<sup>-1</sup> in zone LAA-II, III and IV (Fig. 2.4b).

### A. Zone LAA-I (800 – 585 cm, 1380 – 820 cal yr BP)

Palm tree pollen (5–33%) is mainly from *Mauritia flexuosa* (3–29%). Other palms such as *Iriartea* and *Euterpe/Geonoma* occur less frequently in this zone and the following zones. Tree and shrub pollen (11–83%) are dominant in this zone, mainly represented by Moraceae/Urticaceae (7–67%), except in the lowermost sample (11%) of the core. There are also many other tree and shrub taxa with low percentages (0–4%), such as *Alchornea*, *Acalypha*, *Celtis*, Melastomataceae, *Cecropia*, Fabaceae, *Trema*, *Zanthoxylum*, *Hedyosmum*, *Ficus*, *Luehea*. Malpighiaceae, *Mabea*, Sapindaceae, and *Salix*. Herb pollen (4–82%) is mainly represented by Cyperaceae (0–76%, with the highest percentage in the lowermost sample), Asteraceae (0–15%), and Poaceae (0–6%). Other herb taxa are very rare (<1%) throughout the entire core, including Amaranthaceae/Chenopodiaceae, *Ambrosia*, *Baccharis*, Caryophyllaceae, *Gomphrena*, *Pfaffia*, Iridaceae, Lamiaceae, Liliaceae, *Polygonum*, and Rubiaceae. Pollen grains from the Andes such as *Alnus*, *Clethra*, Ericaceae, and *Myrsine* are very rare throughout the entire core. Aquatic pollen such as *Hydrocotyle* and *Sagittaria* are very rare. Pteridophyta spore contribution is low (2–8%).

### B. Zone LAA-II (585 cm – 445 cm, 820 – 640 cal yr BP)

Values of palm pollen taxa are lower (3–31%) than in the lowest zone LAA-I, except *Mauritia* (21%) and *Euterpe/Geonoma* (10%) at the top sample of this zone. Other Arecaceae pollen is not found in this zone and the upper zones. The percentages of tree and shrub pollen overall decline compared with the lowest zone, but have relatively high values (18–44%), mainly represented by Moraceae/Urticaceae (10–34%). Some of the other tree and shrub taxa maintain the same values as in the previous zone, such

as *Alchornea*, *Acalypha*, and *Celtis*; others decline such as Melastomataceae (<2%), *Cecropia* (<1%), and *Hedyosmum* (<1%), but Sapindaceae (1–3%) slightly increases. The other tree and shrub pollen taxa are continuously very rare (<1%). Values of herb pollen are very high (21–78%), represented by Cyperaceae (16–77%) and Poaceae (0–5%). Asteraceae pollen (<1%) declines to a very low level. The amount of herb pollen declines at the end of this zone and remains rare in the following zones. Pteridophyta values are also very high (2–55%) due to the marked increase of monolete psilate types (2–54%). Other Pteridophyta spore types are rare (<1%), as well as the non-pollen palynomorphs (NPPs), *Gelasinospora*, and *Glomus*.

C. Zone LAA-III (445 cm – 225 cm, 640 – 300 cal yr BP)

This zone is characterized by a marked increase of *Mauritia flexuosa* pollen up to very high and constant values (75–89%), while other palm pollen taxa including *Iriarteia*, *Euterpe/Geonoma* are very rare (<2%). Tree and shrub pollen are continuously lower but still have relatively high values (10–22%), represented by Moraceae/Urticaceae (5–14%). Other tree and shrub pollen taxa, *Alchornea* (0–3%) maintain the same level as in the previous zones, while *Acalypha* and *Celtis* pollen decline (<1%). The other tree and shrub pollen taxa remain rare (<1%) and herb taxa are very rare. Pteridophyta spores (2–13%) decline to a pattern similar as in zone LAA-I, represented by Monolete psilate (0–4%) and *Hymenophyllum* (0–2%).

D. Zone LAA-IV (225 cm – 0 cm, 300 cal yr BP – present)

The uppermost zone is characterised by lower and fluctuating values of *Mauritia flexuosa* pollen (38–92%). Other palm pollen taxa remain rare (<2%). Tree and shrub pollen are more common and mainly represented by Moraceae (3–42%), which shows an opposite fluctuating trend to *Mauritia flexuosa*. *Alchornea*, *Acalypha*, *Celtis*, and Melastomataceae pollen increase to values (0–5%) comparable to zone LAA-II. *Hedyosmum* pollen (0–18%) shows very high values in the lower part of the zone. Other tree and shrub pollen taxa are very rare (<1%) as in the previous zones. Almost all herb pollen taxa are continuously rare (<6%). Only Poaceae slightly increase at the beginning of the zone (5%) and then decline again. Values of Pteridophyta spores are relatively high in the second half of the zone (3–26%), mainly consisting of monolete verrucate types (0–5%) and trilete psilate spores (0–13%). Other pteridophyta are rare in the lower half of the zone, except for *Hymenophyllum* which has a single maximum (12%).

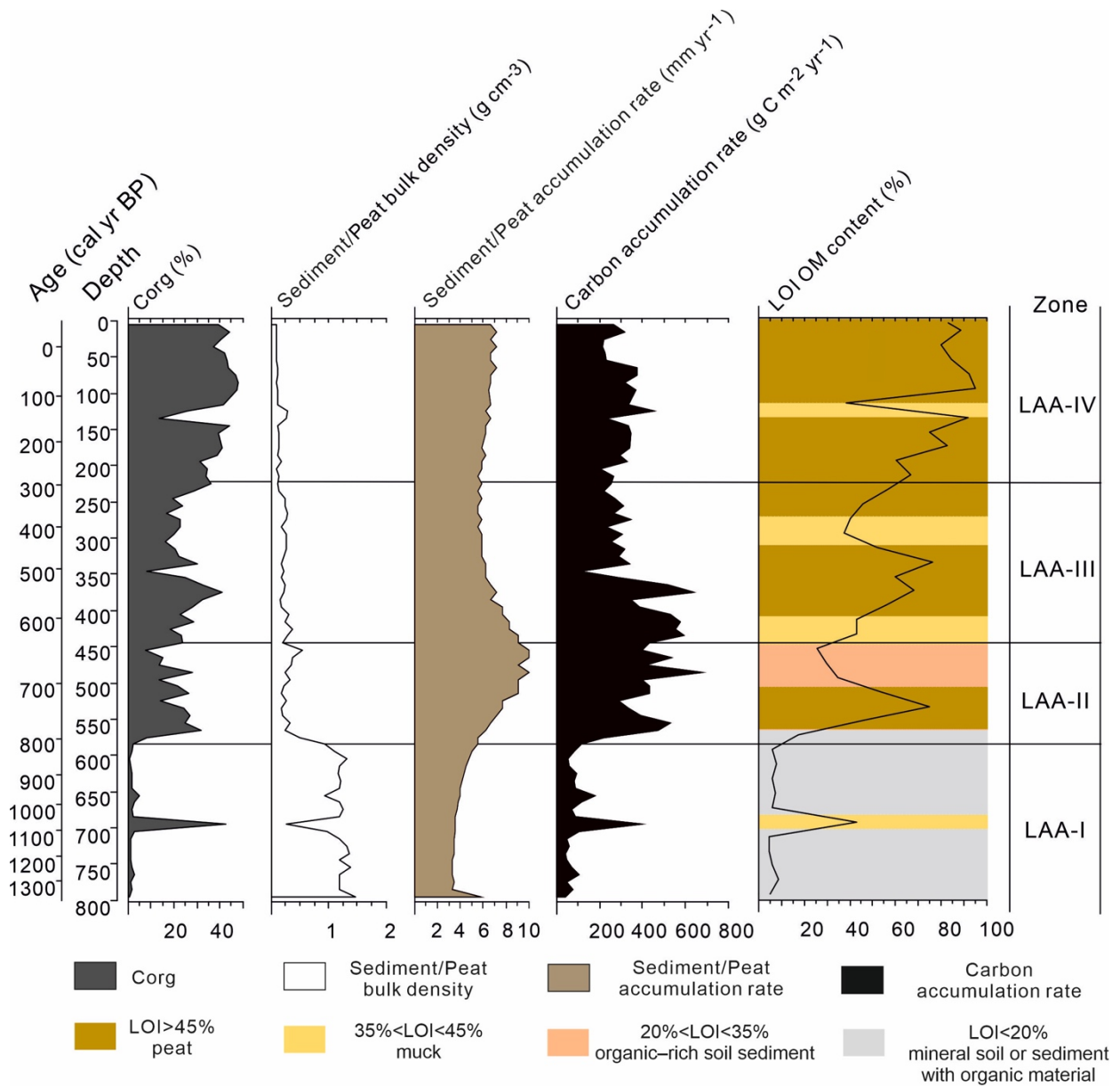
### 2.4.3 LOI and carbon data

LOI data (Fig. 2.3) show that the deposits of the LAA core can be classified according



to Wüst et al. (2003): as “mineral soil or sediment with organic material” (LOI<20%) from 800 to 565 cm core depth (1380–990 cal yr BP), except for a peak at 695 cm (1070 cal yr BP) with 43%, as “organic-rich soil sediment” (20%<LOI<35%) from 505 to 445 cm (700–640 cal yr BP) and as “muck” (35%<LOI<45%) from 705–685 cm (1100–1050 cal yr BP), 445–405 cm (640–590 cal yr BP), 305–265 cm (440–370 cal yr BP) and 125–105 cm (130–100 cal yr BP). All other sections are “peat” (LOI>45%) at the depth of 565–505 cm (990–700 cal yr BP), 445–305 cm (640–440 cal yr BP), 265–125 cm (370–130 cal yr BP) and 105–0 cm (100 cal yr BP to present).

The organic carbon percentage  $C_{org}$  (%), sediment/peat bulk density, sediment/peat and C accumulation rate, are shown in Fig. 2.3.  $C_{org}$  (%) is 1–3% from 800 to 585 cm (1380–820 cal yr BP), excluding a single maximum at 695 cm with 42.6%.  $C_{org}$  (%) is higher from 585 to 0 cm (820 cal yr BP–present) and varies from 7.4 to 47.9% (main=28.5%). The average sediment/peat bulk density is 1.2 g cm<sup>-3</sup> from 800 to 585 cm and 0.2 g cm<sup>-3</sup> from 585 to 0 cm. Sediment/Peat accumulation rate varies between 3.3 and 10 mm yr<sup>-1</sup> (mean=6.1 mm yr<sup>-1</sup>). C accumulation rate varies between 40.3 and 679.2 g m<sup>-2</sup> yr<sup>-1</sup> (mean=281.6 g m<sup>-2</sup> yr<sup>-1</sup>). The average C accumulation rate is 92.7 g m<sup>-2</sup> yr<sup>-1</sup> from 800 to 585 cm (1380–820 cal yr BP), 437.7 g m<sup>-2</sup> yr<sup>-1</sup> from 585 to 355 cm (820–520 cal yr BP), and 289 g m<sup>-2</sup> yr<sup>-1</sup> from 355 to 0 cm (520 cal yr BP to present).



**Fig. 2.3** Loss-on-ignition (LOI, classification based on Wüst et al. (2003)) and carbon content analysis results of the LAA core.

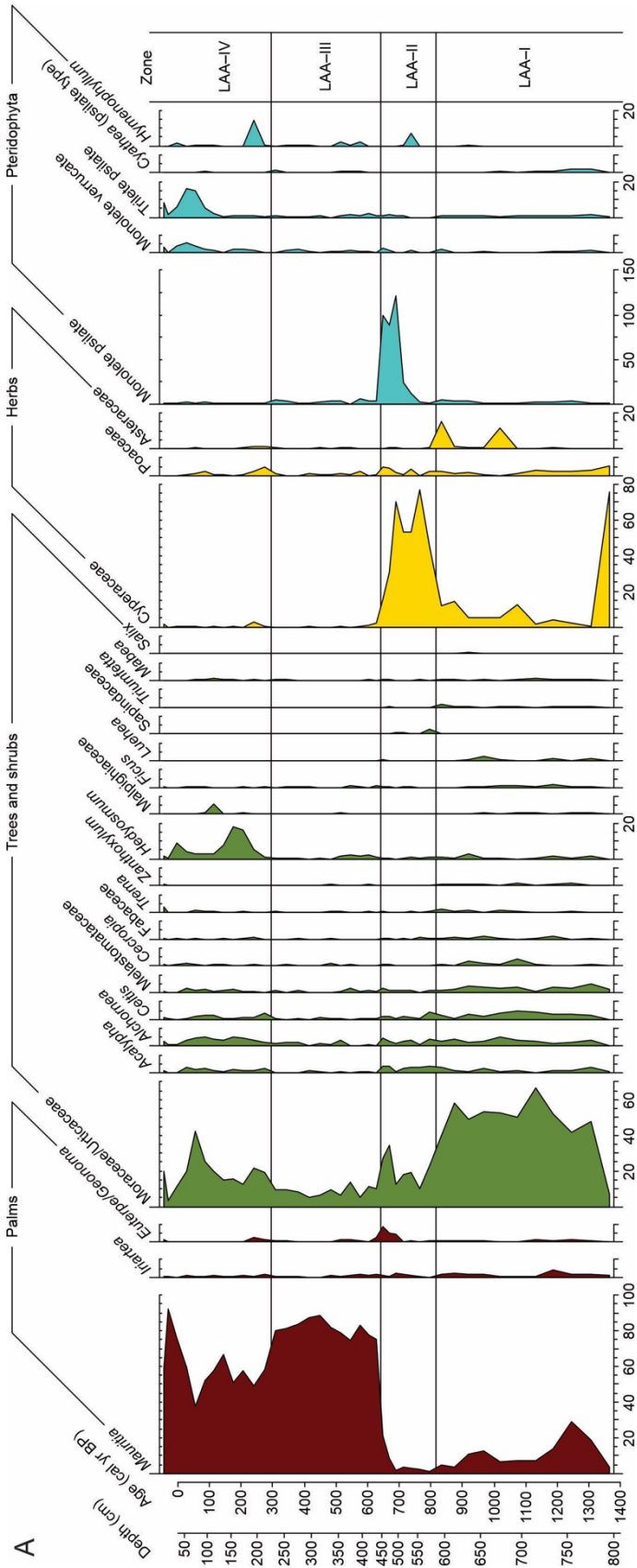
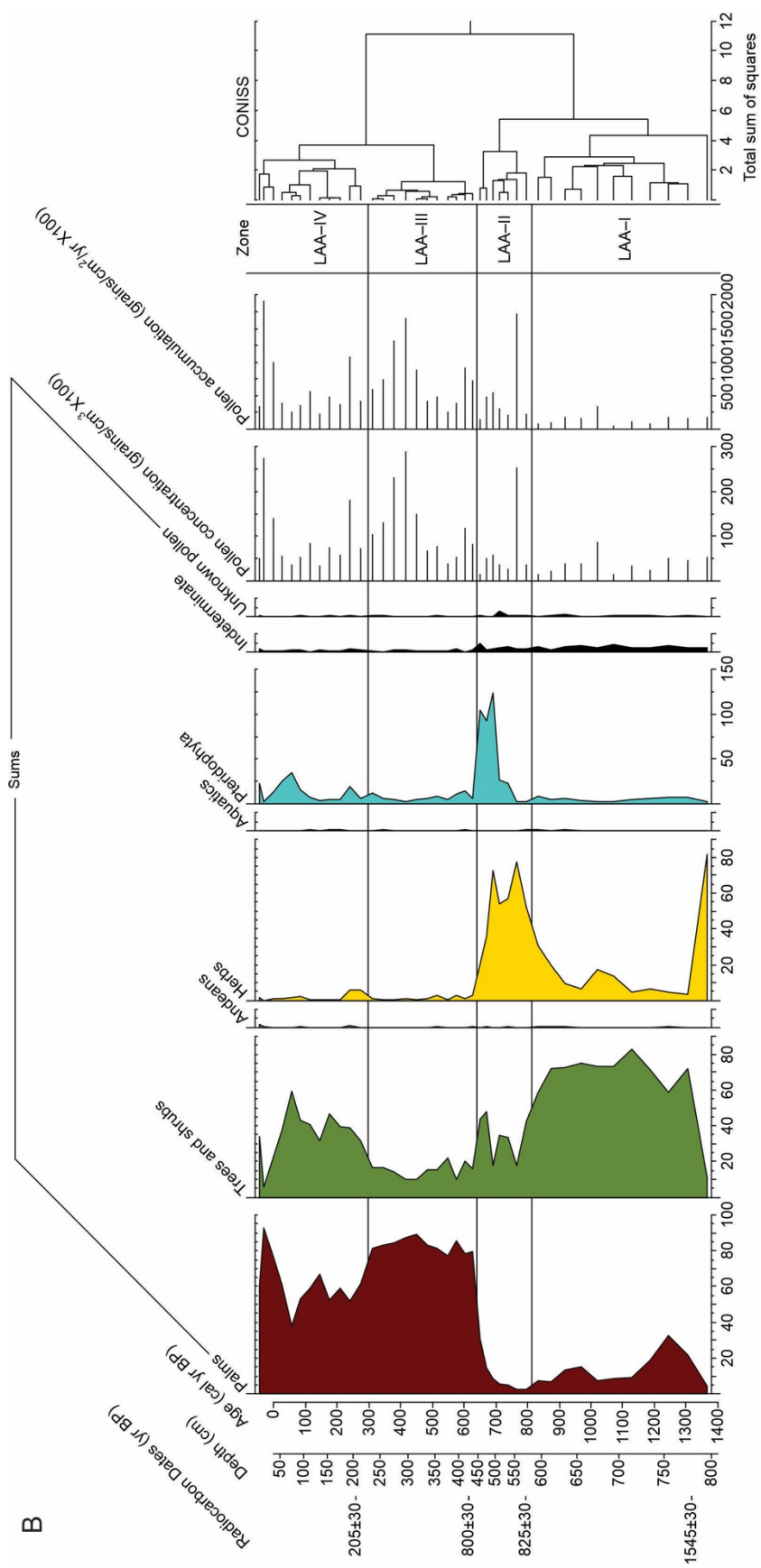


Fig. 2.4(A) Pollen diagram of the LAA core: Percentage diagram of single taxa..



**Fig. 2.4(B)** Pollen diagram of the LAA core: Summary diagram of the grouped pollen taxa, radiocarbon ages, age scale, as well as pollen zones and the CONISS dendrogram

## 2.5 Interpretation and Discussion

### 2.5.1 Late Holocene vegetation and environment as well as the development and dynamics of the aguajal

To interpret the results of the peat, C data (Fig. 2.3), and pollen data (Fig. 2.4), it is necessary to understand first the mechanism of peat and C accumulation in the tropics and the physiological characters of important plants. Net peat and C accumulation are the joint result of gross primary production (GPP), which adds organic materials, and ecosystem respiration (RE, the sum of plant respiration and peat decay) that releases organic materials. These processes are primarily controlled by the water table (Hirano et al., 2012) and to a lesser extent by the available oxygen concentration in the water that influences activities of aerobic bacteria that acts on soil decomposition. Other factors such as the ambient temperatures, humidity, river flooding, and human activities can also strongly influence peatlands (Roucoux et al., 2013; 2017; Lahteenoja et al., 2009a). The physiological characteristics of each important plant are explained in the following. The summary of the vegetation and environment changes is shown in Fig. 2.5.

#### A. Period of 1380 – 820 cal yr BP (800 – 585 cm, zone LAA-I)

In the period between 1380 and 820 cal yr BP, *Mauritia flexuosa* pollen which belongs to palm trees occupied a relatively small proportion in the pollen sum of LAA. It indicates that there might be some small area of *Mauritia* palms but the *aguajal* had not been established yet. This is further supported by low percentages of organic material (OM, 4–17%; Fig. 2.3) that indicates peat had not been formed yet at the coring site, considering tropical peat is defined as having >45% OM (Wüst et al., 2003). Pollen of trees and shrubs occupied the largest proportion in pollen sum of LAA. The frequent pollen types include Moraceae/Urticaceae (most frequent), *Alchornea* (Euphorbiaceae), *Acalypha* (Euphorbiaceae), *Celtis* (Ulmaceae/Urticaceae), Melastomataceae, *Cecropia* (Moraceae/Urticaceae). Even without species-specific vegetation information, the above families of plants frequently grow in *terra firme* that surround LAA at present. Moraceae and Melastomataceae also occur in LAA (report from Eva-Maria Sadowski, unpublished). It indicates that *terra firme* could be the main source of the tree and shrub pollen being transported by wind (while Moraceae and Melastomataceae could also locally from LAA itself). The pure clay sediment, which was a lacustrine deposition, in 800–573 cm (Fig. 2.2 and Table 2.1), indicates that the coring site could be open water (could be pool water from seepages that flow from *terra firme* and/or oxbow lake,

discussed in section 2.5.2) collecting the large proportion of tree and shrub pollen. It is unclear if the very high occurrence of Cyperaceae in only one sample at the base of the core indicates a small marsh or was caused by a fallen flower bud at the coring site. The few Andean pollen grains found in this and the following periods, such as *Alnus*, *Clethra*, Ericaceae, and *Myrsine*, suggest long-distance transport by air from the Andes. They may also be transported by river and deposited at the coring site which would indicate occasional flooding events.

*B. Period of 820 – 640 cal yr BP (585 – 445 cm, zone LAA-II)*

The high occurrence of Cyperaceae pollen and Pteridophyta spore later in this period indicates that the environment of the coring site had been changed from the open water in the period of zone LAA-I into a marsh. Concurrently, the sediment had changed from pure clay in 800–573 cm into peat with clay in 573–443 cm (Table 2.1). The clay could be laden by frequent river flooding (e.g. seasonal). It is supported by the LOI result (Fig. 2.3). OM>45% in the lower part of this period indicates the peat formation, but OM decreased to lower than 45% followed by a decrease in the C content during the time between 690 and 640 cal yr BP despite a high accumulation rate, which may indicate the OM was admixed with allochthonous sediment transported from the river. The deposition mixed with more clay (clayey peat) in the upper part of this period than in the lower part (Fig. 2.2, Table 2.1), indicates the more frequency of river flooding between 690–640 cal yr BP. *Mauritia flexuosa* and *Euterpe/Geonoma* palm pollen occurred in small proportions but started to increase-at the end of this period (670–640 cal yr BP) indicating the beginning of the establishment of the peatland palm swamp. The abundance of ferns infers that the canopy at the beginning of the peatland palm swamp was quite open. This interpretation is supported by the presence of *Euterpe/Geonoma*, characteristic of open palm forests (Kahn and De Granville, 1992; Marchant et al., 2002). The marked decrease of the *terra firme* forest species pollen percentages compared with the period of zone LAA-I, particularly of Moraceae/Urticaceae, may be because of the strong local input of Cyperaceae pollen reducing the proportion of pollen that transported from *terra firme*.

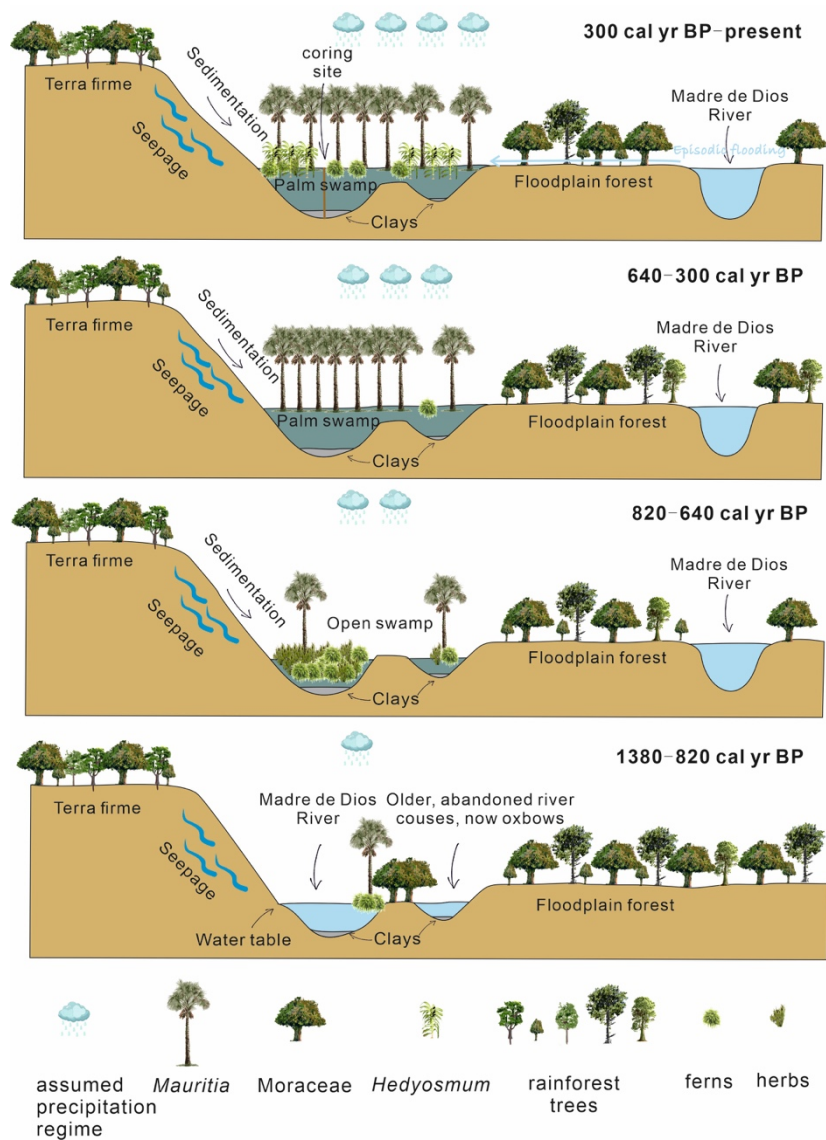
*C. Period of 640 – 300 cal yr BP (445 – 225 cm, zone LAA-III)*

In this period, Cyperaceae pollen and Pteridophyta spore decreased to occupy very small proportions. *Mauritia flexuosa* palm pollen increased rapidly and became the dominant taxa. Since *Mauritia* pollen is typically dispersed only locally, which means its presence in sediment is almost restricted to where this palm is growing (Rull, 1998). Therefore, it can be assumed that the presence of *Mauritia* pollen indicates the presence of *Mauritia* communities at the time of deposition, and its pollen abundance is a reliable

indicator of its population density (Rull, 1998). This suggests that the environment at the coring site had been changed from a marsh in the period in zone LAA–II into a mature *Mauritia* palm swamp (*aguajal*). The rare occurrence of herbs, ferns, and the decline of *Euterpe/Geonoma* suggest that the canopy of the *aguajal* was closed. The interpretation that *aguajal* had been formed since around 640 cal yr BP can be supported by the clay influx was absent above 443 cm (Fig. 2.2, Table 2.1), while OM>45% (Fig. 2.2 and 2.3) that indicates peat accumulated continuously (Wüst et al., 2003). It also indicates the flooding that was frequent in the period of zone LAA–II became rare in this period. This period could be divided into two phases with 520 cal yr BP as the threshold for the OM and C content as well as peat and C accumulation rates. Before 520 cal yr BP (335 cm), OM and C content had increasing trends, while the peat and C accumulation rates were as high as in the period represented by zone LAA II. After 520 cal yr BP, the OM and C content as well as peat and C accumulation rates changed to be lower and stable, but still at relatively high levels. This may indicate that the water table fluctuated allowing the acceleration of the OM decomposition.

*D. Period of 300 cal yr BP – present (225 cm – 0 cm, zone LAA–IV)*

In the most recent period, *Mauritia flexuosa* remained to be the dominant species of the *aguajal* but became mixed with other low-statured and more typical humid montane species such as *Hedyosmum* and ferns (Fig. 2.4a). It indicates that the canopy density of the *aguajal* reduced. The increase of Moraceae/Urticaceae pollen can be explained by its anemophilous character, that increase when the canopy of the *aguajal* was more open. OM values were higher than in all previous periods varying between 60% and 95% with slight fluctuations, except one sample with the value of 38% at 115 cm depth corresponding to the sandy layer at 125–137 cm (Fig. 2.2, Table 2.1) that may indicate an occurrence of high energy flood event/events. Peat and C accumulation rates and C content are also slightly higher than in 520–300 cal yr BP. The relatively stable OM, and slightly higher peat and C accumulation rates as well as C content, may suggest a more or less stable water table and even less river flooding than in 640–300 cal yr BP.



**Fig. 2.5** Summary of the C accumulation and vegetation dynamics about the changes in the environment. From left to right: *terra firme*, dense *aguajal*, open *aguajal*, floodplain forest, Madre de Dios River, which is consistent with the transect in figure 2.1B from northwest to southeast. The switch in the active river channel course from left in 1380–820 cal yr BP to right after 820 cal yr BP shows the process that the river changed its course entirely by cutting through the narrow end of the meander. Consequently, the deep river channel at the escarpment (the left basin in the drawing, corresponding to the northwest in figure 2.1A) was suddenly abandoned and the river main course switched its course to the present situation running along the right side of the *aguajal* (southeast in figure 2.1A) today. The right basin is nowadays an open *aguajal*. The organic matter depth is less than at the coring site. Most likely the right basin is shallower because it reflects an even older stage of the main river course when the river was directly cutting into the escarpment (i.e. the river course eroded the escarpment and gradually moved toward the left side of the drawing before changing its course to the present situation).



## 2.5.2 Factors influencing changes in vegetation, peat, and carbon accumulation

The main changes during the recorded past 1380 years include (Fig. 2.3, 2.4, 2.5), (1) at 820 cal yr BP, the onset of peat and C accumulation, and concurrently the environmental change from open water (Moraceae/Urticaceae dominated in pollen sum) to a marsh (Cyperaceae and Pteridophyta dominated); (2) at 640 cal yr BP, the beginning of the *aguajal* development (*Mauritia flexuosa* dominated) without changes of peat and C accumulation rates; (3) at 520 cal yr BP, a decrease of peat and C accumulation rates without vegetation changes; (4) the vegetation change at 300 cal yr BP, with fluctuations in the proportion of the dominant *Mauritia flexuosa* palms, which lagged (3) for about 220 years.

The LAA is one of typical peatlands in the Madre de Dios region (Fig. 2.1), which are generally located along meandering rivers with one side abutted by steep-faced terrace escarpments (*terra firme*) (Householder et al., 2012). This kind of peatlands was formed often by numerous small and perennial seepages flowing through the cracks in the thick unconsolidated sediment of the *terra firme* and emerging at the interface of the *terra firme* and the blue/grey clay foundation (Ipururu basement) (Campbell et al. 2006; Householder et al., 2012). Considering that the Ipururu basement is impervious, the drainage is poor (Householder et al., 2012), which provides the conditions for the peat and C accumulation. Available Peruvian records from lowlands and the Altiplano indicate a relatively dry climatic condition between 1380 and 820 cal yr BP (Thompson et al., 1986; Rowe et al., 2002; Baker et al., 2005; Bird et al., 2011a, 2011b; Kelly et al., 2017; Swindles et al., 2018). In the lowlands of northern Peru, two dome peatlands in the floodplains recorded the drought event in the period represented by zone LAA I, based on the apparent peat accumulation hiatus at ca. 1800–1100 cal yr BP (Swindles et al., 2018) and the very slow peat accumulation at ca. 1300–400 cal yr BP (Kelly et al., 2017). In the altiplano of Peru, Lake Pumacocha (670 km northwest of LAA) recorded a dry period in 1500–900 cal yr BP that was interpreted to respond to the northward displacement of the Intertropical Convergence Zone (ITCZ, Bird et al., 2011a, 2011b). The record of Quelccaya Ice Cap (150 km southwest of LAA) shows a similar but less pronounced dry period than documented in the Pumacocha record (Thompson et al., 1986; Bird et al., 2011a). Like the Pumacocha record, Lake Titicaca (400 km south of LAA), located at 3810 m elevation near the boundary of Bolivia and Peru recorded a relatively dry event at 1500 cal yr BP, that corresponds to the Bond event 1 (Rowe et al., 2002; Baker et al., 2005; Bond et al., 2001). These dry climatic

records in around 1380–820 cal yr BP indicate that the climate is relatively wet before and after. The relatively wet climate after 820 cal yr BP, which is the beginning of the marsh, may have caused an increase of the water table of the Madre de Dios River that descends from the Andes, which then promoted the peat initiation. Alternatively, the LAA could have developed from an oxbow lake that originated from a river channel cut-off, which is supported by the grey clay deposited in the period between 1380 and 820 cal yr BP (Fig. 2.2, Table 2.1). River levees are naturally established by the sediment deposited on the banks of both sides of the river course when the flooding happened, which are numerous in the Madre de Dios region (Householder et al., 2012). The higher bank could hold more water and to some extent prevent the influence of river flooding, which may help to produce a water-logged environment prompting the initiation of peat and C accumulation. However, there are no traces of river levees surrounding the LAA. The river levees could have been destroyed by a high-energy river flooding, but it is unlikely considering that the lateral migration of the Madre de Dios River was unidirectionally toward the south during the past millennia (Räsänen et al. 1987) and, that Madre de Dios River today and the traces of the ancient river channel are located to the south of LAA (Fig. 2.1a), the influences of river flooding should have been less.

The environment of LAA changed from a marsh to a *Mauritia flexuosa* palm swamp at 640 cal yr BP (Fig. 2.4, 2.5). The absence of visible clay sediment (fluvial sedimentation) indicates a reduced sediment-carrying river flooding (e.g. frequency, degree, duration) around that period. The decreased flooding resulted in a stable water table hence promoting *aguajal* development.

At 520 cal yr BP, peat and C accumulation rates decreased (Fig. 2.3), while the *aguajal* vegetation remained somewhat stable (Fig. 2.4, 2.5). The slow-down in peat accumulation could be explained by water table changes (lead to GPP in the soil decreased and/or RE increased), a reduction in plant productivity, human disturbance (such as slash and burn activities), and river flooding (may lead to peat erosion). The higher pollen accumulation (Fig. 2.4b) and the maintained mature *aguajal* vegetation exclude the possibility of decreasing plant productivity. According to personal communication by locals, human interference was very little until the past years when gold dredging commenced in the neighborhood. River flooding could be excluded from the possible influencing factors as the discussion in section 2.5.1.C. Therefore, the changes in the water table could be the possible explanation for the decreasing of peat and C accumulation at 520 cal yr BP. In general, the water table of peatlands depends on the rate of inflow vs. outflow which may be influenced by climate. The climate

records from the nearby Andes Altiplano show a moisture increase. For example, the Lake Pumacocha record (670 km northwest of LAA) shows a wet period between 550–130 cal yr BP (Bird et al., 2011a), and the ice core data from Quelccaya Ice Cap (150 km southwest of LAA) shows that 450–230 cal yr BP was the wettest period during the last 1000 years (Thompson et al., 1986). Kelly et al. (2014) simulated and calculated water balance at the three peatlands (Quistococha, San Jorge, and Buena Vista) in northern Peru. The simulation suggests that the large amount of water entering Amazonian peatlands via rainfall generally does not leave the system as groundwater flow but rather as surface flow or by evapotranspiration, under the current climate conditions (Kelly et al., 2014). From an airborne Lidar transect overflight, it was noticed that a small area of organic sediment in the center of LAA is slightly above the mean water table. This might be due to a high sandbank underlying the center region and may increase the surface flow from the central region to the margin of the *aguajal*. Probably, the combination of the increase of surface outflow that made the water table decline and the wetter climate that made the water table rise following the more frequent rainfall events may have led to water table fluctuation, as well as an increased input of oxygen-rich rainwater allowing more oxygen to come into the soil speeding up the decay of organic material.

After 300 cal yr BP, the water table became more or less stable indicated by the OM, peat, and C accumulation data (Fig. 2.3, section 2.5.1.D). The vegetation changed to a mixed *Mauritia-Hedyosmum* swamp with ferns, indicating the vegetation became more diverse and with a more open canopy (Fig. 2.4a, 2.5). *Hedyosmum* is known as a typical montane genus that commonly occurs in cool and moist environments, especially in the foothills of the Andes today (Antonelli and Sanmartín, 2011). The strong occurrence of *Hedyosmum* indicates that the climate possibly became cooler and very humid in this period. Nevertheless, so far, no climate record supports that interpretation. Moreover, Householder et al. (2015) investigated the modern taxonomic composition of seven peatlands in Madre de Dios including the swamp of the LAA core, and they found that montane taxa represent a major component of peatland vegetation. Such pattern, so-called “montane bias” was interpreted as habitat tracking of a conserved (ancestral) montane niche on a heterogeneous lowland landscape which could be explained by the high moisture availability and stressful edaphic conditions for peatland habitats (Householder et al., 2015). This provides a possible explanation of the strong occurrence of *Hedyosmum* in the most recent period of LAA and it may suggest that montane bias has occurred since ca. 300 cal yr BP.

### 2.5.3 Comparison with *aguajales* in northern Peru

In this study, we provide the first palynological and peat and carbon accumulation record from the *Mauritia* palm swamp in southern Peru. A comparison with *aguajales* in northern Peru can help to explore potential similar or different long-term development trajectories including vegetation succession and peat and C accumulation for southern and northern Peru. It can reveal whether the controlling factors of *aguajales* development in Peru are regional (refer to the whole of Peru or southern/northern Peru) or local.

#### A. *Vegetation successions*

Contemporaneously with LAA (in the last ca. 1400 years), the vegetation that is shown by the pollen data of the permanently waterlogged *aguajal* in Quistococha “QT”, which is located at the edge of the Amazon floodplain in northern Peru, was seasonally flooded woodland at ca. 1500 cal yr BP lasted ca. 370 years (QT–4c in Roucoux et al., 2013) dominated by Myrtaceae undiff. (22%) and Melastomataceae (9%). The vegetation changed to an opening up of the woodland with the establishment of herbaceous taxa at ca. 1100 cal yr BP lasted ca. 110 years, which was dominated by Poaceae (34%), Cyperaceae (9%), Rubiaceae undiff. (10%) and *Mauritia* t. (9%) (QT–4d in Roucoux et al., 2013), after that *Mauritia* t. (up to 84%) expanded at ca. 1000 cal yr BP and remained to present (QT–5 and QT–6 in Roucoux et al., 2013). In the same period that LAA covered, the vegetation that is shown by the pollen data of the *aguajal* of San Jorge “SJ” bordering the Amazon River towards the north-eastern margin of the PMFB in northern Peru, was a marginal and/or floating mat in the period between 1920 and 650 cal yr BP, which dominated by herbaceous plants (Cyperaceae, Poaceae) and aquatic plant (*Pistia stratiotes*) (SJ–3 in Kelly et al., 2017), after that *Mauritia* t. expanded at ca. 650 cal yr BP and remained to present (SJ–4 and SJ–5 in Kelly et al., 2017). Comparing LAA core with the two records of QT and SJ (Roucoux et al., 2013; Kelly et al., 2017), QT and SJ experienced more complex vegetation succession than LAA. It indicates a variety of vegetation succession among sequences in Peru, which further illustrates that the controlling factor of vegetation change in Peru is not regional. Some significant common points among LAA, QT, and SJ are (1) there was a period of herbaceous taxa (e.g., Cyperaceae, Poaceae) increase before the latest expansion of *Mauritia*, the vegetation pattern of SJ in that period was interpreted as marginal and/or floating mat which is similar with LAA; (2) the timing of the beginning of the latest *Mauritia* expansion were similar (ca. 1000 cal yr BP); (3) they have similar geomorphology, which is a river on one side and terrace on the other side; (4) they all

probably developed from a cut off from the river. The common point (1) illustrates that it is not an accidental event that experienced a period of likely floating mat before *aguajales* development in Peru. Point (2) does not fit all the *aguajales* in Peru, for example, an *aguajal* in Aucayacu, which is located 100–150 km to the west of Quistococha, started to develop at ca. 4000 cal yr BP (Swindle et al., 2017). Point (3) may indicate that peat accumulation often occurred in the places of this kind of geomorphology. Combining the difference of timing of cut-off in QT, SJ, and LAA, with the different vegetation succession of the three sites, point (4) suggests that vegetation succession of Peruvian peatlands might be strongly influenced by the fluvial dynamics (e.g., cut off) in local.

#### B. Peat and carbon accumulation rate

For the nutrient-poor minerotrophic *aguajal* (not convex dome, Lahteenoja et al., 2009b) in Quistococha in northern Peru, peat began to accumulate at ca. 2200 cal yr BP (LOI>45% shown by in Roucoux et al., 2013), peat and C accumulation rates were 1.4–3.3 mm yr<sup>-1</sup> (Roucoux et al., 2013) and 45–125 g m<sup>-2</sup> yr<sup>-1</sup> (Lahteenoja et al., 2009a). For the ombrotrophic *aguajal* (convex dome) in San Jorge in northern Peru (Lahteenoja et al., 2009b), peat began to accumulate between around 2200 to 2400 cal yr BP, with accumulation rate varying between 1.4 to 2 mm yr<sup>-1</sup> except the period between 1300 and 400 cal yr BP with only 0.4 mm yr<sup>-1</sup> peat accumulation rate (Kelly et al., 2017), the C accumulation rate varied between 57–195 g m<sup>-2</sup> yr<sup>-1</sup> (Lahteenoja et al., 2009a). In the last millennium in the two sites above, peat and C accumulation rates were 1.77 mm yr<sup>-1</sup> and 74 g m<sup>-2</sup> yr<sup>-1</sup> in Quistococha and, 1.45 mm yr<sup>-1</sup> and 62 g m<sup>-2</sup> yr<sup>-1</sup> in San Jorg (Lahteenoja et al., 2009a). Swindle et al. (2017) studied peat and C accumulation rates in an ombrotrophic *aguajal* in Aucayacu. The result shows that the peat accumulated during the last 7000 years, peat and C accumulation rates were 0.05–18.2 mm yr<sup>-1</sup> (mean=1.88 mm yr<sup>-1</sup>) and 18–495.7 g m<sup>-2</sup> yr<sup>-1</sup> (mean=70.8 g m<sup>-2</sup> yr<sup>-1</sup>) respectively. In the last millennium, the maximum of peat and C accumulation rates were ca. 10 mm yr<sup>-1</sup> and ca. 400 g m<sup>-2</sup> yr<sup>-1</sup>, respectively (Swindle et al., 2017). Comparison with the above three *aguajales* in northern Peru, the peat and C accumulation rates in LAA (section 2.4.3) in southern Peru were ca. 4 mm yr<sup>-1</sup> and ca. 200 g m<sup>-2</sup> yr<sup>-1</sup> faster than QT and SJ records but were similar with the *aguajal* in Aucayacu in the last millennium. It indicates that peat and C accumulation rates in southern Peru were fast, similar to a few sites in northern Peru, which further suggests that the controlling factor of the peat and C accumulation rates could be a local condition.

## 2.6 Summary and Conclusion

For the first time, the palaeoecological environment of a *Mauritia flexuosa* palm swamp (*aguajal*) which can be an important carbon sink has been studied in southern Peru. The results of the LAA study show that the development of the *aguajal* occurred in four phases: (1) shallow water on the impervious substrate or in an abandoned river oxbow located next to a steep escarpment between *terra firme* (upland) rainforest and floodplain forests (1380–820 cal yr BP), (2) development of an open Cyperaceae swamp (820–640 cal yr BP), (3) a *Mauritia flexuosa* palm swamp (640–300 cal yr BP), and (4) an open canopy and mixed-species *Mauritia flexuosa* palm swamp (300 cal yr BP to present). There are two main changes of peat and C accumulation rates: (1) onset of peat and C accumulation at 820 cal yr BP, (2) of peat and C accumulation after 520 cal yr BP.

We compared our results with other palaeoecological records in *aguajales* in northern Peru. It shows that the dynamics of *aguajales* in Peru were different. The peat and C accumulation rates in southern Peru (LAA) were ca. 4 mm yr<sup>-1</sup> and ca. 200 g m<sup>-2</sup> yr<sup>-1</sup> faster, similar to a few sites in northern Peru. Analyzing dynamics of *aguajales*, which is a kind of typical peatlands in Amazonia, and comparing among different sites allows exploration and prediction of the regional peatlands' development in the future under the potential impact of natural changes.

## Author Contributions

**Bowen Wang:** Formal analysis, Investigation, Writing-Original Draft, Funding acquisition. **Hapsari Kartika Anggi:** Conceptualization, Review & Editing, Supervision. **Viviana Horna:** Conceptualization, Review & Editing, Resources (core collecting). **Reiner Zimmermann:** Conceptualization, Review & Editing, Resources (core collecting). **Hermann Behling:** Conceptualization, Funding acquisition, Review & Editing, Supervision

## Acknowledgments

This study was partly supported by the German Research Foundation (BE-2116/32-1) and the China Scholarship Council (CSC No. 201906190215; for B.W.). We thank Dorothee Dasbach (Chemielabor, ZMT Bremen) for laboratory supports.

## References

- Antonelli, A., Sanmartín, I., 2011. Mass extinction, gradual cooling, or rapid radiation? Reconstructing the spatiotemporal evolution of the ancient angiosperm genus *Hedyosmum* (Chloranthaceae) using empirical and simulated approaches. *Systematic Biology* 60, 596–615.
- Balslev, H., Laumark, P., Pedersen, D., Grández, C., 2016. Tropical rainforest palm communities in Madre de Dios in Amazonian Peru. *Revista Peruana de Biología* 23, 003–0012.
- Baker, P.A., Fritz, S. C., Garland, J., Ekdahl, E., 2005. Holocene hydrologic variation at Lake Titicaca, Bolivia/Peru, and its relationship to North Atlantic climate variation. *Journal of Quaternary Science* 20, 655–662.
- Bird, B.W., Abbott, M.B., Vuille, M., Rodbell, D.T., Stansell, N.D., Rosenmeier, M.F., 2011a. A 2,300-year-long annually resolved record of the South American summer monsoon from the Peruvian Andes. *Proceedings of the National Academy of Sciences* 108, 8583–8588.
- Bird, B.W., Abbott, M.B., Rodbell, D.T. and Vuille, M., 2011b. Holocene tropical South American hydroclimate revealed from a decadal resolved lake sediment  $\delta^{18}\text{O}$  record. *Earth and Planetary Science Letters* 310, 192–202.
- Blaauw, M., 2010. Methods and code for 'classical' age-modelling of radiocarbon sequences. *Quaternary Geochronology*. 5, 512–518
- Bond, G., Kromer, B., Beer, J., Muscheler, R., Evans, M. N., Showers, W., Hoffmann, S., Lotti-Bond, R., Hajdas, I., Bonani, G., 2001. Persistent solar influence on North Atlantic climate during the Holocene. *Science* 294, 2130–2136.
- Campbell, K.E., Frailey, C.D., Romero-Pittman, L., 2006. The pan-amazonian Ucayali peneplain, late neogene sedimentation in Amazonia, and the birth of the modern Amazon river system. *Palaeogeography, Palaeoclimatology, Palaeoecology* 239, 166–219.
- Colinvaux, P. A., De Oliveira, P. E., & Moreno, E., 1999. Amazon: pollen manual and atlas, Harwood Academic Publishers, Amsterdam.
- Dise, N.B., 2009. Peatland response to global change. *Science* 326, 810–811.
- Draper, F.C., Roucoux, K.H., Lawson, I.T., Mitchard, E.T., Coronado, E.N.H., Lähteenoja, O., Montenegro, L.T., Sandoval, E.V., Zarát, R., Baker, T.R., 2014. The distribution and amount of carbon in the largest peatland complex in Amazonia. *Environmental Research Letters* 9, 124017.
- Eva-Maria Sadowski, Vegetationsaufnahmen in *Mauritia*-Sümpfen und einem Terra Firme Wald im Amazonastiefland der Region Madre de Dios im Südosten Perus
- Fægri, K., and Iversen, J., 1989. *Textbook of Pollen Analysis*, fourth ed. Wiley, Chichester, pp.67–89.
- Grimm, E.C., 1987. CONISS: a FORTRAN 77 program for stratigraphically constrained cluster analysis by the method of incremental sum of squares. *Computer Geosciences* 13, 13–35.

- Hapsari, K.A., Biagioni, S., Jennerjahn, T.C., Reimer, P.M., Saad, A., Achnopha, Y., Sabiham, S. and Behling, H., 2017. Environmental dynamics and carbon accumulation rate of a tropical peatland in Central Sumatra, Indonesia. *Quaternary Science Reviews* 169, 173–187.
- Heiri, O., Lotter, A. F., Lemcke, G., 2001. Loss on ignition as a method for estimating organic and carbonate content in sediments: reproducibility and comparability of results. *Journal of paleolimnology* 25, 101–110.
- Hirano, T., Segah, H., Kusin, K., Limin, S., Takahashi, H., Osaki, M., 2012. Effects of disturbances on the carbon balance of tropical peat swamp forests. *Global Change Biology* 18, 3410–3422.
- Hogg, A.G., Hua, Q., Blackwell, P.G., Niu, M., Buck, C.E., Guilderson, T.P., Heaton, T.J., Palmer, J.G., Reimer, P.J., Reimer, R.W., Turney, C.S.M., Zimmerman, S.R.J., 2013. SHCal13 southern hemisphere calibration, 0–50,000 cal BP. *Radiocarbon*. 55, 1889–1903.
- Householder, J.E., Janovec, J.P., Tobler, M.W., Page, S., Lähteenoja, O., 2012. Peatlands of the Madre de Dios River of Peru: distribution, geomorphology, and habitat diversity. *Wetlands* 32, 359–368.
- Householder, J.E., Wittmann, F., Tobler, M.W., Janovec, J.P., 2015. Montane bias in lowland Amazonian peatlands: Plant assembly on heterogeneous landscapes and potential significance to palynological inference. *Palaeogeography, Palaeoclimatology, Palaeoecology* 423, 138–148.
- Gumbrecht, T., Roman-Cuesta, R. M., Verchot, L., Herold, M., Wittmann, F., Householder, E., Herold, N., Murdiyarso, D., 2017. An expert system model for mapping tropical wetlands and peatlands reveals South America as the largest contributor. *Global change biology* 23, 3581-3599.
- Jowsey, P.C., 1966. An improved peat sampler. *New Phytologist*. 65, 245–248.
- Kahn, F., De Granville, J.J., 1992. Palms in the Forest Ecosystems of Amazonia. Springer, Berlin, pp.130 and 107.
- Kelly, T.J., Baird, A.J., Roucoux, K.H., Baker, T.R., Honorio Coronado, E.N., Ríos, M. and Lawson, I.T., 2014. The high hydraulic conductivity of three wooded tropical peat swamps in northeast Peru: measurements and implications for hydrological function. *Hydrological Processes* 28, 3373–3387.
- Kelly, T.J., Lawson, I.T., Roucoux, K.H., Baker, T.R., Jones, T.D., Sanderson, N. K., 2017. The vegetation history of an Amazonian domed peatland. *Palaeogeography, Palaeoclimatology, Palaeoecology* 468, 129–141.
- Lähteenoja, O., Ruokolainen, K., Schulman, L., Oinonen, M., 2009a. Amazonian peatlands: an ignored C sink and potential source. *Global Change Biology* 15, 2311–2320.
- Lähteenoja, O., Ruokolainen, K., Schulman, L., Alvarez, J., 2009b. Amazonian floodplains harbour minerotrophic and ombrotrophic peatlands. *Catena* 79, 140–145.
- Lähteenoja, O., Reategui, Y.R., Räsänen, M., Torres, D.D.C., Oinonen, M., Page, S.,



2012. The large Amazonian peatland carbon sink in the subsiding Pastaza–Marañón foreland basin, Peru. *Global Change Biology* 18, 164–178.
- Malhi, Y, Roberts, J.T, Betts, R.A, Killeen, T.J, Li, W, Noble, C.A., 2008. Climate Change, Deforestation and the Fate of the Amazon. *Science*, 319, 169–172
- Mayle, F.E., Burbridge, R., Killeen, T.J., 2000. Millennial-scale dynamics of southern Amazonian rain forests. *Science* 290, 2291–2294.
- Marchant, R., Almeida, L., Behling, H., Berrio, J.C., Bush, M., Cleef, A., Duivenvoorden, J., Kappelle, M., De Oliveira, P., Teixeira de Oliveira-Filho, A., Lozano-García, S., Hooghiemstra, H., Ledru, M.-P., Ludlow-Wiechers, B., Markgraf, V., Mancini, V., Paez, M., Prieto, A., Rangel, O., Salgado-Labouriau, M.L., 2002. Distribution and ecology of parent taxa of pollen lodged within the Latin American Pollen Database. *Review of Palaeobotany and Palynology* 121, 1–75.
- Nebel, G., Kvist, L.P., Vanclay, J.K., Christensen, H., Freitas, L., Ruiz, J., 2001. Structure and floristic composition of flood plain forests in the Peruvian Amazon: I. Overstorey. *Forest ecology and Management* 150, 27–57.
- Page, S.E., Rieley, J.O., Banks, C.J., 2011 Global and regional importance of the tropical peatland carbon pool. *Global Change Biology* 17, 798–818.
- Puhakka, M., Kalliola, R., Rajasilta, M., Salo, J., 1992. River types, site evolution and succesionall vegetation patterns in Peruvian Amazonia. *Journal of Biogeography* 19, 651–665.
- Räsänen M, Salo J, Kalliola R., 1987. Fluvial perturbation in the western amazon basin: regulation by long term sub-andean tectonics. *Science* 238, 1398–1401.
- Roubik, D. W., Moreno, J. E., 1991. Pollen and Spores of Barro Colorado Island, Vol. 36, Missouri Botanical Garden, the United States.
- Roucoux, K.H., Lawson, I.T., Jones, T.D., Baker, T.R., Honorio Coronado E.N., Gosling W.D., Lähteenoja O., 2013. Vegetation development in an Amazonian peatland. *Palaeogeography, Palaeoclimatology, Palaeoecology* 374, 242–255.
- Roucoux, K.H., Lawson, I.T., Baker, T.R., Del Castillo Torres, D., Draper, F.C., Lähteenoja, O., Gilmore, M.P., Honorio Coronado, E.N., Kelly, T.J., Mitchard, E.T.A., Vriesendorp, C.F., 2017. Threats to intact tropical peatlands and opportunities for their conservation. *Conservation Biology* 31, 1283–1292.
- Rowe, H. D., Dunbar, R. B., Mucciarone, D. A., Seltzer, G. O., Baker, P. A., Fritz, S., 2002. Insolation, moisture balance and climate change on the South American Altiplano since the Last Glacial Maximum. *Climatic Change* 52, 175–199.
- Rull, V., 1998. Biogeographical and evolutionary considerations of *Mauritia* (Arecaceae), based on palynological evidence. *Review of Palaeobotany and Palynology* 100, 109–122.
- Swindles, G.T., Morris, P.J., Whitney, B., Galloway, J.M., Gałka, M., Gallego-Sala, A., Macumber, A.L., Mullan, D., Smith, M.W., Amesbury, M.J., Roland, T.P., Sanei, H., Patterson, R. T., Sanderson, N., Parry, L., Charman D.J., Lopez, O., Valderamma, E., Watson, E.J., Ivanovic, R.F., Valdes, P.J., Turner, T.E.,

- Lähteenoja, O., 2018. Ecosystem state shifts during long-term development of an Amazonian peatland. *Global Change Biology* 24, 738–757.
- Thieme, M., Lehner, B., Abell, R., Hamilton, S.K., Kellndorfer, J., Powell, G., Riveros, J.C., 2007. Freshwater conservation planning in data-poor areas: an example from a remote Amazonian basin (Madre de Dios River, Peru and Bolivia). *Biological Conservation* 135, 484–501.
- Thompson, L.G., Mosley-Thompson, E., Dansgaard, W. and Grootes, P.M., 1986. The Little Ice Age as recorded in the stratigraphy of the tropical Quelccaya ice cap. *Science* 234, 361–364.
- Virapongse, A., Endress, B.A., Gilmore, M.P., Horn, C., Romulo, C., 2017. Ecology, livelihoods, and management of the *Mauritia flexuosa* palm in South America. *Global Ecology and Conservation* 10, 70–92.
- Wüst, R.A., Bustin, R.M. and Lavkulich, L.M., 2003. New classification systems for tropical organic-rich deposits based on studies of the Tasek Bera Basin, Malaysia. *Catena* 53, 133–16

# Chapter 3

## **Holocene environmental changes inferred from an oxbow lake in a *Mauritia* palm swamp (*aguajal*) in the Madre de Dios region, southeastern Peru**

Bowen Wang<sup>a,\*</sup>, Viviana Horna<sup>b,e</sup>, Matthias Heckmann<sup>b,f</sup>, K. Anggi Hapsari<sup>a,d</sup>, Reiner Zimmermann<sup>b,c</sup>, Hermann Behling<sup>a</sup>

*a University of Goettingen, Department of Palynology and Climate Dynamics, Untere Karspüle 2, 37073 Goettingen, Germany*

*b University of Bayreuth, Ecological Botanical Gardens "OBG, 95444 Bayreuth, Germany*

*c University of Hohenheim, Faculty of Natural Sciences 190 a, Forest Ecology and Remote Sensing Group, 70599 Stuttgart, Germany*

*d College of Life and Environmental Sciences, University of Exeter, Exeter, United Kingdom*

*e Max-Planck-Institute for Biogeochemistry, 07745 Jena, Germany*

*f Federal Institute for Geosciences and Natural Resources, Wilhelmstr. 25-30, 13593 Berlin, Germany*

Corresponding author: Bowen Wang [bowen.wang@biologie.uni-goettingen.de](mailto:bowen.wang@biologie.uni-goettingen.de)

Review of Palaeobotany and Palynology (2023) 312, 104863

## Abstract

*Mauritia* peatland palm swamps (locally called *aguajales*) are typical ecosystems in Madre de Dios River floodplains in southeastern Peru. We investigated a sediment core from an oxbow lake in Los Amigos *Aguajal* to reconstruct paleoclimatic changes, vegetation dynamics on a regional scale, and human impact using multi-proxy analysis. The results show that the oxbow lake was part of Madre de Dios River's active meandering system and cut off at ca. 1760 cal yr BP. X-Ray Fluorescence results combined with stratigraphy suggest that since the cutting off, the recorded climate was humid until 540 cal yr BP excepting a shortly drier period of 640–610 cal yr BP, but after 540 cal yr BP the climate became less wet until the present. Pollen results show a stable *terra firme* forest composed primarily by Moraceae/Urticaceae throughout the record. The dense *aguajal* surrounding the oxbow lake developed from 1240 cal yr BP until the present, but canopy was more open during 780–180 cal yr BP. *Hedyosmum* became consecutively abundant since 270 cal yr BP until the present. Charcoal analysis indicated almost no human activity in the study area throughout the record. Comparison of the oxbow lake record and the previously studied palm swamp record both from Los Amigos *Aguajal* shows that: (1) main environmental changes in the palm swamp may correspond to moisture changes; (2) vegetation composition and dynamics on local *aguajal* and more regional scales are similar, except for the missing period of marsh in the oxbow lake. Furthermore, the oxbow lake record shows less wet conditions during the Little Ice Age and relatively wet in the Medieval Climate Anomaly, which is contrary to many records from the Peruvian Andes. This might be related to elevational differences (lowland vs. mountain) and/or non-climate factors and will need further investigation.

## Keywords

late Holocene; oxbow lake; *aguajal*; vegetation and environmental dynamics; Madre de Dios; Peru

### 3.1 Introduction

*Mauritia flexuosa* is an old genus of the Neotropical flora widely distributed in Amazonia, mostly restricted to the Amazon lowlands and the Orinoco basin between 10°N and 10°S latitudes. The earliest occurrence of *Mauritia* pollen dates from near the Cretaceous-Tertiary boundary about 65 million years ago (Rull, 1998). Although *Mauritia flexuosa* grows in different ecosystems ranging from coastal swamps to inland gallery forests (elevations up to ca. 1000 m), the typical *Mauritia flexuosa*-dominated ecosystems in Amazonia are permanently water-logged peatlands.

The “Andes to Amazon Biodiversity Program” (Atrium, 2007) estimates that there are at least 3000 km<sup>2</sup> of *Mauritia*-dominated peatland palm swamps (locally called *aguajal*) are estimated in the Madre de Dios region in southeastern Peru, in western Amazonia. However, despite being a common ecosystem, our understanding of the *aguajales*’ paleoecology in that region is still limited, as there are few palaeoecological studies of these *aguajales*. Only one peat core from the central Los Amigos *Aguajal* in that region, where dense *Mauritia flexuosa* grows, has been investigated (Wang et al., 2022). The study showed that sedimentation started within shallow water (1380–820 cal yr BP), followed by the development of marsh (820–640 cal yr BP), after that the dense *aguajal* developed and the canopy became more open since 300 cal yr BP. Peat and organic carbon (C) accumulation began at 820 cal yr BP with high rates (7.9 mm yr<sup>-1</sup> and 437.7 g m<sup>-2</sup> yr<sup>-1</sup>), which became lower since 520 cal yr BP (6.2 mm yr<sup>-1</sup> and 289 g m<sup>-2</sup> yr<sup>-1</sup>). This study revealed the vegetation dynamics of the locally dense palm swamp and the adjacent *terra firme* forests, and the potential capacity of C storage of the *aguajales* in the Madre de Dios region. However, the pollen record from the dense palm swamp covers only the last millennium and does not provide information on vegetation changes at the regional scale. Furthermore, the drivers of the environmental changes in the dense palm swamp remained unclear because of the lack of local paleoclimatic records with high time resolution in the lowlands of southern Peru. Bush et al. (2007) investigated four lake cores to study the Holocene vegetation, climate, and human impact in southern Peru. However, this study did not provided details about the paleoclimate in the late Holocene.

To obtain a longer and more detailed record of the regional environmental changes, we analyzed an oxbow lake sediment core located at ca. 800 m distance to the studied dense palm swamp within the same *aguajal*. For the analysis of the oxbow lake core, we used the proxies of (a) pollen and spore to infer the vegetation dynamics on a more regional scale; (b) Loss-On-Ignition (LOI) to detect the accumulation of organic material; (c)

charcoal to study the state of human activity; and (d) X-Ray Fluorescence (XRF) to infer hydrological regime and/or paleoclimatic conditions in the lowlands of southern Peru in the late Holocene. The high-resolution XRF data can be combined with the previous palm swamp study to explore past environmental changes in more detail. This will allow us to compare the similarities and differences between southern and northern Peru to discuss the climate dynamics on the scale of Peru during the late Holocene.

This study addresses the following research questions:

How did the local hydrological regime, climate, human activities, and regional vegetation dynamics infer from the oxbow lake record during the Holocene?

Can the local climate dynamics inferred from the oxbow lake record help to further understand the drivers of vegetation, peat, and C dynamics in the palm swamp?

Are environmental changes in vegetation dynamics of the local palm swamp reconstructed from the palm swamp record similar to the regional environment reconstructed from the oxbow lake record?

Are the inferred environmental changes from this study similar to other studies in western Amazonia or the adjacent Andes?

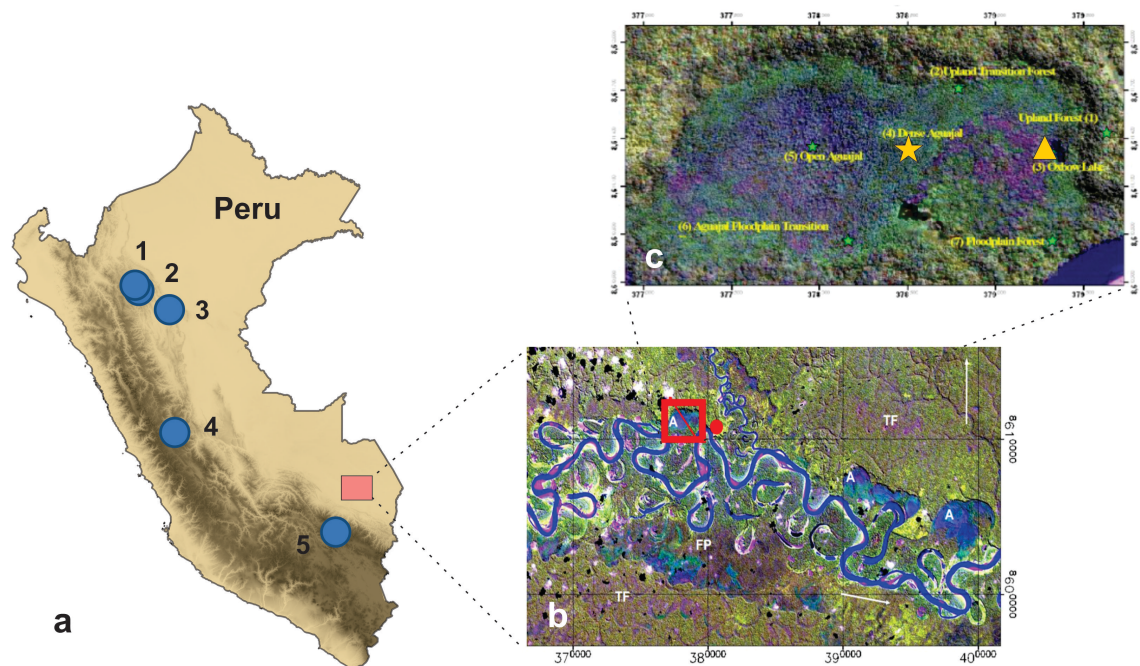
## 3.2 Study area

In southeastern Peru, the Madre de Dios River is a white-water river that descends from the Andes meandering to the southeast at an elevation of about 350 m a.s.l. The river water carries a heavy suspension load of minerals with high concentrations of calcium and has a circumneutral pH (Thieme et al., 2007; Puhakka et al. 1992). The studied oxbow lake is ca. 800 m away from a previously studied palm swamp (Wang et al., 2022), which both are located in Los Amigos *Aguajal* on the floodplain of the northern Rio Madre de Dios (Fig. 3.1).

The climate of the Madre de Dios region is warm, humid, and seasonal. Los Amigos research station CICRA (Centro de Investigación y Capacitación Rio Los Amigos, Fig. 3.1b) provides a five-year climate record from 2000 to 2006. The record shows the mean annual precipitation from 2700 to 3000 mm. More than 80% of the annual rainfall occurs between October and May. The mean annual temperature is around 24°C with maxima up to 39°C (CICRA). Episodic cold Antarctic air influx from the southeast, locally called “Friajes”, may cause significant cooling down to 8°C.

The oxbow lake, locally called “Pozo de Don Pedro”, is surrounded by *Mauritia*-dominated Los Amigos *Aguajal* on the floodplain of the Rio Madre de Dios (Fig. 3.1). The upland forests (*terra firme*) grow on a flat table land adjacent to and ca. 30 m above Los Amigos *Aguajal*. A steep escarpment incline limits the northern side of Los Amigos

*Aguajal* (Fig. 3.1c). Los Amigos *Aguajal* is waterlogged. *Mauritia flexuosa*, the dominant palm of Los Amigos *Aguajal*, is a single-stemmed, long-lived, and dioecious palm that can grow up to 30–40 m in height and 60 cm of stem diameter with an average canopy cover of up to 75% (Virapongse et al., 2017). Areas on the floodplain of the Rio Madre de Dios that are either regularly flooded or growing on nutrient-rich substrate sustain floodplain forests with common families such as Moraceae, Arecaceae, Meliaceae, and Rubiaceae (Nebel et al., 2001). *Terra firme* forests grow on higher elevations outside the influence of floods. They grow on nutrient-poor soils and are generally more diverse and often older than floodplain forests. Frequent species include *Geonoma deversa* and *G. macrostachys* (both Arecaceae), *Hevea guianensis* (Moraceae) and *Mabea* (Euphorbiaceae) which are typical Amazonian forest trees (Balslev et al., 2016).



**Fig. 3.1** Map of Madre de Dios region. (a) Map of Peru with the location of paleoclimatic records discussed in the text. The shading indicates altitude, the darker the color the higher the altitude, the data is from Shuttle Radar Topography Mission (SRTM) 90 m Digital Elevation Database (DEM). The pink rectangular shows our study area in the Madre de Dios region. Other paleoclimatic sites are represented by blue circles, including 1) Palestina cave (870 m a.s.l, Apaéstegui et al., 2014); 2) Cascayunga cave (two speleothems connected: CAS-A (930 m a.s.l) and CAS-D (841 m a.s.l), Reuter et al., 2009); 3) Lake Limón (600 m a.s.l, Parsons et al., 2018); 4) Pumacocha cave (4300 m a.s.l, Bird et al., 2011b); 5) Quelccaya Ice Cap (5670 m a.s.l, Thompson et al., 2013). (b) Landsat image of the middle course of the Madre de Dios showing *Mauritia* palm swamps (*aguajales*, deep blue-green) and open peatlands (purple-blue) along the left banks north in the vicinity of the Rio de Los Amigos research station CICRA (red circle). The small river entering from the top is the Rio de Los Amigos. The location of the proposed *aguajal* transect study is indicated by a red line cutting across the *aguajal* west of the station. The floodplain (FP) with wetlands and peatland palm swamps is on both sides sharply limited by steep escarpments with *terra firme* forests (TF) on top. At the *terra firme* (bottom) ancient river terraces and traces of former meandering river channels from an abandoned floodplain system are visible. (Image: Landsat ETM+ scene Path 3, Row 96, 23.5.2000, Bands 7/4/2, Projection: UTM 19S, WGS-84). (c) Landsat TM image of the research site west of the Los Amigos Research Station. The yellow triangle is the location of the Los Amigos Lake (LAL) study. The yellow star is the location of the palm swamp study (Wang et al., 2022).

### 3.3 Methods

#### 3.3.1 Core sampling and chronology

A 288 cm-long sediment core is and was collected using a Livingstone piston-corer from an oxbow lake (12.56°S, 70.11°W), here called Los Amigos Lake (LAL), in the *Mauritia* palm swamp called Los Amigos *Aguajal* (LAA) in Madre de Dios region in southern Peru (Fig. 3.1). The stratigraphy of the core was from visual description.

Five 2 cm<sup>3</sup> organic bulk samples were sent to the Poznań Radiocarbon Laboratory, Poland for radiocarbon dating. We constructed an age-depth model using Bacon script (Blaauw and Christen, 2011), which was calibrated using the SHCal13.14C southern hemisphere calibration curve (Hogg et al., 2013).

#### 3.3.2 Pollen and charcoal analysis

For pollen analysis, a total of 31 subsamples of 1 cm<sup>3</sup> with approximately 10 cm interval were collected along the oxbow lake core. Before the processing, we added one tablet of exotic *Lycopodium* spores (20,846 per tablet) to each sample for calculation of pollen concentration (grains/cm<sup>3</sup>) and pollen accumulation rate (grains/cm<sup>2</sup>/yr). All samples were processed using standard pollen analytical techniques and acetolysis (Faegri and Iversen, 1989). We identified pollen grains and spores using the reference collection of



the Department of Palynology and Climate Dynamics of University of Göttingen and available literature (e.g. Roubik and Moreno, 1991; Colinvaux et al., 1999). A total of 27 samples were counted mostly up to 300 terrestrial pollen grains. Four depth samples (at 60, 70, 172, and 277 cm) had no or very little pollen grains and were not included in the data set. We used TILIA software of version 2.6.1 to calculate and plot the pollen and spore diagram (Grimm, 1987). In the diagram, we grouped all the taxa into ecological groups, such as palms, trees and shrubs, herbs, Andean tree taxa (pollen taxa which occur in the Andes), aquatics, and pteridophyta. The pollen and spore taxa presented in the diagram are percentages of the pollen sum. Pollen sum includes the groups of palms, trees and shrubs, herbs, and Andean tree taxa. “Monolete” and “Trilete” represent morphological form types of fern spores that cannot further be identified. CONISS was used for the cluster analysis of terrestrial pollen taxa (Grimm, 1987). For charcoal analysis, we took subsamples of 1 cm<sup>3</sup> at the same depths at which pollen subsamples were taken. Each subsample was prepared following the method developed by Stevenson and Haberle (2005). First, each subsample was dispersed in 5-10 ml 10% KOH for 24h, then 6% hydrogen peroxide (H<sub>2</sub>O<sub>2</sub>) was used to remove organic material and left overnight, after that sieving through a 125 µm sieve.

### 3.3.3 Loss-On-Ignition (LOI) analysis

LOI analysis is used to determine the organic material (OM) in the sediment and was performed according to Heiri et al. (2001). We took 1 cm<sup>3</sup> sample at approximately 10 cm intervals along the oxbow lake core. These are the same depths used for pollen sampling. All samples were dried at 105°C for 24 h and then combusted at 550°C for 4 h. The LOI value (%), that is OM content, each sample of which was calculated as the percentage of the difference between the weight after combustion at 550°C (W<sub>c</sub>) and the weight after drying at 105°C (W<sub>dry</sub>) divided by W<sub>dry</sub>:

$$\text{LOI OM content (\%)} = \frac{W_{\text{dry}} - W_{\text{c}}}{W_{\text{dry}}} * 100$$

### 3.3.4 X-Ray Fluorescence (XRF)

Non-destructive XRF scanning was performed with an Itrax Core scanner (Cox Analytical Systems) at the University of Bremen, Institute of Geography in Germany. The oxbow lake core was scanned at a resolution of 5 mm using a Mo X-ray tube (30 kV, 18 mA) with a dwell time of 0.5 s per step. To improve the signal-to-noise ratio four consecutive spectra were later combined and reprocessed with the scanning software (Q-spec, Cox Analytical Systems) to achieve a spatial resolution of 2 mm with a dwell time of 40 s. Raw element data (integrated peak areas as total counts) were

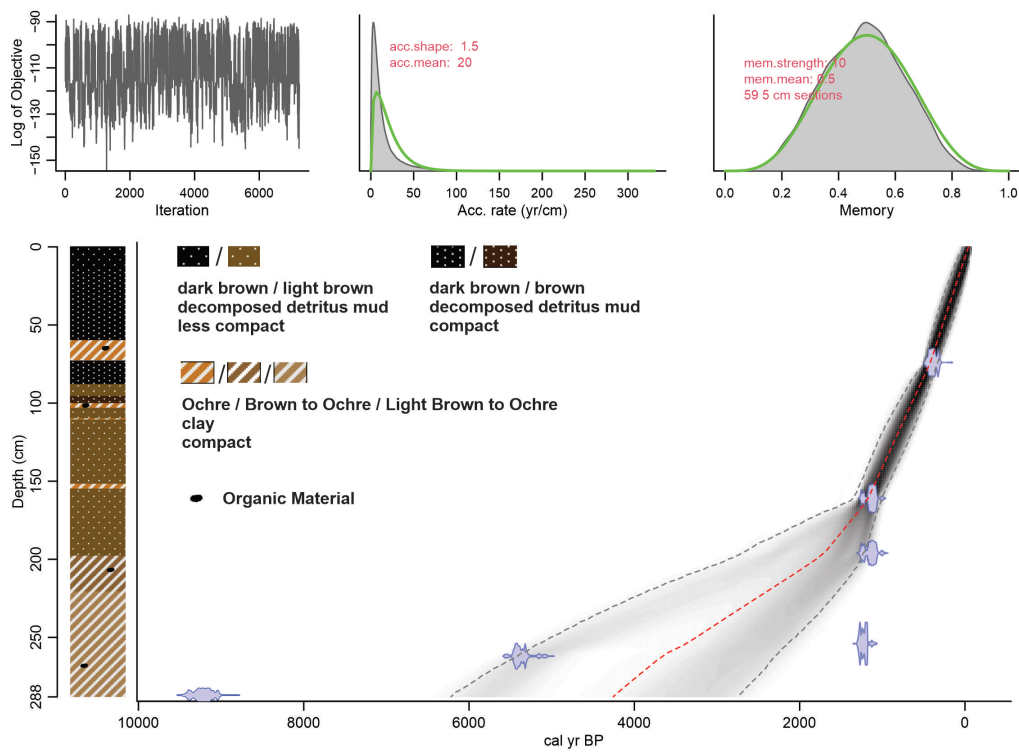
normalized by the coherent scatter radiation (coh) to minimize matrix effects. Si/coh, K/och, Ti/coh, Ca/coh, and ratios of Ca/Ti, Fe/Mn were provided.

### 3.4 Results

#### 3.4.1 Stratigraphy and chronology

Fig. 3.2 and Table 3.1 show the stratigraphy of the oxbow lake core from Madre de Dios. From 288 to 198 cm, the core material is brown or light brown to ochre fine clay with little organic material (Fig. 3.2, Table 3.1). From 198 to the top, the core material mainly consists of different shades of brown decomposed fine detritus mud, with some layers of ochre fine clay (73–60 cm, 103–100 cm, 111–110 cm, and 155–152 cm) containing very little organic material.

The five Accelerator Mass Spectrometry (AMS) radiocarbon dating results (Table 3.2) and the age-depth model (Fig. 3.2) show that the sediment was deposited since ca. 4260 cal yr BP. The sediment accumulation rate is relatively low in the depth of 288–200 cm (4260–1800 cal yr BP) that is 0.36 mm/yr, but it is much higher in 200–0 cm (1800 cal yr BP to present) which is 1.09 mm/yr (Fig. 3.2).



**Fig. 3.2** Stratigraphy and age-depth model of the Los Amigos Lake (LAL) record. The central dotted red line indicates the ‘best’ model based on the weighted mean age. The outer grey dotted lines with grey shading between them indicate 95% confidence intervals. The purple points are the dates of the tested samples.

Depth (cm)	Description
0–16	dark brown decomposed fine detritus mud, less compact
16–88	dark brown decomposed fine detritus mud, compact 60–73 cm: ochre fine clay, compact (with very little organic material)
88–198	light brown decomposed fine detritus mud, less compact 96–100 cm: brown decomposed fine detritus mud, compact 100–103, 110–111, 152–155 cm: ochre fine clay, compact (100–103 cm with very little organic material)
198–220	brown to ochre fine clay, compact (with very little organic material)
220–288	light brown to ochre fine clay, compact (with very little organic material)

**Table 3.1** Stratigraphy of the Los Amigos Lake (LAL) core.

Depth (cm)	Lab. Code	Radiocarbon dates ( <sup>14</sup> C yr BP)	Calibrated age (cal yr BP)	Dated material (OM)	d13C
74	Poz-119192	355±30	420	mud	-31.1±0.6
161	Poz-128987	1265±30	1174	mud	-32.6±0.5
196	Erl-12178	1273±38	1708	mud	-
254	Poz-122519	1355 ± 30	3375	clay	-30.2±0.2
262	Poz-132740	4670±40	3655	clay	-29.9±0.3
287	Poz-125486	8280 ± 50	4234	clay	-33.5±1.0

**Table 3.2** Radiocarbon dates from the Los Amigos Lake (LAL) core.

### 3.4.2 Pollen and charcoal data

In total 112 pollen and spore taxa were identified, which include 17 unknown pollen types (Appendix I). Important taxa are shown in the pollen diagram (Fig. 3.3a). Three pollen zones (LAL-I to LAL-III, Fig. 3.3) are recognized, based on the constrained cluster analysis on terrestrial pollen percentages using CONISS (Grimm, 1987). Pollen concentration and accumulation rates have similar trends (Fig. 3.3b). Both were relatively low in the core depth of 288–222 cm (4260–2440 cal yr BP) and increased since that. In the period of 4260–2440 cal yr BP, ranges of pollen concentration and

accumulation rates were 3000–30,000 grains/cm<sup>3</sup> and 100–1000 grains/cm<sup>2</sup>/yr, respectively. After 2440 cal yr BP to the present, they were 8000–120,000 grains/cm<sup>3</sup> and 1000–14,000 grains/cm<sup>2</sup>/yr. The charcoal accumulation rate was low throughout the record, which was less than 4 particles/cm<sup>2</sup>/yr for each sample (Fig. 3.3b).

A. Zone LAL-I (288–161 cm, 4260–1140 cal yr BP, 12 samples)

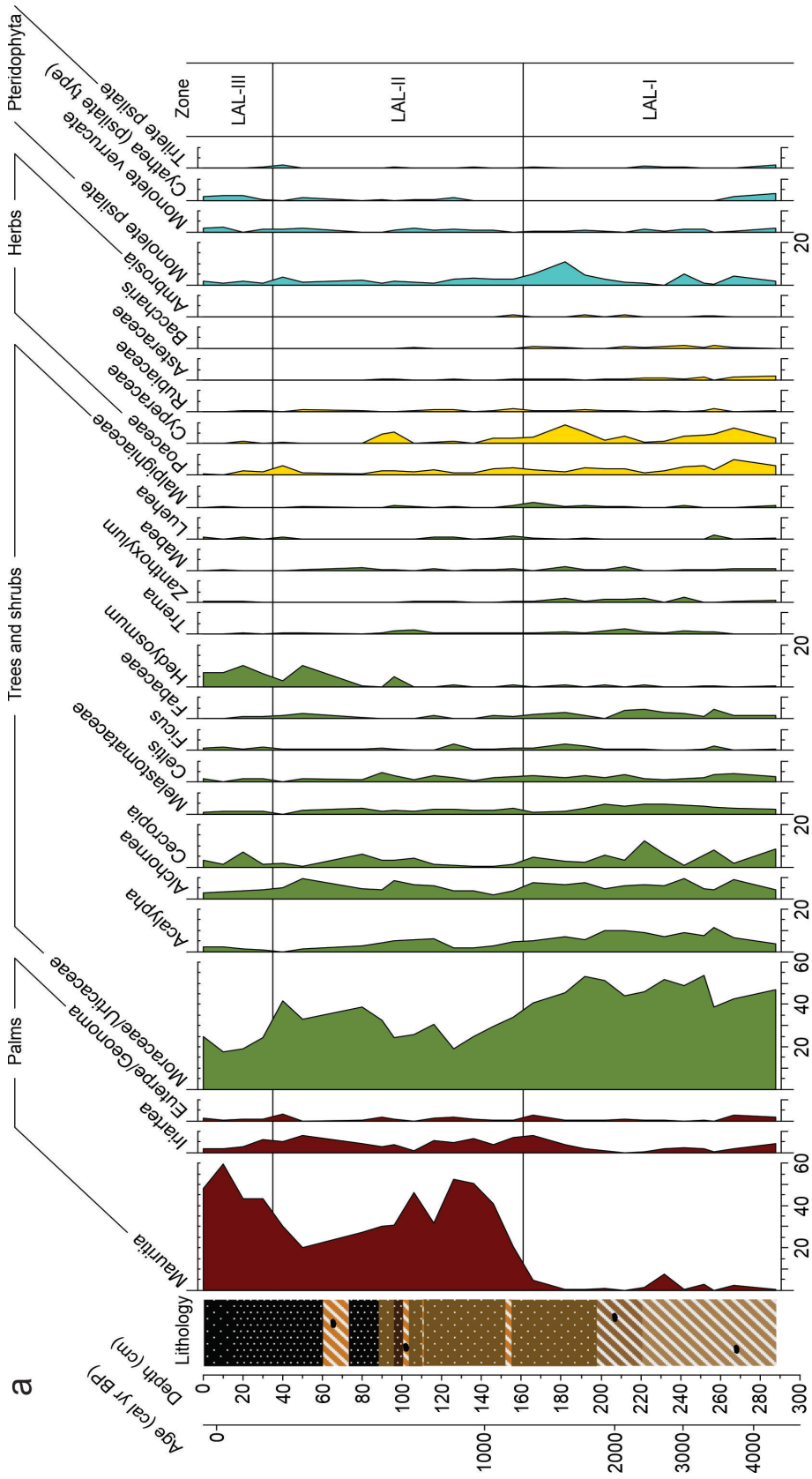
Palm pollen is low in this zone, with low amounts of *Mauritia* (<8%), *Iriartea* (<4%, except the uppermost sample of this zone with 8%), and *Euterpe/Geonoma* (<3%). Tree and shrub pollen are dominant in this zone, mainly represented by Moraceae/Urticaceae (39–54%), *Acalypha* (4–11%), *Alchornea* (4–9%), *Cecropia* (1–12%), Melastomataceae (1–5%). Other tree and shrub pollen taxa with relatively low percentages (<4%) are *Celtis*, *Ficus*, *Hedyosmum*, *Trema*, *Zanthoxylum*, *Mabea*, *Luehea* and some species of Fabaceae and Malpighiaceae families. Herb pollen is represented mainly by Poaceae (1–8%) and Cyperaceae (1–9%). Other herb taxa are rare, such as Asteraceae and Rubiaceae with values of <2%. Pteridophyta spores are mainly from Monolete psilate (<10%), other taxa such as Monolete verrucate, *Cyathea* (psilate type) and Trilete psilate are rare (<3%). Aquatics and Andean tree taxa are rare throughout the record (<2% for each taxa in each sample).

B. Zone LAL-II (161–35 cm, 1170–180 cal yr BP, 11 samples)

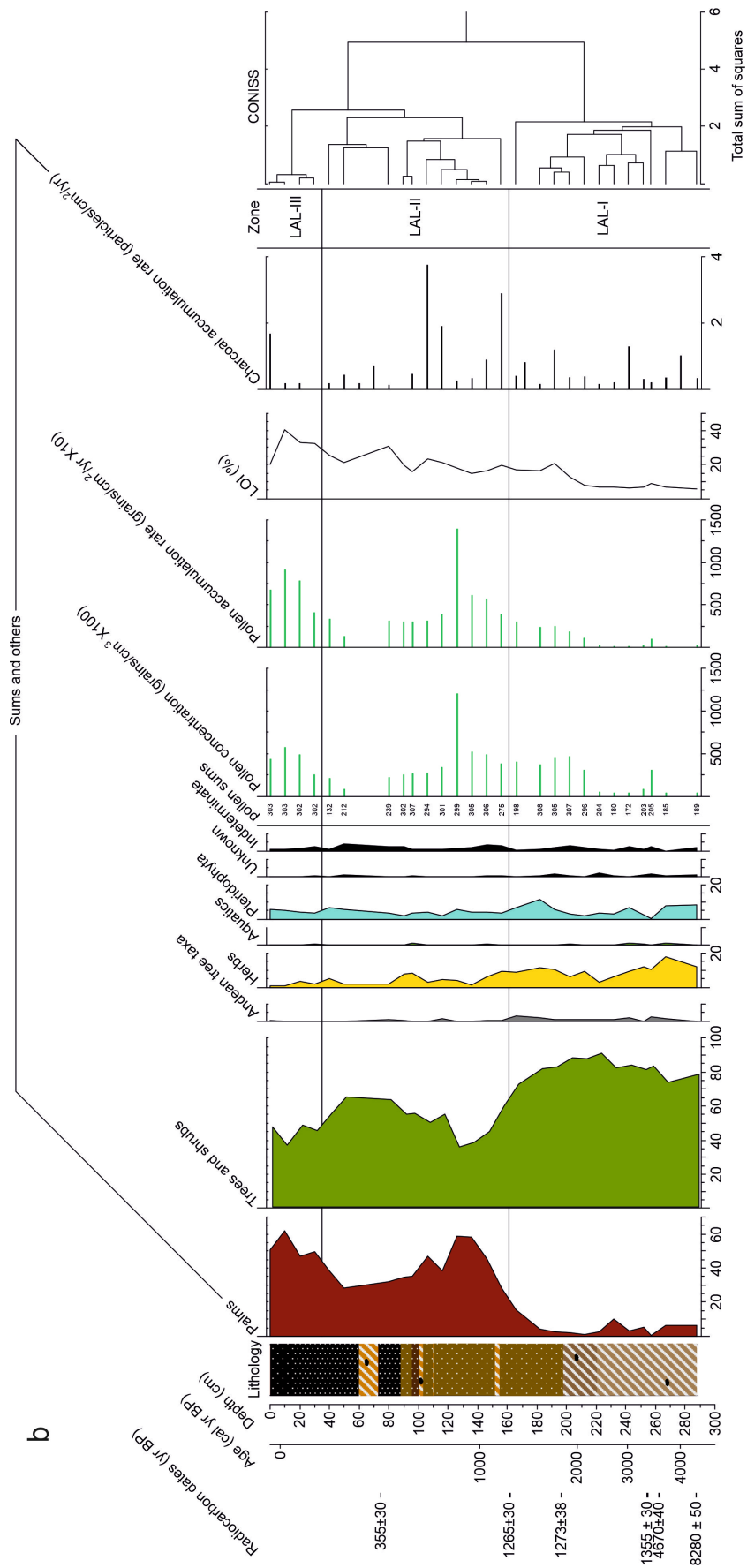
Compared with zone LAL-I, this zone is characterized by a marked increase of *Mauritia* pollen (20–52%). Other palm pollen, such as the values of *Iriartea* are higher (4–8%), while *Euterpe/Geonoma* remains rare (<3%). Moraceae/Urticaceae pollen decreased but is still abundant (19–42%). *Hedyosmum* pollen has an increase from the middle to the uppermost part of this zone with a maximum value of 10%. Other tree and shrub pollen taxa almost remain at the same level as in zone LAL-I. Herb pollen taxa show slight decrease compared to zone LAL-I, both Poaceae and Cyperaceae are <5%, and the pollen values of Asteraceae and Rubiaceae are lower than 0.4% and 2% respectively. The values of Pteridophyta taxa are also lower than in zone LAL-I, including Monolete psilate (1–4%), Monolete verrucate (<2%), *Cyathea* (psilate type) (<1%) and Trilete psilate (<1%).

C. Zone LAL-III (35–0 cm, 180 cal yr BP to the present, 4 samples)

Compared with zone LAL-II, percentages of *Mauritia* pollen are higher (43–60%), while *Iriartea* pollen (2–6%) and *Euterpe/Geonoma* pollen (<1%) remain at the same level. Moraceae/Urticaceae pollen decline (18–25%). *Hedyosmum* values vary from 6 to 10%. Values of other tree and shrub pollen taxa have no pronounced changes. Herb pollen taxa decline with values of lower than 2%. Fern spores are lower than 2%.



**Fig. 3.3a** Pollen diagram from the oxbow lake record showing the temporally changing proportions (%) of major pollen taxa.



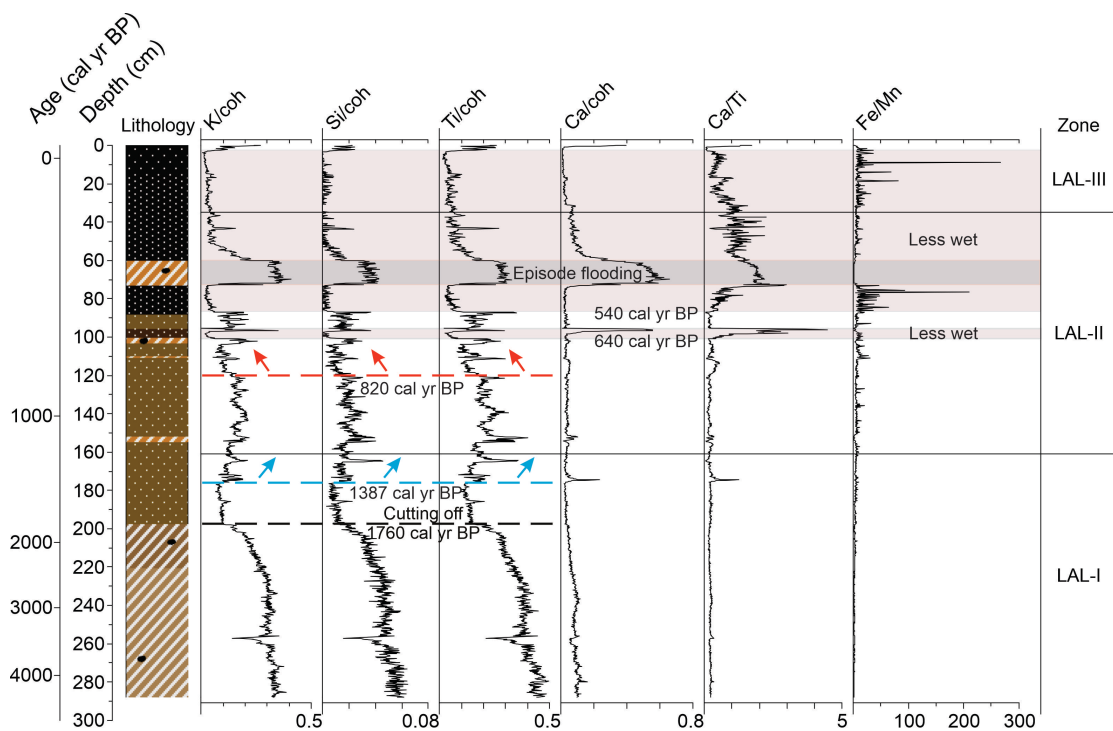
**Fig. 3.3b** Diagram of the total pollen percentages of each life form, pollen zones and the CONISS dendrogram, pollen concentration and accumulation rate, LOI, charcoal, radiocarbon ages as well as age scale.

### 3.4.3 LOI data

From the base to the top of the core, the material is mainly “mineral soil/sediment” (LOI<20%), except at 192, 116–106, 90–20, and 0 cm, where the material can be classified as “OM rich soil” (20%<LOI<35%). At 10 cm that is the maximum value of LOI in the oxbow lake core (41%), which can be classified as “muck” (35–45%). The classification is based on Wüst et al. (2003).

### 3.4.4 XRF data

The XRF data shows a similar trend in the coherent scatter radiation (coh)-normalized elements K, Si, Ti. These have high counts in the depths of 288–198 cm, 73–60 cm, and the top ca. 3 cm of the core, and are low in 100–96 cm, 88–73 cm, 60–3 cm, and relatively high but lower than the high parts in the other parts of the core. Both the Ca/Ti ratio and the coh-normalized Ca counts have peaks at 174 cm, 96–98 cm, 73–60 cm, and at the top part ca. 0.4 cm. The Ca/Ti ratio is lower than the peaks, but remains high at 60–0.4 cm. The Fe/Mn ratio is high at 88–73 cm, and at 35–0 cm.



**Fig. 3.4** XRF scanning results of the Los Amigos Lake (LAL) core. Grey-pink shading represents the less wet period. The darker shading indicates a flooding event.

## 3.5 Interpretation and Discussion

### 3.5.1 Late Holocene environmental reconstruction

#### A. Period of 4260–1170 cal yr BP (288–161 cm, zone LAL-I)

During the period of 4260–1170 cal yr BP, the sediment deposition of the coring site changed from continuous clay into mainly fine detritus mud at 198 cm, which is at ca. 1760 cal yr BP. Also, the sediment accumulation rate and OM increased since that time (Fig. 3.2, 3.3b). Furthermore, the elements Si, K, and Ti, which generally indicate allochthonous detrital and/or clay inputs (Marshall et al., 2011; Moreno et al., 2011; Stansell et al., 2013), decreased since 1760 cal yr BP (Fig. 3.4). All these changes at ca. 1760 cal yr BP indicate that the environment of the oxbow lake coring site changed from an active into a passive fluvial system, forming an oxbow lake, probably due to the cutting off from the main course of the Madre de Dios River. Before the cutting off, the coring site may have experienced a period of low fluvial activity because the deposits between 220–198 cm (2380–1760 cal yr BP) remained clay but darker in color than the lower section (Fig. 3.2; Table 3.1). This can also be supported by the increase in pollen concentration and accumulation rates in the deposits upper than 222 cm (Fig. 3.3b).

The pollen assemblage was relatively stable during the period of zone LAL-I, either before or after the cutting-off (Fig. 3.3). Moraceae/Urticaceae was dominant, and other rainforest trees such as *Acalypha* (Euphorbiaceae), *Alchornea* (Euphorbiaceae), *Cecropia* (Moraceae/Urticaceae) and Melastomataceae were frequent, showing the main vegetation composition of the Madre de Dios study region. Those families frequently occur in the *terra firme* and/or the floodplain forests near the coring oxbow lake today. Considering that Moraceae and *Cecropia* are wind pollinated and therefore often overrepresented (Gosling et al., 2009), these trees should be fewer in the actual environment than pollen recorded. A small amount of pollen of Andean origin, probably transported by the river, occurred throughout this period (Fig. 3.3b). It suggests a possible continuous influence of the Madre de Dios River on the coring site, which can be arisen by river flooding when local, upstream, and/or seasonal rainfall was high, causing highstands of the river. However, it cannot be excluded that pollen of Andean origin was transported by wind. Palm tree pollen of *Mauritia flexuosa*, *Iriartea*, and *Euterpe/Geonoma* was rare but started to increase since 1240 cal yr BP (166 cm, Fig. 3.3), which indicates that the *aguajal* surrounding the oxbow lake today has started to form since that time, probably at the border of a larger oxbow lake where the water



table was shallow.

The rate of charcoal accumulation shows some fluctuations but is very low throughout the oxbow lake record. This could indicate that there was very little or no human influence in the late Holocene in the study area.

*B. Period of 1170–180 cal yr BP (161–35 cm, zone LAL-II)*

Since the cutting off was dated at 1760 cal yr BP, the coring site has been an oxbow lake and lasted to the present as only limnic deposits accumulated, covering the whole period of zone LAL-II. The ratio of Ti/coh changes in lakes can reflect allochthonous detrital input as Ti is released from Ti-bearing rocks by physical erosion (Cohen, 2003; Haberzettl et al., 2007a) and as Ti is insensitive to redox variations (Haug et al., 2001). The allochthonous input can arise from runoff (Haberzettl et al., 2005, 2007a, 2007b), rainfall (Haug et al., 2003), and seepages from the nearby *terra firme*. Hence, the higher ratio of Ti/coh from the sediment of this oxbow lake may represent a wetter environment with larger runoff, more precipitation, seepages, and flooding. Si/coh and K/coh were similar to Ti/coh, with higher values indicating more allochthonous detrital and/or clay inputs.

Calcareous deposition (main CaCO<sub>3</sub>) in lakes can be produced by five combined processes of primary inorganic precipitation, photosynthesis (e.g., assimilation of CO<sub>2</sub> by aquatic plants), biogenic processes (e.g., skeletons), classical allochthonous input, and diagenetic reactions (Haberzettl et al., 2005). For the Ca in the oxbow lake record, the source of photosynthesis can be excluded because the spore of aquatic plants is very rare (Fig. 3.3b). Even though biogenic processes and diagenetic reactions cannot be excluded, there is no evidence to support such sources. Below 88 cm (540 cal yr BP), the Ca/coh values are low while values of Ti/coh, Si/coh, and K/coh are high, except a Ca/coh peak in (100–96 cm, 640–610 cal yr BP). However, above 88 cm, Ca/coh changes follow Ti/coh, Si/coh, and K/coh, which indicates that the Ca/coh values of the upper part were from allochthonous input by river flooding. High Ti/coh, Si/coh, and K/coh almost throughout the oxbow lake record, but Ca/coh changes following them only occurred since 540 cal yr BP. Furthermore, Ca/coh occupied more proportion in the input mineral material indicated by the increase of Ca/Ti during 640–610 cal yr BP and since 540 cal yr BP. This may indicate that more calcareous was produced by primary inorganic precipitation on a regional scale. The primary inorganic CaCO<sub>3</sub> precipitation can be an indicator of moisture, with a less wet climate resulting in the precipitation of carbonate. It is because high rainfall usually means increased cloudiness which causes the temperature to decrease, and the solubility of CaCO<sub>3</sub> increases (means less CaCO<sub>3</sub> precipitation) with the lower temperature (Haberzettl et

al., 2005). However, it is not excluded that the increased Ca/coh was caused by unknown river dynamics that eroded and transported more Ca-rich mineral material into the oxbow lake since 540 cal yr BP.

High Fe/Mn ratios are considered as an indicator of reducing and/or anaerobic conditions because of the higher solubility of Mn versus Fe under those conditions (Cohen, 2003). In turn, anoxic conditions indicate a higher accumulation of organic matter.

Based on the indications of changes in the elements above, combining the XRF data (Fig. 3.4) with the pollen and spore record (Fig. 3.3), LOI data (Fig. 3.3b), and the stratigraphy (Fig. 3.2; Table 3.1), the environmental changes during this period (1170–180 cal yr BP) can be interpreted. Since the cutting-off (1760 cal yr BP, top part in the period of zone LAL-I) until 640 cal yr BP, the values of Ti/coh, Si/coh, and K/coh were generally intermediate, which may indicate a relatively overall wet climate. However, there were still changes in the period of 1760–640 cal yr BP. For example, the values of Ti/coh, Si/coh, and K/coh increased indicating a wetter climate between 1390 and 820 cal yr BP, but decreased while Ca/Ti slightly increased maybe indicate less wet conditions during 820–640 cal yr BP. There were also three layers of ochre fine clay during that time, at the depths of 155–152 cm (1120–1090 cal yr BP), 111–110 cm (740–730 cal yr BP), and 103–100 cm (670–640 cal yr BP) concurrent with higher values of Ti/coh, Si/coh, and K/coh, indicating flooding events.

However, from 640 up to 180 cal yr BP, except for the short period of 610–540 cal yr BP (96–88 cm) which have similar conditions to the period of 1760–640 cal yr BP, the continuously high values of Ca/Ti and low Ti/coh indicate a less wet climate on a regional scale. The sediment was mainly brown detritus mud except for the ochre fine clay at 73–60 cm core depth (410–330 cal yr BP). Even though the age model shows that the clay layer was formed and lasted for 120 years, the high values of Ti/coh, Si/coh, and K/coh indicate that it could also be a single flooding event. Almost no pollen accumulated during that time (70–60 cm, Fig. 3.3b) which supports this interpretation. Furthermore, during the period of 540–410 cal yr BP, the high values of Fe/Mn and low values of Ti/coh, Si/coh, and K/coh, both indicate that the oxbow lake was almost isolated from the Madre de Dios River allowing the accumulation of OM which supported by the increase of LOI since 540 cal yr BP.

Pollen data shows that since the beginning of this period, *Mauritia flexuosa* increased fast and became dominant, indicating a dense *aguajal* surrounding the oxbow lake. However, since 780 cal yr BP (116 cm) *Mauritia flexuosa* decreased but remained abundant, which indicates that the surrounding *aguajal* became less dense with a more

open canopy. The palm *Iriartea* was abundant throughout this period. As *Iriartea* occurs in well-drained upland forests (Duivenvoorden, 1995), and the vegetation survey of Sadowski (unpublished data) shows that *Iriartea* grows in the *terra firme* forest east of the oxbow lake today, *Iriartea* pollen recorded by the oxbow lake core should be from that *terra firme* (e.g., by seepages) rather than from the *aguajal* surrounding the oxbow lake. *Hedyosmum* became consecutively abundant since 270 cal yr BP (50 cm).

### C. Period of 180 cal yr BP to the present (35–0 cm, zone LAL-III)

Compared with the last 150 years of the period of zone LAL-II (330–180 cal yr BP), the deposition of the period of zone LAL-III remained consecutively dark brown detritus mud (Fig. 3.2, Table 3.1). The values of Ti/coh, Si/coh, and K/coh are stable on the lowest level in the record. Ca values also decreased which can be explained as Ca in the oxbow lake was transported together with Ti, Si, and K by occasional river flooding (section 3.5.1.B). Ca/Ti ratios decreased but remained relatively high (Fig. 3.4) compared to the lower part of the record. The changes of those elements indicate that the climate became wetter but not as wet as during the period of 1760–640 cal yr BP. Furthermore, the increased Fe/Mn ratios (Fig. 3.4) and LOI values (Fig. 3.3b) indicate that the oxbow lake has higher OM accumulation, which further indicates that the oxbow lake had less connection to the Madre de Dios River. This is supported by the absence of Andean pollen (Fig. 3.3b) during this period.

*Mauritia flexuosa* increased again, while dwarf *Hedyosmum* remained at the same level since 270 cal yr BP (Fig. 3.3a), indicating that the surrounding *aguajal* became denser but still with an open canopy. *Iriartea*, which may grow in the *terra firme* forests east to the oxbow lake, remained abundant but decreased since the middle of the period of zone LAL-III (Fig. 3.3a). Peaks of K/coh, Si/coh, Ti/coh, Ca/coh, and Ca/Ti (Fig. 3.4) were registered at the end of this period, similar to the period of 410–330 cal yr BP. These peaks may indicate flooding events or gold mining activities in the study area.

## 3.5.2 Further interpretation of the drivers of the changes in the palm swamp

The climate signal indicated by the oxbow lake record allows a better understanding of the drivers of the environmental changes of the palm swamp record (Wang et al., 2022). The main changes in the palm swamp record include (1) start of the sediment accumulation in a water pond since 1380 cal yr BP; (2) start of peat and C accumulation with a transition from open pond to marsh since 820 cal yr BP; (3) transition from marsh to *aguajal* since 640 cal yr BP; (4) decrease in peat and C accumulation rates since 520 cal yr BP, but remaining on a relatively high level; (5) openness of the *aguajal* canopy

with the increase of *Hedyosmum* since 300 cal yr BP.

The values of Ti/coh, Si/coh, and K/coh increased since 1390 cal yr BP (176 cm; Fig. 3.4) in the oxbow lake record indicating a wetter climate. Hence, it might be that the wetter climate caused more seepages merging on an impervious substrate (consisted by blue/grey clay, Householder et al., 2012) or a meander cutting off from the Madre de Dios River, which formed the initial water pond.

For the start of peat and C accumulation the values of Ti/coh, Si/coh, and K/coh decreased since 820 cal yr BP (120 cm; Fig. 3.4) in the oxbow lake record indicating a less wet local climate. Therefore, a new inference of the driver of this change is that less flooding and local seepages went into the palm swamp under a not so wet regional climate, resulting in a relatively stable water table facilitating the onset of the peat and C accumulation.

For the change that the marsh transferred to an *aguajal*, the previously studied palm swamp showed that the development of the *aguajal* was caused by less flooding evidenced by absent of visible clay particles after 640 cal yr BP, because *Mauritia* cannot tolerate deep flooding (Roucoux et al., 2013; Pennington et al., 2004). Combined with the oxbow lake record, the less wet climate evidenced by the high values of Ca/Ti during 640–610 cal yr BP might be one of the drivers that facilitated less flooding.

Without the local climate record in the previous palm swamp study, the driver for the decrease of peat and C accumulation rates was speculated using the climate record from the Andes Altiplano which shows wet climate during the Little Ice Age (LIA; 550–130 cal yr BP) (Bird et al., 2011a). However, the oxbow lake record shows that the local climate became less wet since 540 cal yr BP compared with before. Therefore, a more probable inference is that the lower local water table developed under a not so wet regional climate led to the decrease in peat and C accumulation rates in the palm swamp since 520 cal yr BP.

The driver of the change to a more open *aguajal* with the increase of *Hedyosmum* in the understorey is still not clear. The vegetation survey from Sadowski (unpublished data) suggested that *Hedyosmum* is more frequent when the *aguajal* is more open because of better light conditions in the shrub layer. However, the abundance of *Hedyosmum* did not always change inversely to the abundance of *Mauritia flexuosa* (Fig. 3.3a). From the perspective view that *Hedyosmum* is a montane genus (Antonelli and Sanmartín, 2011) tracking an ancestral montane niche (e.g., high moisture availability) on the peatlands as habitats in the Madre de Dios region (Householder et al., 2015), moisture is expected to influence the growth of *Hedyosmum* in the study area. However, the changes in *Hedyosmum* abundance did not always follow the

reconstructed climate change in this study.

### 3.5.3 Comparison of the pollen records of the palm swamp and oxbow lake

Similar vegetation composition and dynamics could be observed between the record from the palm swamp (Wang et al., 2022) which only represents the central dense *aguajal* and this study which represents a region scale including the studied swamp, nearby *terra firme* forests, and floodplain forests (Fig. 3.1c). The oxbow lake record started at ca. 4260 cal yr BP and the palm swamp record at ca. 1380 cal yr BP, in which both local environments were characterized first by open water before the *aguajal* developed. The formation of a marsh dominated by Cyperaceae from ca. 820 to 640 cal yr BP, shown in the palm swamp record, is missing in the oxbow lake record. The reason for the missing is not clear yet. The marked increase in *Mauritia flexuosa*, indicating the formation of the *aguajal*, is dated in the oxbow lake record at ca. 1170 cal yr BP and in the palm swamp record at ca. 640 cal yr BP. This time difference can be explained by the earlier formation of the *aguajal* in the eastern part than in the central part of the studied swamp. Furthermore, *Mauritia flexuosa* pollen in the palm swamp is more abundant than in the oxbow lake record (70% vs 38% on average) since the formation of the *aguajales*. This may be caused by a strong local input of *Mauritia flexuosa* pollen within the *aguajal* itself.

Before the formation of the *aguajal*, values of Moraceae/Urticaceae pollen in both records were similar (ca. 47% on average) reflecting the regional condition of Moraceae/Urticaceae occupation. After the *aguajal* establishment, Moraceae/Urticaceae pollen in the oxbow lake record was generally higher than in the palm swamp record (28% vs 16% on average). This might be because of the higher local input of the *Mauritia flexuosa* pollen and the more closed canopy in the palm swamp. Other frequent rainforest taxa, such as *Acalypha*, *Alchornea*, and *Cecropia* were also more abundant in the oxbow lake record than in the palm swamp record, even before the development of *aguajales*. The reason might be due to the location of the oxbow lake coring site closer to the *terra firme* forest than the palm swamp site and/or a stronger regional input of pollen at the oxbow lake. Interestingly, *Iriartea* pollen was more frequent in the oxbow lake record than in the palm swamp record (5% vs. 1% on average). This might be also due to the different locations, as *Iriartea* grows more often in *terra firme* forests. *Hedyosmum* pollen started to increase at a similar time in both records, which was 300 cal yr BP in the palm swamp record and 270 cal yr BP in the oxbow lake record. The values of *Hedyosmum* pollen in both records were also similar

(5–10%), except for the short period of 210–180 cal yr BP shown by two pollen samples with higher values in the the palm swamp record (16–18%). This indicates that the *aguajal* at the palm swamp site had a more open canopy during 210–180 cal yr BP. Overall, the different local conditions and the location within the studied swamp caused the differences in the pollen records.

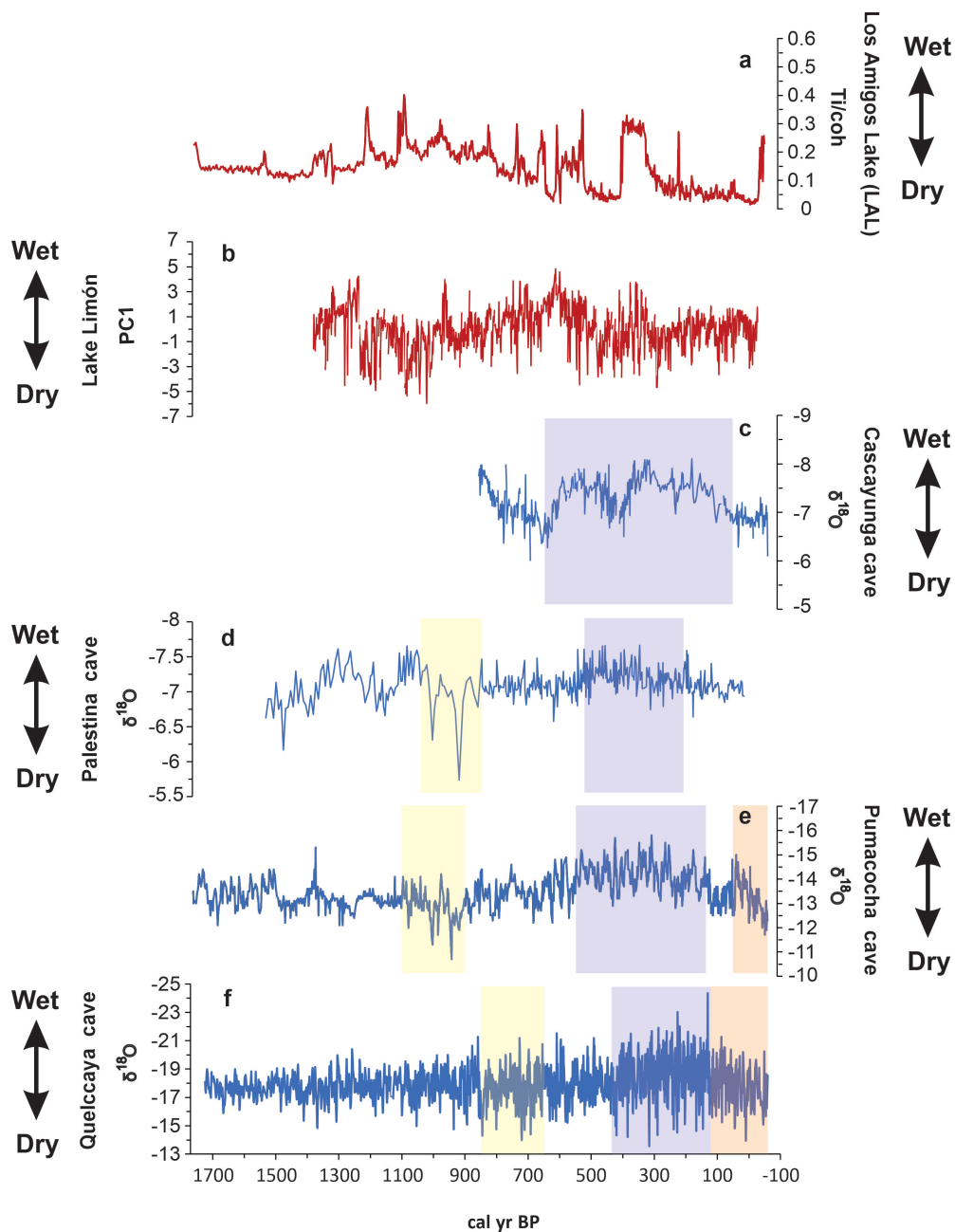
### 3.5.4 Comparison with other records in Peru

Even though the time of the beginning and the duration of the climate changes were different, many Peruvian Andes records from the north to south (Apaéstegui et al., 2014; Reuter et al., 2009; Bird et al., 2011b; Thompson et al., 2013) demonstrate that the climate pattern that was wetter in the so-called LIA and drier in the Medieval Climate Anomaly (MCA) and/or the current warm period (CWP) in the last two millennia (Fig. 3.5c, d, e, f). However, the result of Ti of the oxbow lake was opposite to the climate pattern of the Peruvian Andes, which shows lower Ti values indicating less wet conditions during the LIA (regarding the period of 410–330 cal yr BP with high Ti values as a flooding event, section 3.5.1.B) and higher values indicating wetter conditions during MCA and CWP (Fig. 3.4, 3.5a). Generally, the amount of rainfall in the Andes should influence the Ti content in the oxbow lake record by runoff and flooding (e.g., frequency, gradient) from the Madre de Dios River that descends from the Andes. However, as there are only a few Andean pollen grains accumulated throughout the oxbow lake record, the Ti accumulated in the oxbow lake should mainly be related to erosion by local rainfall and seepages. Therefore, one possible explanation for the different climate patterns between the Peruvian Andes and the oxbow lake study area is the antiphasing precipitation between the altiplano and lowlands in Peru. However, it cannot be excluded that non-climate disturbances influence the oxbow lake and other existing records. For example, the changes in Ti values in the oxbow lake record are possibly influenced by the establishment and destruction of river levees.

The Lake Limón record, which is principal component one (PC1) calculated from the elemental time series of XRF, is from the lowland of northern Peru (Parsons et al., 2018; Fig. 3.5b). This PC1 record is positively correlated with the abundance of the terrestrial elements (e.g., Ti) and negatively correlated with Ca abundance, which has relatively similar trend to our oxbow lake record during LIA. Compared with the records from the nearby Andes (Fig. 3.5c, d), Parsons et al. (2018) found that the Andes records are also not always consistent with the Lake Limón record, even though these records (Fig. 3.5b, c, d) should have similar background hydroclimatic variability because they show similarly hydroclimate-sensitive paleoclimate spectra. Therefore, they thought these records either record non-climatic noise in different ways, or the signals of these records

were misinterpreted.

From the different climate trends between the lowlands (this study and the Lake Limón record; Figure 3.5a, b) and the existing records in the Peruvian Andes (Figure 3.5c, d, e, f), we inferred two possibilities: (1) the precipitation can increase as the elevation from the lowland to the Andes rise; (2) the paleoclimate records may include the non-climatic signals that disturb our interpretation of climate changes. Therefore, it is necessary to study more lowland records in Peru to explore if the different climate trends between highlands and lowlands are a regional phenomenon, and test methods to remove the non-climate factor in the palaeoecological records in the future.



**Fig. 3.5** Los Amigos Lake (LAL) record and other Peruvian paleoclimate records. All other records data are downloaded from the National Oceanic and Atmospheric Administration (NOAA) paleoclimate website, including: (a) Los Amigos Lake (LAL) record (ca. 350 m a.s.l, this study); (b) Lake Limón (600 m a.s.l, Parsons et al., 2018); (c) Cascayunga cave (two speleothems connected: CAS-A (930 m a.s.l) and CAS-D (841 m a.s.l, Reuter et al., 2009); (d) Palestina cave (870 m a.s.l, Apaéstegui et al., 2014); (e) Pumacocha cave (4300 m a.s.l, Bird et al., 2011b); (f) Quelccaya Ice Cap (5670 m a.s.l, Thompson et al., 2013). The purple shade represents the Little Ice Age (LIA). The yellow shades represent the Medieval Climate Anomaly (MCA) and the current warm period (CWP). Curve (a) represents Ti result of Los Amigos Lake (LAL) record that was normalized by coherent scatter radiation. Curve (b) represents Principal Component 1 (PC1) that explains the most variance (40%) in the study of Lake Limón, which is strongly driven by Ti and is positively correlated with the abundance of the terrestrial elements Al, K, Ti, Fe, and Rb, and negatively correlated with Ca abundance. At least one standard deviation below the mean can be identified as drought, and vice versa. The curves (c), (d), (e), and (f) are speleothems  $\delta^{18}\text{O}$  records colored blue. More negative  $\delta^{18}\text{O}$  values reflect more precipitation and vice versa. The curves a and b are mainly contributed by Titanium (Ti) colored red. The higher values of Ti/coh reflect wetter, and vice versa.

### 3.6 Summary and Conclusion

To better understand the *aguajales* in the Madre de Dios region, in this paper we studied a 288 cm-long sediment core from an oxbow lake in the Los Amigos *Aguajal* to reconstruct paleoclimate changes, vegetation dynamics on a regional scale, human impact, and OM accumulation since 4260 cal yr BP.

The XRF results combined with stratigraphy and OM changes show that the coring site belonged to a meander of the Madre de Dios River, and was cut off at 1760 cal yr BP. The climate was wet in 1760–540 cal yr BP excepting a short drier period of 640 – 610 cal yr BP, subsequently becoming less wet until the present. However, it cannot be fully excluded that the changes were influenced by non-climatic factors.

Pollen of Moraceae/Urticaceae is always the dominant family in the pollen spectra of the record since 4260 cal yr BP, which mainly grows on the nearby *terra firme*. Other rainforest trees/shrubs such as *Acalypha*, *Alchornea*, and Melastomataceae were also frequent. The *aguajal* dominated by *Mauritia flexuosa* surrounding the oxbow lake developed since 1240 cal yr BP until the present, but with a more open canopy during the period of 780–180 cal yr BP. *Hedyosmum* became consecutively abundant since 270 cal yr BP. The charcoal results indicate that there was almost no human activity in the study area throughout the record.

A comparison of the environmental changes in the palm swamp record with the paleoclimate changes shown by the oxbow lake record indicates that the environmental changes in the palm swamp may correspond to changes in wetter and less wet



conditions. Comparing the pollen and spore records of the oxbow lake and the palm swamp, we found that the vegetation composition and dynamics on the local *aguajal* and regional scales are similar except for the missing period of marsh in the oxbow lake record. There are also differences in the percentages of each main taxa between the two records.

Comparing the oxbow lake results with other paleoclimate records in Peru, we found that the oxbow lake record show opposite climate changes to many Peruvian Andes records. The different climate changes between the lowlands and the altiplano also occurred in northern Peru. The reason for this difference is not clear, but two possible directions can be considered: (1) the influence of the elevation differences (lowland vs. mountain); (2) non-climate disturbances influencing the oxbow lake record and existing records in Peru. Therefore, we suggest to study more records in Peruvian lowlands and considering how to remove the non-climate factor in the palaeoecological records in the future.

## Acknowledgments

This study was supported by the China Scholarship Council (CSC No. 201906190215; for B.W.) and partly by the German Research Foundation (BE-2116/32-1). We thank Prof. Dr. Henry Hooghiemstra for his helpful and constructive review.

## References

- Antonelli, A., Sanmartín, I., 2011. Mass extinction, gradual cooling, or rapid radiation? Reconstructing the spatiotemporal evolution of the ancient angiosperm genus *Hedyosmum* (Chloranthaceae) using empirical and simulated approaches. *Syst. Biol.* 60, 596–615.
- Apaéstegui, J., Cruz, F.W., Sifeddine, A., Espinoza, J.C., Guyot, J.L., Khodri, M., Santini, W., 2014. Hydroclimate variability of the northwestern Amazon basin near the Andean foothills of Peru related to the South American Monsoon System during the last 1600 years. *Climate of the Past* 10, 1967-1981.
- Atrium, 2007. Biodiversity Information System for the Andes to Amazon Biodiversity Program. Botanical Research Institute of Texas. <http://atrium.andesamazon.org>.
- Balslev, H., Laumark, P., Pedersen, D., Grández, C., 2016. Tropical rainforest palm communities in Madre de Dios in Amazonian Peru. *Revista Peruana de Biología* 23, 3-12.
- Bird, B.W., Abbott, M.B., Rodbell, D.T., Vuille, M., 2011a. Holocene tropical South American hydroclimate revealed from a decadal resolved lake sediment  $\delta^{18}\text{O}$  record. *Earth and Planetary Science Letters* 310, 192–202.

- Bird, B.W., Abbott, M.B., Vuille, M., Rodbell, D.T., Stansell, N.D., Rosenmeier, M.F., 2011b. A 2,300-year-long annually resolved record of the South American summer monsoon from the Peruvian Andes. *Proceedings of the National Academy of Sciences* 108, 8583–8588.
- Blaauw, M., Christen, J.A., 2011. Flexible paleoclimate age-depth models using an autoregressive gamma process. *Bayesian analysis* 6, 457-474.
- Bush, M. B., Silman, M. R., Listopad, C. M. C. S., 2007. A regional study of Holocene climate change and human occupation in Peruvian Amazonia. *Journal of biogeography* 34, 1342-1356.
- Cohen, A.S. 2003: *Paleolimnology. The history and evolution of lake systems*. Oxford University Press.
- Duivenvoorden, J. E., 1995. Tree species composition and rain forest-environment relationships in the middle Caquetá area, Colombia, NW Amazonia. *Vegetatio* 120, 91-113.
- Faegri, K., and Iversen, J., 1989. *Textbook of Pollen Analysis*, fourth ed. Wiley, Chichester, pp. 34, 67-89.
- Gosling, W.D., Mayle, F.E., Tate, N.J., Killeen, T.J., 2009. Differentiation between Neotropical rainforest, dry forest, and savannah ecosystems by their modern pollen spectra and implications for the fossil pollen record. *Review of Palaeobotany and Palynology* 153, 70-85.
- Grimm, E.C., 1987. CONISS: a FORTRAN 77 program for stratigraphically constrained cluster analysis by the method of incremental sum of squares. *Comput. Geosciences* 13, 13-35.
- Heiri, O., Lotter, A.F., Lemcke, G., 2001. Loss on ignition as a method for estimating organic and carbonate content in sediments: reproducibility and comparability of results. *Journal of Paleolimnology* 25, 101-110.
- Haberzettl, T., Fey, M., Lücke, A., Maidana, N., Mayr, C., Ohlendorf, C., Schäbitz, F., Schleser, G.H., Wille, M., Zolitschka, B., 2005. Climatically induced lake level changes during the last two millennia as reflected in sediments of Laguna Potrok Aike, southern Patagonia (Santa Cruz, Argentina). *Journal of Paleolimnology* 33, 283–302.
- Haberzettl, T., Corbella, H., Fey, M., Janssen, S., Lücke, A., Mayr, C., Ohlendorf, C., Schäbitz, F., Schleser, G.H., Wille, M., Wulf, S., Zolitschka, B., 2007a. Lateglacial and Holocene wet-dry cycles in southern Patagonia: chronology, sedimentology and geochemistry of a lacustrine record from Laguna Potrok Aike, Argentina. *The Holocene* 17, 297–310.
- Haberzettl, T., Kück, B., Wulf, S., Anselmetti, F., Ariztegui, D., Fey, M., Janssen, S., Lücke, A., Mayr, C., Ohlendorf, C., Schäbitz, F., Schleser, G., Wille, M. and Zolitschka, B. 2007b: Hydrological variability in southeastern Patagonia and explosive volcanic activity in the southern Andean Cordillera during Oxygen Isotope Stage 3 and the Holocene inferred from lake sediments of Laguna Potrok Aike, Argentina. *Palaeogeography, Palaeoclimatology, Palaeoecology*.

- Haug, G. H., Hughen, K. A., Sigman, D. M., Peterson, L. C., & Rohl, U., 2001. Southward migration of the intertropical convergence zone through the Holocene. *Science* 293, 1304–1308.
- Haug G., Gunther D., Peterson L., Sigman D., Hughen K. and Aeschlimann B. 2003. Climate and the collapse of Maya civilization. *Science* 299: 1731–1735.
- Hogg, A.G., Hua, Q., Blackwell, P.G., Niu, M., Buck, C.E., Guilderson, T.P., Heaton, T.J., Palmer, J.G., Reimer, P.J., Reimer, R.W., Turney, C.S.M., Zimmerman, S.R.J., 2013. SHCal13 southern hemisphere calibration, 0-50,000 cal BP. *Radiocarbon* 55, 1889-1903.
- Householder, J.E., Janovec, J.P., Tobler, M.W., Page, S., L\"ahteenoja, O., 2012. Peatlands of the Madre de Dios River of Peru: distribution, geomorphology, and habitat diversity. *Wetlands* 32, 359–368.
- Householder, J.E., Wittmann, F., Tobler, M.W., Janovec, J.P., 2015. Montane bias in lowland Amazonian peatlands: plant assembly on heterogeneous landscapes and potential significance to palynological inference. *Palaeogeography Palaeoclimatology Palaeoecology* 423, 138–148.
- Marshall, M.H., Lamb, H.F., Huws, D., Davies, S.J., Bates, R., Bloemendal, J., Boyle, J., J.Leng, M., Umler, M., Bryant, C., 2011. Late Pleistocene and Holocene drought events at Lake Tana, the source of the Blue Nile. *Global and Planetary Change* 78, 147-161.
- Moreno, A., L\"opez-Merino, L., Leira, M., Marco-Barba, J., Gonz\'alez-Samp\'eriz, P., Valero-Garc\'es, B.L., L\"opez-S\'aez, J.A, Santos, L., Mata. P., Ito, E., 2011. Revealing the last 13,500 years of environmental history from the multiproxy record of a mountain lake (Lago Enol, northern Iberian Peninsula). *Journal of Paleolimnology*, 46, 327-349.
- Nebel, G., Kvist, L.P., Vanclay, J.K., Christensen, H., Freitas, L., Ru\'ız, J., 2001. Structure and floristic composition of flood plain forests in the Peruvian Amazon: I. Overstorey. *Forest Ecology and Management* 150, 27-57.
- Parsons, L.A., LeRoy, S., Overpeck, J.T., Bush, M., C\'ardenes-Sand\'ı, G.M., Saleska, S., 2018. The threat of multi-year drought in western Amazonia. *Water resources research* 54, 5890-5904.
- Pennington, T.D., Reynel, C., Daza, A., 2004. *Illustrated Guide to the Trees of Peru*. David Hunt, Sherborne, UK (848 pp.).
- Polissar, P. J., Abbott, M.B., Wolfe, A.P., Bezada, M., Rull, V., Bradley, R.S., 2006, Solar modulation of Little Ice Age climate in the tropical Andes, *Proc. Natl. Acad. Sci. U. S. A.*, 103, 8937– 8942
- Reuter, J., Stott, L., Khider, D., Sinha, A., Cheng, H., Edwards, R.L, 2009. A new perspective on the hydroclimate variability in northern South America during the Little Ice Age. *Geophysical Research Letters* 36, L21706.
- Roucoux, K.H., Lawson, I.T., Jones, T.D., Baker, T.R., Honorio Coronado, E.N., Gosling, W.D., L\"ahteenoja, O., 2013. Vegetation development in an Amazonian peatland. *Palaeogeography, Palaeoclimatology, Palaeoecology*. 374, 242–255.

- Roubik, D.W., Moreno, J.E., 1991. Pollen and Spores of Barro Colorado Island, Monographs in Systematic Botany, Vol. 36, Missouri Botanical Garden, the United States.
- Rull, V., 1998. Biogeographical and evolutionary considerations of *Mauritia* (Arecaceae), based on palynological evidence. Review of Palaeobotany and Palynology 100, 109-122.
- Stansell, N.D., Rodbell, D.T., Abbott, M.B., Mark, B.G., 2013. Proglacial lake sediment records of Holocene climate change in the western Cordillera of Peru. Quaternary Science Reviews, 70, 1-14.
- Stevenson, J., Haberle, S., 2005. Macro Charcoal Analysis: a Modified Technique Used by the Department of Archaeology and Natural History. Australian National University, Canberra.
- Thieme, M., Lehner, B., Abell, R., Hamilton, S.K., Kellndorfer, J., Powell, G., Riveros, J.C., 2007. Freshwater conservation planning in data-poor areas: an example from a remote Amazonian basin (Madre de Dios River, Peru and Bolivia). Biological Conservation 135, 484-501.
- Thompson, L.G., Mosley-Thompson, E., Davis, M.E., Zagorodnov, V.S., Howat, I.M., Mikhailenko, V.N., Lin, P.N., 2013. Annually resolved ice core records of tropical climate variability over the past~ 1800 years. Science 340, 945-950.
- Puhakka, M., Kalliola, R., Rajasilta, M., Salo, J., 1992. River types, site evolution and successional vegetation patterns in Peruvian Amazonia. Journal of Biogeography 19, 651-665.
- Virapongse, A., Endress, B.A., Gilmore, M.P., Horn, C., Romulo, C., 2017. Ecology, livelihoods, and management of the *Mauritia flexuosa* palm in South America. Global Ecology and Conservation 10, 70-92.
- Wang, B., Hapsari, K.A., Horna, V., Reiner, Z., Behling, H., 2022. Late Holocene peatland palm swamp (*aguajal*) development, carbon deposition and environment changes in the Madre de Dios region, southeastern Peru. Palaeogeography, Palaeoclimatology, Palaeoecology 594, 110955.
- Wüst, R.A., Bustin, R.M. and Lavkulich, L.M., 2003. New classification systems for tropical organic-rich deposits based on studies of the Tasek Bera Basin, Malaysia. Catena 53, 133-163.

# Chapter 4

## **Holocene vegetation dynamics, carbon deposition, sea level changes, and human impact inferred from the Lagoa da Fazenda core in the Baía de Caxiuanã region, northern Brazil**

<sup>a</sup> Wang, B., <sup>b</sup> Costa, M.L., <sup>b</sup> Valente, G.J.S.S., <sup>b</sup> Santos, P.H.C., <sup>a</sup> Behling, H.

<sup>a</sup> University of Goettingen, Department of Palynology and Climate Dynamics, Untere Karspüle 2, 37073 Goettingen, Germany

<sup>b</sup> Federal University of Pará, Geosciences Institute, Campus of Guamá, 66075-110 Belém/Pará, Brazil

Corresponding author: Bowen Wang [bowen.wang@biologie.uni-goettingen.de](mailto:bowen.wang@biologie.uni-goettingen.de)

Quaternary Science Reviews (2024) 327, 108520.

## **Abstract**

Tropical peat deposits as a potential carbon (C) stock are important to global climate change. Hence, it is necessary to explore the mechanism of formation and dynamics of tropical peat ecosystems. Up to present, the paleoecology of peat ecosystems in eastern Amazonia is still little known. We did a multi-proxy analysis including pollen and spores, LOI, organic C, macro-charcoal, minerals and chemical composition of a 395-cm-long radiocarbon dated sediment core, named Lagoa da Fazenda (LF), from a blocked river channel of the Baía de Caxiuanã in eastern Amazonia. This study site is representative of a net of former small river valleys with carbon deposits in eastern Amazonia. The study results indicate that the peat with organic C deposits originated from a local inundated forest which started at ca. 7000 cal yr BP. Inundations were caused by the Atlantic sea level rise. The Atlantic sea level further rose since ca. 5000 cal yr BP. Peat and C accumulation rates remained at a high level since the beginning but became lower and more fluctuating since 2600 cal yr BP influenced by river flooding, which may have been caused by soil erosion due to human activities in the region. The local vegetation changed from an inundated forest to a Cyperaceae swamp since 1800 cal yr BP until the present. A strong local human influence was recorded since ca. 260 cal yr BP.

## **Keywords**

Holocene; eastern Amazonia; peat; organic carbon accumulation; Atlantic sea level; vegetation dynamics, human activities

## 4.1 Introduction

New estimates show that tropical peatlands cover an area of 1700,000 km<sup>2</sup>, containing 7268 km<sup>3</sup> of peat (Gumbrecht et al., 2017) and 152-288 gigatons (Gt) of carbon (C) storage (Riberio et al., 2021). This is much more than the former estimation of 440,000 km<sup>2</sup>, 1758 km<sup>3</sup>, and 88.6 Gt, respectively (Page et al., 2011). This points out the underestimation of peat C stock in tropical peatlands and their influence on global changes. Different to peatlands in temperate regions, where the relationship between ecosystem dynamics, C accumulation and climate is well studied, tropical peatlands are little known and have their mechanism of peat formation and vegetation coverage (Riberio et al., 2021). In the tropics, South America potentially holds the largest natural peatlands but their palaeoenvironment is little known (Riberio et al., 2021). Available palaeoecological studies of peatlands focus on western Amazonia especially in Peru (Kelly et al., 2017; Roucoux et al., 2013; Swindle et al., 2018; Wang et al., 2022). Furthermore, most of the peatlands in South America are distributed in Amazonia (Xu et al., 2018), and little is known about northeastern Amazonia.

Our study site, called Lagoa da Fazenda, is part of an abandoned river with peat deposition from the Baía de Caxiuanã region belonging to the Caxiuanã River system in northeastern Amazonia. Baía de Caxiuanã is an inland bay with many blocked rivers, which is frequent in river systems in the lowlands of northeastern Amazonia. Therefore, we studied the sediment core from the LF as a representative archive in a network of infilled river channels in northeastern Amazonia. From the LF archive, we will explore past vegetation and fire dynamics, climate change and human impact as well as processes of peat and organic C accumulation by methods of pollen and spore, macro-charcoal, Loss-On-Ignition (LOI), organic C as well as mineralogical and geochemical analysis. This study is conducted to address the following main research questions:

1. How were the past vegetation dynamics in the study region?
2. Since when and how did the low-lying river valleys start to accumulate peat and organic C in eastern Amazonia?
3. How did the peat and organic C accumulation rates change over time in this region?
4. What factors may have influenced the vegetation dynamics as well as peat and organic C accumulation rates?

## 4.2 Study area

The studied sediment core of Lagoa da Fazenda (LF, 1°46'51" S, 51°25'19" W, 3 m above sea level) is from an abandoned river of the Baía de Caxiuanã, which nowadays

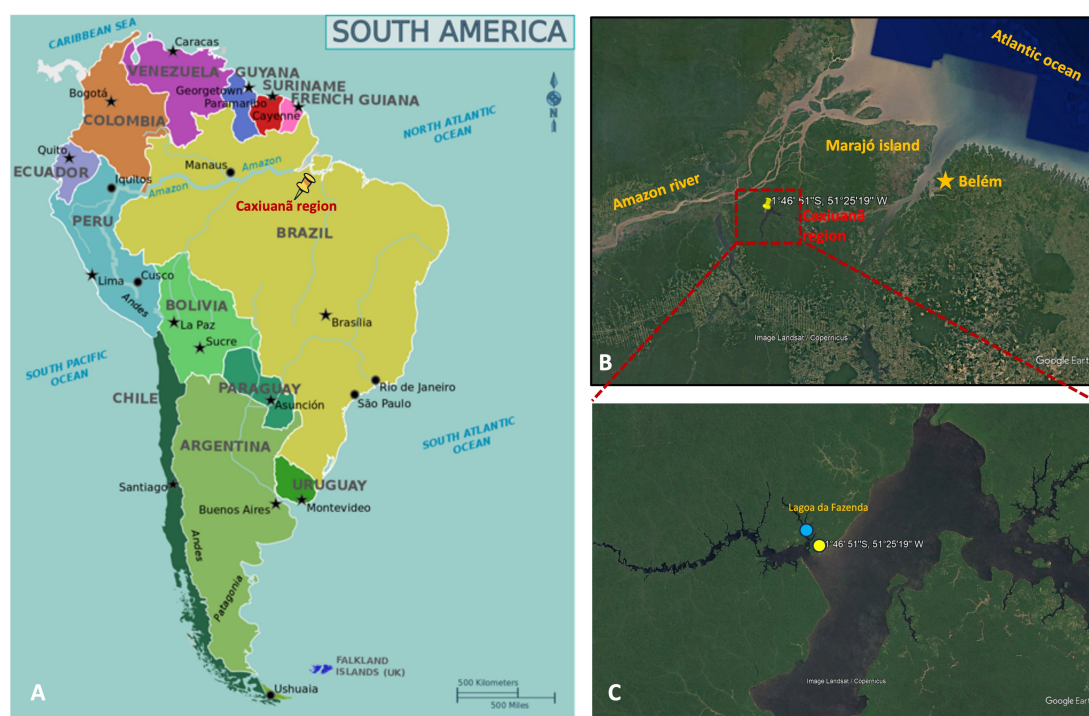
is a small swamp in the rainforest. The site is located ca. 350 km to the west of Belém City (Pará State) in northern Brazil (Fig. 4.1). The Baía de Caxiuanã is a shallow inland bay, which is about 40 km long and 8–15 km wide with water depths ca. 2–5 m, lying on the relatively flat plain between the Xingu River and the Pacajá River. The west bank of the inland bay is the Caxiuanã National Forest Reserve. Amazonian rainforests occur on deep latosols and spodosols (areas with white sand) derived from cretaceous sedimentary rocks from the Alter do Chão Formation and Quaternary sedimentary rocks of the Barreiras Formation. In the Caxiuanã National Forest Reserve, the research station “Estação Científica Ferreira Penna” (ECFPn, 1°44'07" S, 51°27'47" W) is located, which is ca. 7 km northwest of the coring site. The recorded average fluctuations of water levels at ECFPn from December 1995 to April 1996 is 33 cm (Hida et al., 1997). The fluctuating water level is influenced by low and high tides, ranging between 17 and 21 cm. A small east-flowing stream drained the bay via Baía de Portel, Baía do Melgaço, and Rio Pará to the Atlantic Ocean. No modern connection exists between the bay and the Amazon River (ca. 80 km northwest of the coring site). A warm, humid tropical climate controls the study site, without marked dry periods (Nimer, 1989). The climate station Breves is about 100 km east of the coring site. Here, the mean annual temperature is about 26°C, the highest measured temperature is 32.9°C, and the lowest is 22.2°C (Moraes et al., 1997). Mean annual precipitation is about 2500 mm (1969–1980).

Around 85% of the area is covered by unflooded upland forests called *terra firme*, and most of the other area is covered by inundated forests called *várzea* and *igapó*. Forests in the study area are highly diverse. Lisboa et al. (1997) and Ferreira et al. (1997) show that 2452 plant species with a diameter breast height >10 cm were recorded on studied plots (13 hectares) at the ECFPn. The most common tree families and species of *terra firme* forest are *Rinorea guianensis* (Violaceae), *Tetragastris panamensis* (Bursaceae), *Lecythis idatimon*, *Eschweilera coriacea* and *E. grandiflora* (Lecythidaceae), and *Vouacapua americana* (Caesalpiniaceae), Melastomataceae, and Moraceae. Characteristic species of *várzea* forest are *Virola surinamensis* (Myristicaceae), *Pachira aquatica* (Bombacaceae), *Euterpe oleracea* and *Mauritia flexuosa* (Arecaceae). Small areas of savanna-like vegetation with a dominance of herbaceous plants (e.g., Cyperaceae, Poaceae), formed by inundation or human activity, are also found in this region.

Humans have lived in this region since the Pre-Columbian era which is evidenced by several archaeological sites with black soils (*terra preta*) along the shore of the Baía de Caxiuanã (Kern and Costa, 1997). Thermoluminescence-dated ceramic fragments are



not older than 720 yr BP (Kern, 1996). The Rio Curuá record shows a marked occurrence of fires in the study region suggesting the increased human presence since ca. 2500 cal yr BP (Behling and Costa, 2000).



**Fig. 4.1** A: Location of the study area, near Caxiuana bay, in South America. B: Google map of Caxiuana region in northern Brazil. The yellow thumbtack shows the coring site of Lagoa da Fazenda (LF). C: Google map of LF coring site (yellow circle) and previously studied Rio Curuá record (Behling and Costa, 2000; blue circle) in the Caxiuana region.

## 4.3 Methods

### 4.3.1 Core sampling and chronology

The sediment core is 395 cm long and taken from the deepest area of the LF site in northern Brazil (Fig. 4.1), which was collected using a Russian Corer taking sections of 50 cm length. The stratigraphy (Fig. 4.2) of this core was done by visual description. Five samples were taken for Accelerator Mass Spectrometry (AMS) radiocarbon dating, and dated in the Poznań Radiocarbon Laboratory, Poland. The sample at 83 cm ( $3610 \pm 35$  yr BP) was excluded because of possible contamination with old fluvial deposits of probably clay (Table 4.2). The other four dates (Table 4.2) were calibrated by the SHCal20C southern hemisphere calibration curve (Hogg et al., 2013), and the 0 cm ( $-48$  cal yr BP) was calibrated by the calendar dates calibration curve, were used to construct an age-depth model by the Bacon script (Blaauw and Christen, 2011).

### 4.3.2 Pollen and spore analysis

For pollen analysis, a total of 51 pollen samples of 0.5 cm<sup>3</sup> each were taken in about 8 cm intervals along the core. Each sample was taken with a volume of 0.5 cm<sup>3</sup>. Before processing, we added one tablet of exotic *Lycopodium* spores (9666±212) to each sample for calculation of pollen concentration (grains cm<sup>-3</sup>) and pollen accumulation rate (grains cm<sup>-2</sup> yr<sup>-1</sup>). We prepared all samples using standard pollen analytical techniques and acetolysis and mounted each sample with glycerine (Faegri and Iversen, 1989). We identified pollen and spore grains using the reference collection of the Department of Palynology and Climate Dynamics and available literature (e.g. Roubik and Moreno, 1991; Colinvaux et al., 1999). A total of 48 samples were counted. The samples at 248, 312, and 328 cm core depth were not counted as they contained very few pollen grains. Among the counted 48 samples, 44 samples were counted over 300 grains, but 4 samples (at 120, 136, 152, and 168 cm) had relatively low pollen concentrations and were counted to 150 grains for each sample. We used TILIA software of version 2.6.1 to calculate and plot the pollen and spore diagram. The pollen and spore taxa presented in the diagram are percentages of the pollen sum which only includes terrestrial pollen. We grouped all the taxa into broad life forms, including palms, trees and shrubs, herbs, aquatics, and pteridophyta. CONISS module of the TILIA software was used for the cluster analysis of the percentage values of the terrestrial pollen taxa (Grimm, 1987).

### 4.3.3 Macro-charcoal analysis

For charcoal analysis, we continuously took samples of 1 cm<sup>3</sup> in 2 cm thickness. Each charcoal sample was prepared following the method developed by Stevenson and Haberle (2005). First, each sample was dispersed in 5–10 ml 10% KOH for 24h, then we used 6% hydrogen peroxide (H<sub>2</sub>O<sub>2</sub>) to remove organic material and left overnight. At last, each subsample was wet sieved through a 125 µm sieve.

### 4.3.4 Loss-On-Ignition (LOI) and organic C analysis

LOI analysis in this study was carried out according to Heiri et al. (2001). We took a sample of 0.5cm<sup>3</sup> for LOI at each depth same as the pollen sample. The LOI organic material (OM) content of each sample was calculated by the percentage of the difference between the weight after 24 hours of drying at 105°C (W<sub>dry</sub>) and the weight after 4 hours of combustion at 550°C (W<sub>c</sub>) divided by W<sub>dry</sub>:

$$\text{LOI OM content (\%)} = \frac{W_{\text{dry}} - W_{\text{c}}}{W_{\text{dry}}} * 100$$

A total of 51 samples for organic C analysis were taken along the LF core at the same

depth as the pollen samples. The volumes for C samples range from 0.5 to 6 cm<sup>3</sup>. Each sample was dried at 70 °C for 24 hours, and then was finely ground in an agate mortar. Each ground dry sample was weighed ( $W_{\text{dry and ground}}$  (g)) and tested for the percentage of total C content ( $C_{\text{total}}$  (%)) and the percentage of total nitrogen content ( $N_{\text{total}}$  (%)) by Elementar Vario EL III. After that, each sample was burnt at 600°C for 5 hours and weighed ( $W_{\text{burn}}$  (g)). The percentage of inorganic C content in each burn sample ( $C_{\text{burn}}$  (%)) was tested by Elementar Vario EL III. This test requires that the quality of the material after burning for each sample is at least 20 mg. The percentage of organic C content in each sample ( $C_{\text{org}}$  (%)) was calculated by:

$$C_{\text{org}} (\%) = C_{\text{total}}(\%) - C_{\text{burn}}(\%) * \frac{W_{\text{burn}}}{W_{\text{dry and ground}}}$$

The ratio of organic C to total N for each sample was calculated by:

$$\frac{C}{N} = \frac{C_{\text{org}}(\%)}{N_{\text{total}}(\%)}$$

#### **4.3.5 Chemical composition analysis by portable X-ray Fluorescence (pXRF)**

In total 11 samples (depth in 395–390 cm, 330–325 cm, 280–275 cm, 230–225 cm, 180–175 cm, 130–125 cm, 94–89 cm, 70–65 cm, 45–40 cm, 30–25 cm, and 10–5 cm) were taken for semiquantitative chemical composition analysis by pXRF, which were performed in the Institute of Geosciences of the Federal University of Pará. All material was homogenized and formed a single set. Analysis with pXRF was performed on the aggregate pellet of each sample, repeated at least twice. The analyzed elements are represented by their respective oxides ( $\text{Al}_2\text{O}_3$ ,  $\text{SiO}_2$ ,  $\text{TiO}_2$ ,  $\text{Fe}_2\text{O}_3$ ,  $\text{MgO}$ ,  $\text{P}_2\text{O}_5$ ,  $\text{K}_2\text{O}$ ,  $\text{CaO}$ ) with only sulphur (S) being represented in its elemental form, which were determined directly on the pressed natural dried samples. Furthermore, by difference, considering the pXRF results as a total, the LOI was calculated, therefore an approximate value.

#### **4.3.6 Mineralogical identification by X-ray diffraction (XRD)**

The 11 samples mentioned in the chemical composition analysis (section 4.3.5) were also used for mineralogical analysis by XRD. This analysis was performed by a Bruker D2 Phaser X-ray diffractometer equipped with a Cu anode and a Ni-k $\beta$  filter, at the Federal University of Pará, Brazil. We used the powder method. The diffractometer was set in the  $\theta$ - $\theta$  Bragg-Brentano geometry with a Linear Lynxeye detector. Each sample was ground in an agate mortar and measured in reflection mode from 5° to 70° 2 $\theta$  range with 0.02° step size and 38.4 s per step counting time. The mineral characterizations

were performed using the software High Score Plus 5.0, with the aid of the database of the Powder Diffraction Files from the International Centre for Diffraction Data.

### **4.3.7 Mineral identification by Scanning Electron Microscope (SEM) with Energy Dispersive Spectroscopy (EDS)**

In addition to identifying the minerals by XRD, SEM/EDS allows to identify other minerals, which can also obtain images and semi-quantitative (spot and chemical mapping) chemical analysis of the identified minerals. Among the 11 geochemical analysis samples (sections 4.3.5, 4.3.6), the samples of 395–390 cm, 230–225 cm, 130–125 cm, 30–25 cm, and 10–5 cm were analysed by SEM/EDS. In this analysis, the Hitachi TM3000 Scanning Electron Microscope coupled to a Swift ED300 Energy Dispersive X-ray Fluorescence Spectrometer was used, with voltage acceleration from 5 to 15 kV and with SDD detector (161 eV Cu-K $\alpha$ ) from the Institute of Geosciences of the Federal University of Pará. The analysis was performed under a low vacuum without metallization.

## **4.4 Results**

### **4.4.1 Stratigraphy and chronology**

The 395-cm-long LF core consists of decomposed compact black to dark brown peat with a few plant fragments (383–82 cm) containing grey clay materials in the depth of 105–100 cm and wood fragments in the depth of 395–383 and 198–87 cm, compact clay with different shades of grey to black colours (82–16 cm) containing visible charcoal particles in the depth of 58–56 cm and 51–49 cm, decomposed dark brown to brown peat with plant fragments (16–0 cm) (Fig. 4.2; Table 4.1).

The four AMS radiocarbon dates are 6110 $\pm$ 40, 3570 $\pm$ 35, 1800 $\pm$ 35, 150 $\pm$ 30 yr BP at the depth of 395, 188, 55, and 28 cm, respectively (Table 4.2). Based on the dates, the age-depth model was established, which shows that the sediment of the LF sediment record started to accumulate since ca. 7000 cal yr BP.

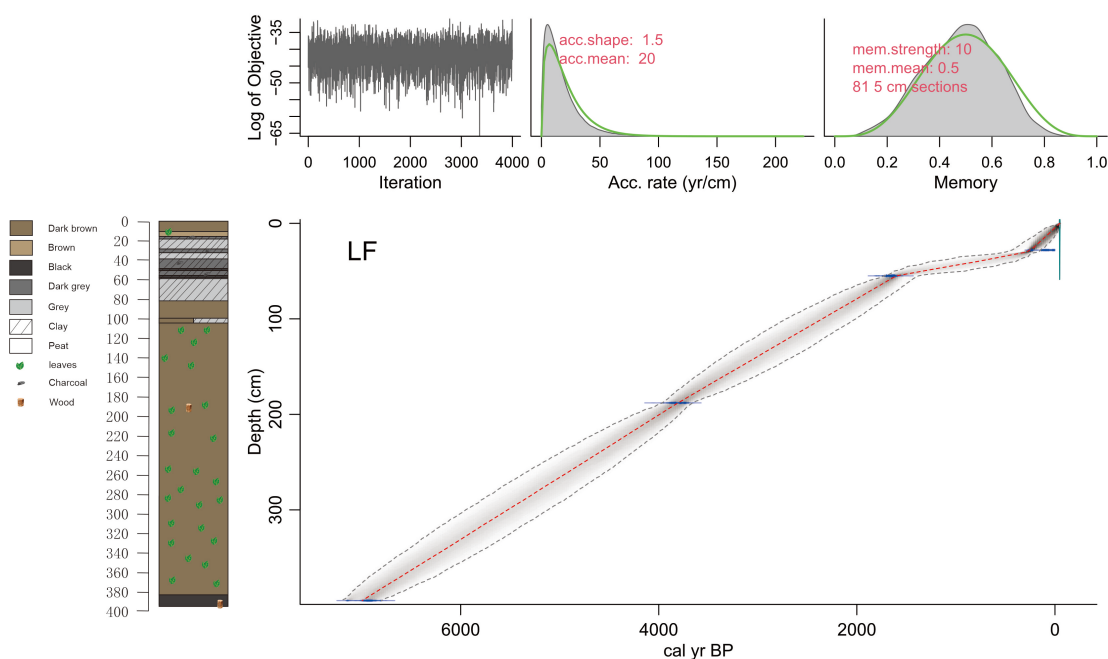
Depth (cm)	Description
16–0	Peat, decomposed, compact 9–0 are dark brown with a few plants 16–9 are brown with more plants
82–16	Grey clay, decomposed, compact 59–37 (58–56 and 51–49 are black), 35–29, 19–16 are dark grey, with visible charcoal

---

395–82	Dark brown peat, decomposed, compact, remained many plants such as leaves fragment
	105–100 with grey clay
	395–394, 198–87 with big wood fragment
	395–383 is black

---

**Table 4.1** Stratigraphy of the LF core.



**Fig. 4.2** Stratigraphy and age-depth model of the LF record. The central dotted red line indicates the ‘best’ model based on the weighted mean age. The outer grey dotted lines with grey shading between them indicate the 95% confidence intervals. The five purple points include four dates of the tested samples and one date at the depth of 0 cm which is the year (1998 CE) of drilling the studied core.

---

Depth(cm)	Lab. Code	Radiocarbon dates ( <sup>14</sup> C yr BP)	Calibrated age (cal yr BP)	Material
28	Poz-159205	150±30	255	Clay
55	Poz-159206	1800±35	1601	Charcoal
83	Poz-149800	3610±35	2066	Peat with clay
188	Poz-144438	3570±35	3804	Wood
395	Poz-144439	6110±40	6994	Wood

---

**Table 4.2** Radiocarbon dates from the LF core.

#### 4.4.2 Pollen and macro-charcoal data

A total of 153 different pollen and spore taxa were identified in the LF core, which

includes 53 unknown pollen types. Important taxa are shown in the pollen diagram (Fig. 4.3). Four pollen zones (LF-I to LF-IV) are recognized, based on terrestrial pollen percentages using constrained cluster analysis CONISS (Grimm, 1987). Pollen concentration and accumulation rate have similar trends throughout the whole core (Fig. 4.3B). Pollen concentration and accumulation rates are relatively low in zone LF-Ia, which are 22000–81000 grains cm<sup>-3</sup> and 1400–5200 grains cm<sup>-2</sup> yr<sup>-1</sup>, respectively. Since the beginning of LF-Ib to the present, they were higher, 22000–490000 grains cm<sup>-3</sup> and 1400–26000 grains cm<sup>-2</sup> yr<sup>-1</sup>, respectively (Fig. 4.3B). The charcoal accumulation rate was low (<0.6 particles cm<sup>-2</sup> yr<sup>-1</sup>) from zone LF-I to LF-IVa, but during LF-IVb, it was higher, which is 0.29–4.5 particles cm<sup>-2</sup> yr<sup>-1</sup> (Fig. 4.3B).

#### A. Zone LF-I (395–248 cm, 7000–4700 cal yr BP)

In zone LF-Ia (395–284 cm, 7000–5300 cal yr BP), tree and shrub pollen is dominant (76–90%), which is represented by *Mabea* (12–41%), *Virola* (8–25%), Melastomataceae (1–24%), Fabaceae (2–12%), *Podocalyx* (1–8%), *Pachira aquatica* (<11%), Moraceae (<10%), *Clusia* (<7%), *Banara/Xylosma* (<6%), Rubiaceae (<5%). Other tree and shrub taxa have relatively low percentages (<3% for each taxon), such as *Cecropia*, *Macrolobium*, *Protium*, *Sloanea*, Anacardiaceae, Apocynaceae, *Didymopanax*. Palm pollen has relatively low value (1–7%), which is represented by *Euterpe/Geonoma* (<5%), *Mauritia* (<4%) and *Mauritiella* (<3%). *Euterpe/Geonoma* became rare (<1%) in the upper part of this zone. Values of herb pollen are relatively low, mainly represented by Cyperaceae (1–7%), Poaceae (1–4%), and Asteraceae (<3%). Aquatics (<2%) and Pteridophyta spores (<4%) have low values throughout the record.

In zone LF-Ib (284–248 cm, 5300–4700 cal yr BP) most pollen and spore taxa have similar values as in zone LF-Ia. The difference is the increase of *Mabea* (27–41%) and decrease of Melastomataceae (1–10%), Rubiaceae (<1%), Fabaceae (3–5%) and *Macrolobium* (<1%). *Euterpe/Geonoma* remain rare as in the upper part of zone LF-Ia. Poaceae slightly decreases (<1%).

#### B. Zone LF-II (248–116 cm, 4700–2600 cal yr BP)

Compared with zone LF-Ib, zone LF-IIa (248–180 cm, 4700–3700 cal yr BP) is characterized by remaining high values of *Mabea*, increases of *Podocalyx* (1–27%) and Melastomataceae (7–41%), but decreases of *Virola* (1–11%), Fabaceae (<6%) and *Clusia* (<4%). Other tree and shrub taxa remain at low levels. In this zone, palm pollen originates mainly from *Mauritiella* (<3%), which has a small increase at the beginning but is lower in the upper part of the zone. Herb pollen is mainly from Cyperaceae (<14%), which also has higher values in the lower part but decrease in the upper part.

Values of Asteraceae (<1%) is lower than in zone LF-I.

Compared with zone LF-IIa, in zone LF-IIb (180–116 cm, 3700–2600 cal yr BP), pollen of *Mabea* (19–41%) and *Podocalyx* (2–16%) remain abundant. However, *Virola* (13–31%) markedly increases, Fabaceae (<14%) increases to the same level as in zone LF-I with fluctuations, while Melastomataceae (5–14%) markedly decreases. Other tree and shrub taxa remain at low values. Palms have lower values due to the decrease of *Mauritiella* pollen (<1%). Herb remains at a low level, with a small decrease of Cyperaceae (<2%) and an increase of Poaceae (1–4%).

#### C. Zone LF-III (116–68 cm, 2600–1800 cal yr BP)

Compared with zone LF-IIb, values of Melastomataceae (15–34%) increase, while *Mabea* (4–18%) markedly decreases to a low level. *Podocalyx* (<1%) becomes very rare, *Virola* (12–21%) slightly decreases but is still relatively abundant. *Ficus* (1–13%), *Clusia* (<5%), *Alchornea* (<3%), *Sloanea* (<3%), *Macrolobium* (1–4%), Malpighiaceae (1–4%) increase. Other tree and shrub taxa almost remain at the same occurrence as zone LF-IIb. Palm taxa remain rare. Poaceae pollen (<1%) are rare.

#### D. Zone LF-IV (68–0 cm, 1800 cal yr BP to present)

Compared with zone LF III, in zone LF-IVa (68–28 cm, 1800–260 cal yr BP), percentages of *Banara/Xylosma* (3–12%) markedly increase. *Virola* (7–22%) and Melastomataceae pollen (4–23%) remain abundant. Pollen of *Mabea* (1–3%) decrease, and *Ficus* (<3%), *Clusia* (<1%), *Alchornea* (<1%), *Sloanea* (<1%), *Macrolobium* (<1%), Malpighiaceae (<2%) became rare. Moraceae increases (2–9%). Cyperaceae (20–48%) greatly increases and is the dominant pollen taxa in the lower part of this zone but is lower in the upper part (5–11%).

Compared with zone LF-IVa, in zone LF-IVb (28–0 cm, 260 cal yr BP to present), values of *Cecropia* pollen (1–50%) strongly increase, while *Banara/Xylosma* (<2%), Melastomataceae (5–12%) and *Virola* (3–13%) decrease. Rubiaceae (<4%) and *Macrolobium* (<1%) slightly increase. Cyperaceae (4–44%) markedly increase to the level same as the lower part of zone LF-IVa.

### 4.4.3 LOI and organic C data

Results of LOI are shown in Fig. 4.4. From 395–116 cm (7000–2600 cal yr BP), the sediment of the LF core can be classified as “peat” (LOI>45%). From 116–68 cm (2600–1800 cal yr BP), the sediment is mixed by “peat”, “muck” (35%<LOI<45%), “organic-rich soil sediment” (20%<LOI<35%), and “mineral soil or sediment with organic material” (LOI<20%). From 68–28 cm (1800–260 cal yr BP), the sediment consists of “organic-rich soil sediment” and “mineral soil or sediment with organic material”. From 28–0 cm (260 cal yr BP to the present), the sediment changed from

“mineral soil or sediment with organic material” to “organic-rich soil sediment”, and then to “peat”. The classification is according to Wüst et al. (2003).

Trends of  $C_{org}$  (%) are similar to LOI (Fig. 4.4). From 395–116 cm (7000–2600 cal yr BP),  $C_{org}$  (%) is high and relatively stable with fluctuations of around 50%, with lower values of 17–36 % in 280–272 cm core depth (5200–5100 cal yr BP). From 116–68 cm (2600–1800 cal yr BP),  $C_{org}$  (%) has stronger fluctuations with values of 7–45%. From 68–28 cm (1800–260 cal yr BP),  $C_{org}$  (%) has the lowest values in the whole record with 4–13%. From 28–0 cm (260 cal yr BP to the present),  $C_{org}$  (%) increases from 5% to 30%.

Bulk density changes are opposite to LOI and  $C_{org}$  (%). Values are low (0.09–0.32 g cm<sup>-3</sup>) from 395–116 cm core depth (7000–2600 cal yr BP), then become high (0.16–0.95 g cm<sup>-3</sup>) from 116–28 cm (2600–260 cal yr BP), and then decrease (0.28–0.88 g cm<sup>-3</sup>) from 28–0 cm (260 cal yr BP to the present).

Changes in peat/sediment and organic C accumulation rates are similar (Fig. 4.4). From 395–68 cm (7000–1800 cal yr BP), peat and organic C accumulation rates are high and stable with values of 0.56–0.67 mm yr<sup>-1</sup> and 29–66 g m<sup>-2</sup> yr<sup>-1</sup>, respectively. From 68–28 cm (1800–260 cal yr BP), sediment and organic C accumulation rates are lower with the values of 0.18–0.6 mm yr<sup>-1</sup> and 11–37 g m<sup>-2</sup> yr<sup>-1</sup>, respectively. From 28–0 cm (260 cal yr BP to the present), peat/sediment and organic C accumulation rates increased to 0.44–0.98 mm yr<sup>-1</sup> and 19–85 g m<sup>-2</sup> yr<sup>-1</sup>, respectively.

C/N ratios stay at high levels in 395–68 cm core depth (7000–1800 cal yr BP) with values of 21–57% (Fig. 4.4). From 68–0 cm (1800 cal yr BP to the present), C/N decreases to 14–22%.

#### 4.4.4 Chemical composition by pXRF

The results of the chemical analyses of the 11 samples using pXRF for the LF core are shown in Fig. 4.6. From 395–284 cm (7000–4700 cal yr BP, LF-I), SiO<sub>2</sub> (31.6%), Al<sub>2</sub>O<sub>3</sub> (10.4–11.4%), TiO<sub>2</sub> (1.1%), K<sub>2</sub>O (1.05–1.13%) mainly display moderate contents, while Fe<sub>2</sub>O<sub>3</sub> (1.8%), S (0.06–0.07%), LOI (52.93–53.78%, indirectly measured by pXRF, the same as below in this section) are relatively low. Only in the depth of 395–390 cm (ca. 7000 cal yr BP) was observed an expressive variation, in which SiO<sub>2</sub> (11.2%), Al<sub>2</sub>O<sub>3</sub> (6.28%), TiO<sub>2</sub> (0.06%), K<sub>2</sub>O (0.09%) are low, but Fe<sub>2</sub>O<sub>3</sub> (2.86%), S (1.17%), and even LOI (78.25%) are high. From 284–116 cm (4700–2600 cal yr BP, LF-II), also SiO<sub>2</sub> (5.47–14.3%), Al<sub>2</sub>O<sub>3</sub> (4.24–7.69%), TiO<sub>2</sub> (0.03–0.1%), K<sub>2</sub>O (0.05–0.08%) are low, but Fe<sub>2</sub>O<sub>3</sub> (2.01–2.95%), S (1.44–2.05%), LOI (72.72–84.14%) are high. From 116–68 cm (2600–1800 cal yr BP, LF-III), the chemical composition is similar to the depth of 284–116 cm, only Fe<sub>2</sub>O<sub>3</sub> (0.05%) and S (0.02%) are very low.



From 68–28 cm (1800–260 cal yr BP, LF-IVa), SiO<sub>2</sub> (59.3–63%), Al<sub>2</sub>O<sub>3</sub> (19.3–24.6%), TiO<sub>2</sub> (1.31–1.55%), K<sub>2</sub>O (1.44–1.93%), Fe<sub>2</sub>O<sub>3</sub> (2.16–3.03%) show the highest values of the whole record, while S (0.01%) and LOI (6.93–12.77%) are lowest. From 28–0 cal yr BP, SiO<sub>2</sub> (45.2%), Al<sub>2</sub>O<sub>3</sub> (11.3%), TiO<sub>2</sub> (1.2%), K<sub>2</sub>O (1.16%), Fe<sub>2</sub>O<sub>3</sub> (1.93%) slightly decrease, while S (0.05%) and LOI (37.79%) are higher. The two LOI calculation methods used in this study are general LOI analysis (section 4.3.4) and the LOI indirectly calculated from pXRF results (section 4.3.5). The results of the latter method (section 4.3.5) include the LOI in minerals, their values are in the same order as the results of general LOI analysis, reinforcing the classification of the LF sediments in section 4.4.3.

#### **4.4.5 Mineralogical composition by XRD**

The mineralogical composition of the 11 samples identified by XRD along the LF core is shown in Fig. 4.5. From 395–284 cm (7000–4700 cal yr BP, LF-I), the inorganic fraction to the sediment mainly consists of quartz, kaolinite and mica, and some anatase. In the depth of 395–390 cm (ca. 7000 cal yr BP) the abundances of quartz, kaolinite and mica are still lower, and anatase was not detected, while cristobalite and montmorillonite were present. From 248–116 cm (4700–2600 cal yr BP, LF-II), the mineralogical composition is similar to 395–390 cm, but without montmorillonite. The low concentration of minerals in 248–116 cm is compensated by the high abundance of LOI, represented mainly by carbonaceous OM from peat. From 116–0 cm (2600 cal yr BP to the present, LF-III and LF-IV), the mineralogical composition is slightly distinct from the interval 395–284 cm (except for 395–390 cm), which consists of abundant quartz, kaolinite, mica sometimes with illite, and anatase. Goethite, which is Fe oxyhydroxide, extend oscillating in low contents throughout the record. The results of mineralogical composition reinforce the classification of sediments in section 4.4.3.

#### **4.4.6 Mineral phases after SEM/EDS**

The images of mineral granules, plant detritus, sponges, diatoms, and charcoal particles identified by SEM/EDS for the five samples, which in the core depth of 395–390, 230–225, 130–125, 30–25, and 10–5 cm, are shown in Fig 4.7. The semi-quantitative (spot and chemical mapping) chemical analysis results of the identified minerals for the five samples are shown in Table 4.3. Among the minerals identified by SEM/EDS throughout the core, iron sulphide stands out considered mainly as pyrite, in addition, were identified as barite, zircon, ilmenite, Ti-magnetite, and rutile. Pyrite was found in all five samples (Fig. 4.7A, B, D, I, J, Table 4.3), being as rhomboids, framboids, and micrometric aggregates, especially in plant tissues. In addition to iron sulphide and

plant tissues, sponges, diatoms, and charcoal particles were identified in different samples. In the sample of 395–390 cm (ca. 7000 cal yr BP, LF-Ia), barite appears as isolated crystals ranging from 10 to 30  $\mu\text{m}$  (Fig. 4.7A), rarely as aggregates. In the sample of 230–225 cm (ca. 4400 cal yr BP, LF-IIa), barite also occurs, spicule of cauxi sponges (Fig. 4.7B). In the sample of 130–125 cm (ca. 2800 cal yr BP, LF-IIb), large quartz fragments and spicules of cauxi were identified (Fig. 4.7E, F). In the sample of 30–25 and 10–5 cm (ca. 260 cal yr BP to the present, LF-IVb), diatoms, cauxi sponges, a mica flake, quartz, and clay aggregates were identified (Fig. 4.7G–J). Hematite and/or goethite are present as accessories throughout the entire core.

Element	Weight % (1)	Weight % (2)	Weight % (3)	Weight % (4)	Weight % (5)	Weight % (6)	Weight % (7)	Weight % (8)	Weight % (9)	Weight % (10)
Carbon				25.289	66.343	61.296	-	-	-	
Oxygen	45.593	43.287	40.943	53.902	30.742	36.253	55.385	63.730	56.407	63.453
Magnesium	0.620	-	-	-	-	-	0.479		0.424	-
Sodium									0.605	-
Aluminum	17.775	4.951	1.868	0.217	1.030	1.015	16.354	13.045	15.931	9.461
Silicon	27.625	5.406	1.928	20.591	1.010	0.859	23.396	17.322	21.059	20.557
Sulfur	1.224	8.577	11.870	-	0.426	0.290	0.267	0.882	-	1.526
Potassium	2.558	0.390	-	-	-	-	1.271	0.671	4.523	1.250
Titanium	1.042	-	-	-	-	-	0.659	-	0.297	-
Iron	3.564	-	-	-	0.449	0.288	2.189	4.349	0.755	2.766
Calcium	-	0.382	-	-	-	-				0.988
Barium	-	37.006	43.391	-						

**Table 4.3** Results of SEM/EDS point chemical analyses for the LF core tested by (1): quartz, cristobalite, montmorillonite, kaolinite, mica, pyrite, goethite/hematite, anatase in the core depth of 395–390 cm; (2): barite, montmorillonite, mica-illite in 395–390 cm; (3): barite and kaolinite in 395–390 cm; (4): cauxi sponges composed by cristobalite and carbonaceous organic matter in 230–225 cm; (5) and (6): detrital carbonaceous matter with kaolinite, quartz and traces of pyrite in 230–225 cm; (7): mineral matrix represented by montmorillonite, kaolinite, quartz, and traces of pyrite in 130–125 cm; (8): a mica-illite grain with pyrite and Fe oxide in 30–25 cm (SEM image is shown in Fig. 7I); (9): mica-illite in 30–25 cm, undulated platy form; (10): mineral matrix in 10–5 cm, which is made of montmorillonite, mica-illite, kaolinite and pyrite.

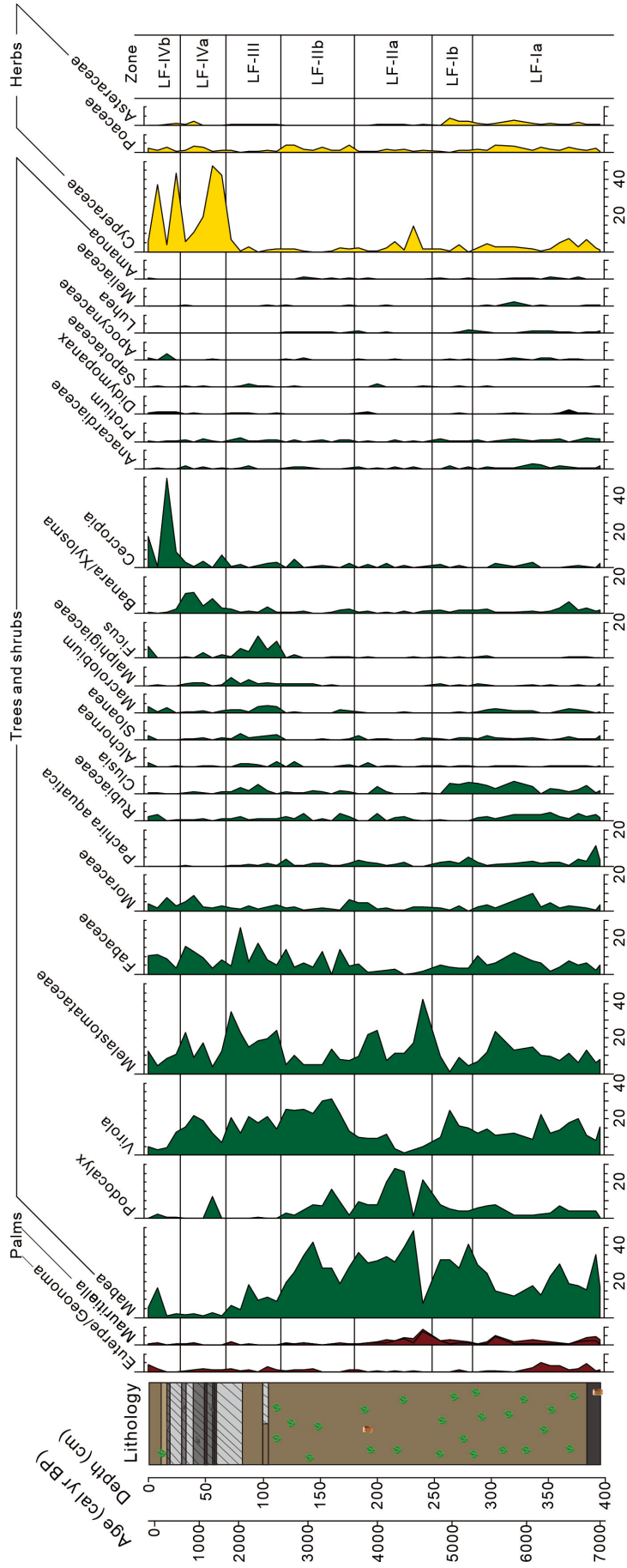
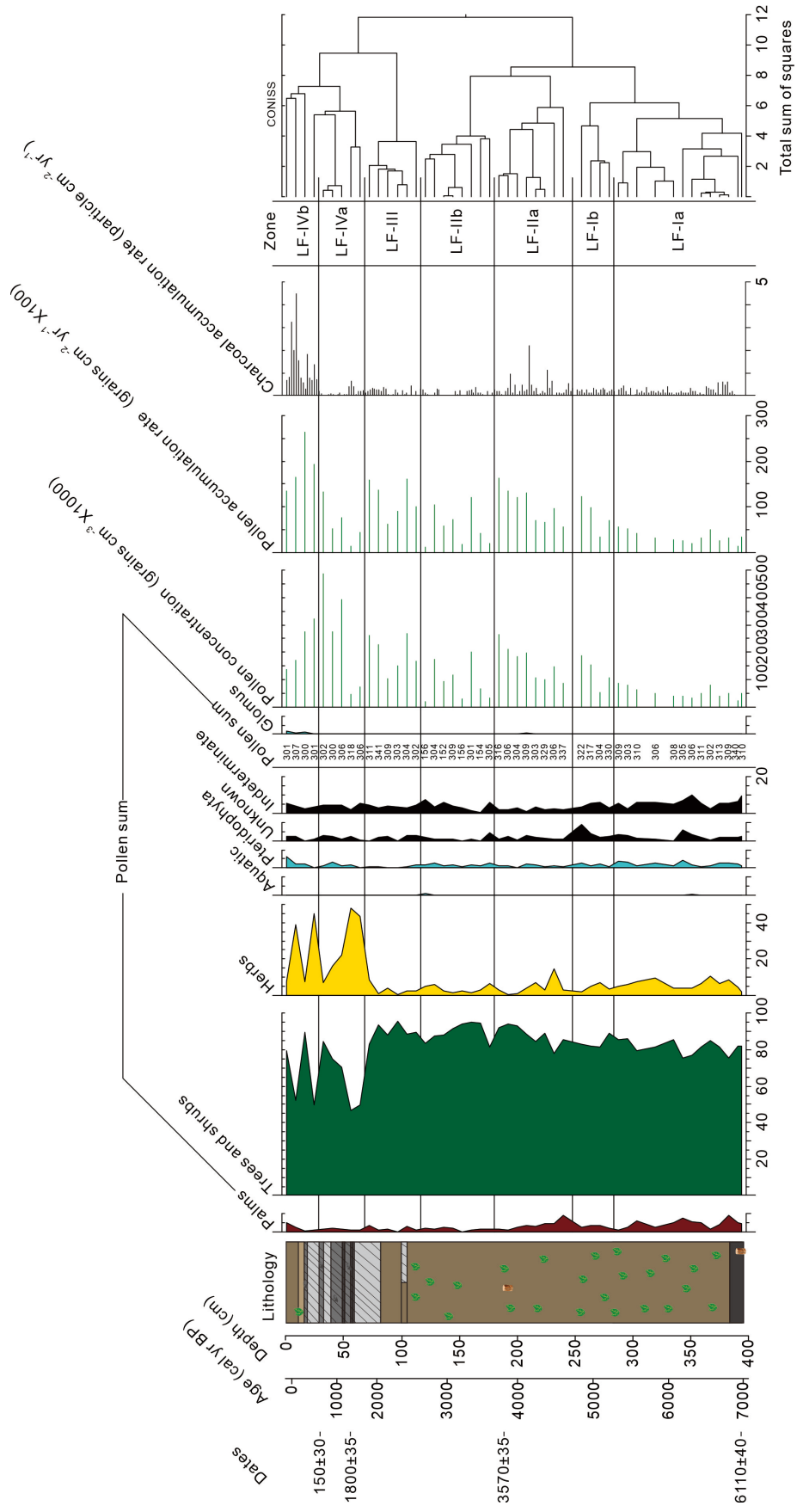
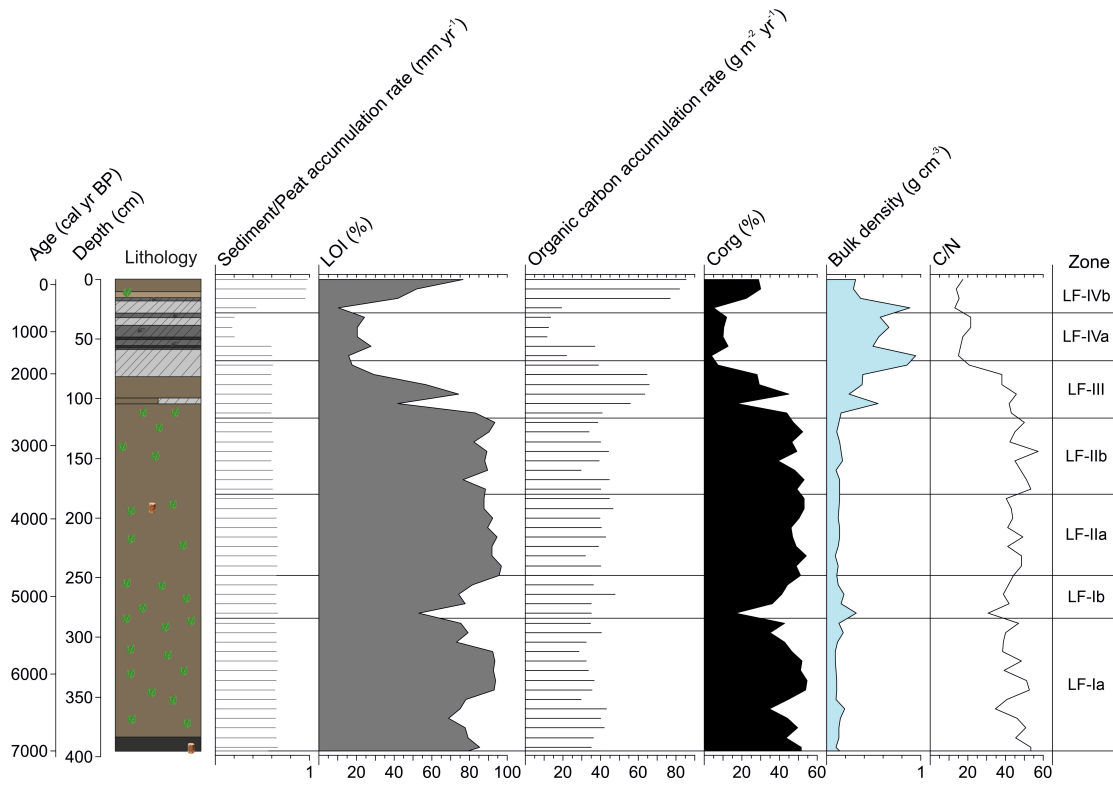


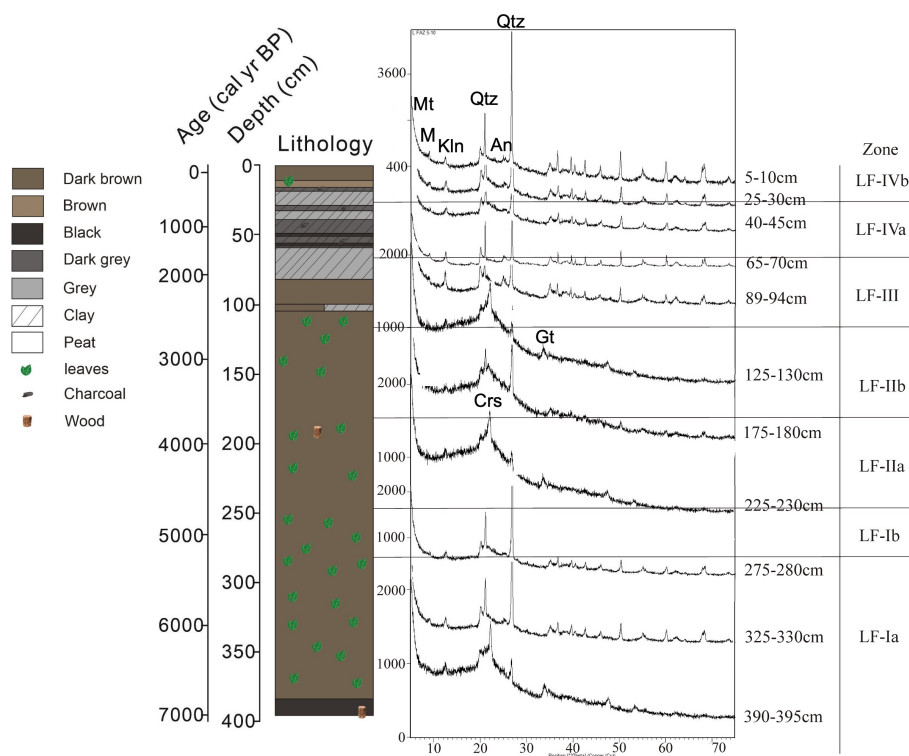
Fig. 4.3A Pollen diagram from the LF record with the percentages of each taxa.



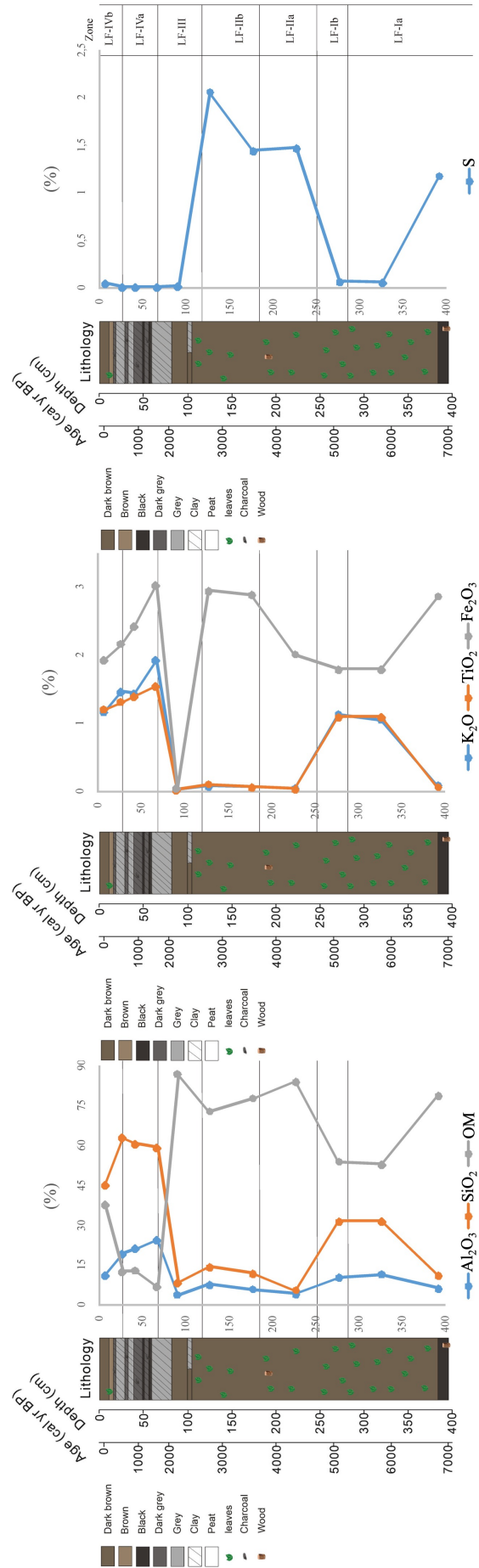
**Fig. 4.3B** Diagram of the total pollen percentages of each life form, pollen zones and the CONISS dendrogram, pollen concentration and accumulation rate, macro-charcoal accumulation rate, radiocarbon ages as well as the age scale.



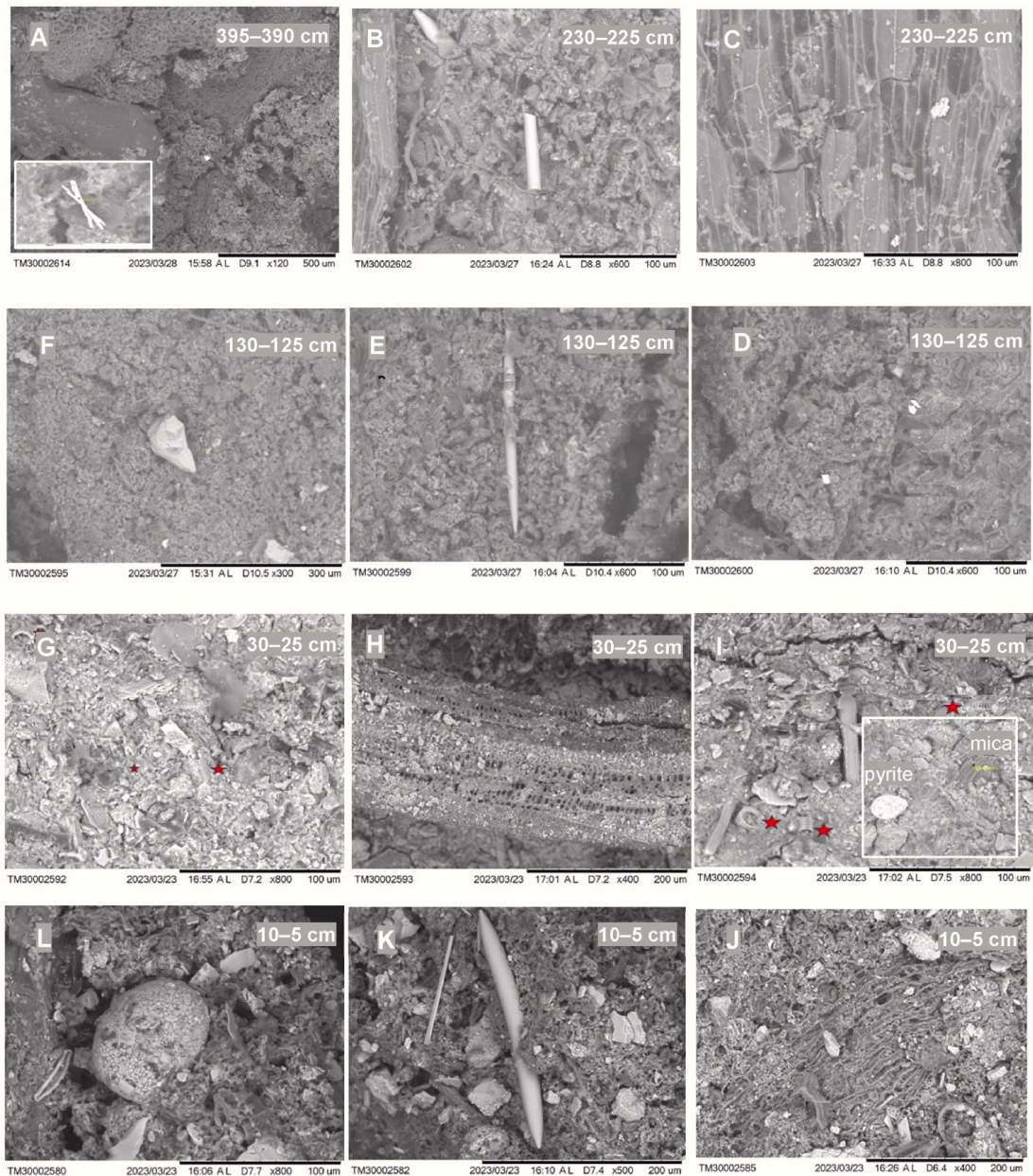
**Fig. 4.4** Loss-on-ignition and organic carbon analysis results of the LF core.



**Fig. 4.5** Mineralogical identification by X-ray diffraction (XRD) for the LF core, analysed by 11 samples. Qtz: quartz; Kln: kaolinite; Mt: montmorillonite; Crs: cristobalite; M: mica-illite; An: anatase; Gt: goethite.



**Fig. 4.6** Chemical composition by portable X-ray Fluorescence (pXRF) for the LF core, analysed by the same 11 samples as XRD. No Sodium (Na) mineral has been detected by XRD, hence Na<sub>2</sub>O is considered to be equal to zero. Organic material (OM) obtained by difference from 100%.



**Fig. 4.7** A: Mineral granules and plant detritus with pyrite micro aggregates and barite crystals (illustrated in the small image in the bottom left corner) in the core depth of 395–390 cm. B: Aggregates of minerals with punctuations of pyrite, plant detritus and cauxi-type spicules in 230–225 cm. C: Detail of plant tissue in 230–225 cm; D: Mineral and plant aggregates punctuated by tiny pyrite crystals in 130–125 cm. E: The same aggregate as D with the presence of a whole cauxi spicule. F: Aggregates of minerals and OM detritus with large quartz fragments and spicules in 130–125 cm. G: Aggregates of mineral grains, diatoms (indicated by red stars) and OM detritus in the core depth of 30–25 cm. H: Detail of a plant tissue detritus at the same depth as A. I: Aggregate of sponge and diatom (red stars) fragments also in 30–25 cm, a pyrite framboid and mica flake are shown in the small image in the bottom right corner. J: Plant material with quartz, clay aggregates, and pyrite framboids in 10–5 cm. K: Well developed cauxi sponges, and minerals fragments in 10–5 cm. L: A pyrite framboid and diatom (on the left of framboid) in 10–5 cm.

## 4.5 Interpretation and Discussion

### 4.5.1 Late Holocene environmental reconstruction

#### A. Period of 7000–4700 cal yr BP (395–248 cm, zone LF-I)

The sediment deposits of the period from 7000–4700 cal yr BP (zone LF-I) is dominated by dark brown peat, which is decomposed, compact, and plant remains such as leaf fragments (Fig. 4.2). The mineral deposition is mainly constituted of quartz, kaolinite, illite/mica, and some amorphous materials (decomposed organic matter) that represent the dispersed cellulosic texture (Fig. 4.5). Anatase and/or rutile are also detected, but pyrite is absent. This mineralogical dominance is confirmed by the relatively moderate contents of SiO<sub>2</sub>, Al<sub>2</sub>O<sub>3</sub>, Fe<sub>2</sub>O<sub>3</sub>, and LOI (analysed in geochemical samples by pXRF differences) and relatively high contents of K<sub>2</sub>O and TiO<sub>2</sub> with low S (Fig. 4.6), which represents the continental sediment provenance probably from *terra firme* (Barreiras or Alter do Chão Formations). However, during the period of 7000–6900 cal yr BP (395–390 cm, base of zone LF-Ia), the amorphous material (e.g., plants, Fig. 4.7A) predominates over the identified continental minerals. Its low levels of Al<sub>2</sub>O<sub>3</sub>, SiO<sub>2</sub>, K<sub>2</sub>O and TiO<sub>2</sub> stand out, while the levels of Fe<sub>2</sub>O<sub>3</sub>, S and LOI are high (Fig. 4.6). The relatively high contents of Fe and S are found as aggregates of pyrite and other iron barium sulphide, probably precursors of pyrite (Fig. 4.7A). Some S formed isolated barium sulphate like barite (small image in the low left corner of Fig. 4.7A). The relatively high concentration of S and organic material indicates reducing environmental conditions at the lowest part of the studied core. S may come from the incursion of oceanic water and alga development close to the studied area. Barium can support the ocean water influence. The oceanic influence at 7000–6900 cal yr BP may indicate that the onset of the sediment accumulation in the study area is driven by Atlantic sea level rise causing the block of the former river.

The high values of LOI (53–96%, same resolution as pollen samples) during the period of 7000–4700 cal yr BP (Fig. 4.4), indicate the beginning and continuing peat accumulation. The trend of organic C content is like in LOI. The peat and organic C accumulation rates were high and relatively stable. These data indicate an inundated environment during this period. Even though not fully synchronized, the relatively lower values of LOI and organic C content in the upper part of this period indicating the low-energy allochthonous input (e.g., flooding), corresponding to the inference of “continental sediments” indicated by mineral and geochemical results.

The pollen record during this period is divided into two subperiods (Fig. 4.3). During the period of 7000–5300 cal yr BP (zone LF-Ia), the pollen record was characterized by



the high abundance of *Virola*, *Mabea*, Melastomataceae and Fabaceae. *Virola* is a large to intermediate rainforest tree (Marchant et al., 2002) that typically grows in inundated forests (Ferreira et al., 1997). The values of *Virola* pollen may represent the abundance of *Virola* plants and the degree of inundation in the local area, as the pollinators of *Virola* are insects (Poinar and Steeves, 2013; Steeves, 2011). Therefore, the high abundance of *Virola* indicates that the inundated forest of the coring site was formed since 7000 cal yr BP. *Mabea* is also a large rainforest tree that often grows in a well-drained (e.g., *terra firme*) environment in Amazonia, but can also occur in seasonally inundated forests (Marchant et al., 2002; Gentry et al., 1993). *Mabea* could be anemophilous (Jablonski, 1967). However, pollinators of *Mabea* could also be bats (Steiner, 1983) and other animals such as mammals, birds, and insects (Viera and de Carvalho-Okano, 1996). The large amount of *Mabea* may indicate the existence of well-drained forests near the coring site. Contrary to *Virola* and *Mabea*, Melastomataceae is a dwarf plant. It could be lianas, dwarf shrubs or trees (Marchant et al., 2002; Colinvaux et al., 1996), generally grow in both well-drained (e.g., *terra firme*) and inundated (e.g., swamp) environments (Somavilla and Graciano-Ribeiro, 2012). The most common pollination strategy of Melastomataceae is local pollination by bees (Dellinger et al., 2022). Therefore, Melastomataceae in this study area mainly grow in the understory of the local inundated forest and/or nearby *terra firme* forests, which can be the indicator of the canopy openness of these forests. This inference can be supported by that the frequency of Melastomataceae is roughly opposite to tall *Virola* and/or *Mabea* throughout our record. Therefore, the relatively high amount of Melastomataceae during this period may indicate a relatively open canopy in the study area. Fabaceae is very diverse in Amazonia, which could be trees of different sizes, shrubs, lianas, and herbs occupying the niches of the understory to the upper canopy (Augusto Gomes de Souza, 2023). They can live in different kinds of environments of Amazonia, such as grasslands, dry deciduous forests, seasonally inundated and tidal forests. However, the dynamics of Fabaceae are still not clear. Moraceae, *Podocalyx*, Rubiaceae, and *Clusia* were relatively frequent and are trees or shrubs that can grow in well-drained environments (Marchant et al., 2002), probably in nearby *terra firme* forests. The presence of Cyperaceae, palms (*Euterpe* and *Mauritiella*), and *Pachira aquatica*, which are generally common in swamp forests (Marchant et al., 2002), indicates the occurrence of small palm swamp areas in the local inundated forest.

Compared with the period of 7000–5300 cal yr BP (zone LF-Ia), the main changes in the period of 5300–4700 cal yr BP (zone LF-Ib) are the increase of *Mabea*, and the decrease of Melastomataceae. It may indicate the expansion of well-drained forests with more closed canopy near the coring site. As the frequency of *Virola* remains at the same level as zone LF-Ia, the local inundated forest almost has not changed.

B. *Period of 4700–2600 cal yr BP (248–116 cm, Zone LF-II)*

The sediment deposits of this period (zone LF-II) were continuously dark brown peat (Fig. 4.2). Probably due to the low resolution of the mineralogical and chemical data, the two subperiods of the pollen record (zone LF-IIa and IIb) could not be identified. The mineralogical and chemical composition of this period resembles the period of 7000–6900 cal yr BP (earliest period in zone LF-Ia), which differs from the period of 7000–4700 cal yr BP. Amorphous materials, which are often in cellulosic form (vegetation) and spongy materials (Fig. 4.7B–F), predominated over crystalline ones. The restricted crystalline materials are represented by quartz, kaolinite, goethite, and sometimes cristobalite. The low contents of SiO<sub>2</sub> and Al<sub>2</sub>O<sub>3</sub> confirm the restricted presence of kaolinite and quartz. The low values of K<sub>2</sub>O and TiO<sub>2</sub> confirm the almost absence of illite/mica and anatase and/or rutile, respectively. The relatively high Fe<sub>2</sub>O<sub>3</sub> contents confirm the presence of goethite and other iron oxides. Part of the iron is also found as pyrite by SEM/EDS (Fig. 4.7B, D), corresponding to the high content of S (Fig. 4.6). Cristobalite often partially composes the sponges (Fig. 4.7B, E). Indicated by the marked presence of sponges (Fig. 4.7B, E), the domain of fresh waters in the period of 4700–2600 cal yr BP is reinforced. However, the high S content suggests some ocean water incursion that can promote significant algal activity, if discharges from other S sources (e.g., volcanic activity, groundwater flowing through sulphur-bearing rocks, and industrial activity; volcanic and industrial activities are unknown in this region during this time).

The values of LOI, organic C content, peat and organic C accumulation rates remained high and more stable during the whole period of 4700–2600 cal yr BP than in the period of 7000–4700 cal yr BP (Fig. 4.4). It indicates that the environment remained inundated, and the low-energy flooding stopped. This inference corresponds to low levels of terrestrial minerals and chemical components.

The pollen record during this period is divided into two subperiods (Fig. 4.3). In the period of 4700–3700 cal yr BP (zone LF-IIa), *Virola* decreased, while Melastomataceae increased. It indicates that the canopy of the inundated forest was more open. Concurrently, *Podocalyx* increased. *Podocalyx* generally grows as small trees in warm regions (Díaz et al., 2007). Duque et al. (2001) investigated plants along the middle stretch of the Caquetá River in Colombian Amazonia. They found in total of 24 individuals of *Podocalyx* with 2.7–39 cm diameter at breast high (dbh). Among the individuals, 9 grow in swamps, 6 grow in well-drained floodplains, and 9 grow in well-drained uplands. Therefore, the marked increase of *Podocalyx* may grow in understories of both locally inundated forests dominated by *Virola* and nearby well-drained terra

*firme* forests dominated by *Mabea*. Combined with the marked decrease of *Virola*, the marked increase of *Podocalyx* may support the inference that the canopy of the locally inundated forest was more open. However, although the pollination of *Podocalyx* is little known, considering the open canopy of the inundated forest, it is possible that *Podocalyx* pollen was (partly) transported by wind.

Compared with the period of 4700–3700 cal yr BP, during the period of 3700–2600 cal yr BP (zone LF-IIb), *Virola* markedly increased while Melastomataceae and *Podocalyx* decreased. This indicates the re-formation of the inundated forest dominated by *Virola* with a more closed canopy.

### C. Period of 2600 cal yr BP to the present (116–0 cm, Zone LF-III, LF-IV)

The sediment deposits during this period (zones LF-III and LF-IV) are formed by alternated brown and grey clays, sometimes black, with some charcoal, leaves and peat. There are no mineralogical and chemical contrasts for the periods of the two identified pollen zones, except for the abundance of mineral phases. The minerals predominate over the amorphous materials (Fig. 4.5). They are mainly represented by kaolinite, quartz, and illite/mica, which is the same as the upper part of the period of 7000–4700 cal yr BP (zone LF-I). From 1800 cal yr BP to the present, relatively high contents of  $\text{Al}_2\text{O}_3$ ,  $\text{SiO}_2$ ,  $\text{K}_2\text{O}$  and  $\text{Fe}_2\text{O}_3$  stand out (Fig. 4.6), which confirms the great dominance of kaolinite, quartz, illite/mica and, probably goethite/hematite. Concurrently, the lowest values of LOI (by pXRF difference), tested in the mineral and geochemical samples (Fig. 4.6) highlight the lowest presence of organic material throughout the sediment core. Although chemical composition analysis by pXRF shows very low S values in the whole period, pyrite framboids were frequently observed in the tissues of micro vegetation fragments in the depth of 30–25 cm and 10–5 cm (zone LF-IVb, Fig. 4.7I, J, L). Sponges are also present (Fig. 4.7I, K) and may contain cristobalite. In the last 10 cm, the  $\text{Al}_2\text{O}_3$  and  $\text{SiO}_2$  contents decrease while the LOI (by pXRF difference) increases (Fig. 4.6), showing the lower contribution of minerals and strong accumulation of organic material in the surface layer. The mineralogical and chemical data in this period suggest that the studied site has suffered greater continental contributions and lost the influence of possible incursions of oceanic waters, becoming eminently a freshwater environment. It is worth to note that the loss of oceanic water influence cannot reflect a sea regression because ca. 1 m height of sediment was accumulated since 2600 cal yr BP.

Analysed in the same resolution as pollen samples, results of LOI, bulk density, organic C content, and peat and organic C accumulation rates (Fig. 4.4) show their changes in a higher time resolution than the LOI (by pXRF difference) results from the

geochemical samples (Fig. 4.6), which follows well with the periods of pollen zones (zone LF-III, LF-IVa, and LF-IVb).

Compared with the period of 4700–2600 cal yr BP, from 2600 to 1800 cal yr BP (zone LF-III), peat and organic C accumulation rates remained high (Fig. 4.4), which indicates that the environment remained an inundated environment. However, the existence of the clay layer (105–100, 82–68 cm, Fig. 4.2), and the lower and fluctuated LOI and organic C content (Fig. 4.4) indicate an influence of river flooding. In terms of vegetation, *Mabea* markedly and *Virola* slightly decreased, while Melastomataceae increased. This may indicate that the local inundated forest and well-drained forests in the surroundings had more open canopies. Another characteristic of this period is the marked increase of *Ficus*, and the increase of *Clusia*, *Alchornea*, *Sloanea*, *Macrolobium*, and Malpighiaceae, which are plants with a wide ecological range (Marchant et al., 2002). *Ficus* and *Clusia* are common in both well-drained environments such as *terra firme* forests (Duivenvoorden and Cleef, 1994) and seasonally inundated forests such as gallery forests (Keating, 2000). Also, Malpighiaceae can be prevalent in different ecological environments (Gentry, 1993). *Alchornea* and *Sloanea* are large trees that often grow in *terra firme* forests (Duivenvoorden and Cleef, 1994; Pivello et al., 1999). *Macrolobium* is common in black water-flooded forests called *igapó* in Brazilian Amazonia and poorly drained upland forests (Duivenvoorden, 1995). Therefore, the changes in the pollen record during the period of 2600–1800 cal yr BP cannot indicate a uniform environmental change, which might be caused by the flooding influence. The marked decrease of *Podocalyx* may also be influenced by flooding. Furthermore, *Cecropia* slightly increased, even though the local occurrence were not high. *Cecropia* is a secondary forest tree (Gentry, 1993), which suggests human disturbance. However, considering the low values of macro-charcoal (Fig. 4.3B), the human influence may be from the surrounding areas.

During 1800–260 cal yr BP (zone LF-IVa), the sediment deposits were clay with different coloured layers. The sediment accumulation rate was lower. LOI, organic C content, and organic C accumulation rate decreased (Fig. 4.4). These changes indicate that the sediment during this period was strongly influenced by allochthonous input such as river flooding from surrounding areas. Therefore, the pollen record may represent the vegetation on a more regional scale. *Virola* and Melastomataceae slightly decreased, which indicates still areas of the local inundated forests. *Mabea*, *Ficus*, *Clusia*, Malpighiaceae, *Macrolobium*, *Alchornea*, and *Sloanea* decreased but still existed. However, Cyperaceae markedly increased with fluctuations. The high abundance of Cyperaceae indicates the formation of a local Cyperaceae swamp. The

fluctuations may be caused by the strong influence of flooding. Furthermore, *Banara* strongly increased. *Banara* is a shrub which often occurs within secondary forests in Brazil (Gentry, 1993; Marchant et al., 2002). The low values of macro-charcoal (Fig. 4.3B) indicate that human activities did not occur in the local area during this period. Therefore, the increase of *Banara* may be due to river flooding and human activities on a more regional scale.

During the period of 260 cal yr BP to the present (zone LF-IVb), the sediment changed from clay to mainly peat with clay layers. Also, LOI, organic C, and peat and organic C accumulation rates increased, like the period of zone LF-III. These changes indicate that flooding became less at the top of the LF record. Cyperaceae remained in high abundance, which indicates that the local environment remained an open swamp dominated by Cyperaceae. *Virola* and Melastomataceae decreased. *Mabea* slightly increased but was still at low levels. *Banara* markedly decreased, while *Cecropia* markedly increased. Combined with the high values of macro-charcoal (Fig. 4.3B), the high abundance of *Cecropia* indicate that the local environment during this period was strongly influenced by human activities. As *Virola* is a large tree and contains red latex, that can be extracted to produce a hallucinogenic power (Gentry, 1993), the decrease of *Virola* is also possible due to use by humans.

#### **4.5.2 Comparison with other records**

The LF record shows that the onset of the sediment accumulation is probably caused by the Atlantic sea level rise, indicated by the relatively high value of S during ca. 7000–6900 cal yr BP. This inference can be supported by the previous palaeoecological study of the lake-like Rio Curuá record, which is also from an abandoned river of Baía de Caxiuanã, ca. 7 km distance to the LF record (Behling and Costa, 2000). The Rio Curuá record shows that the Rio Caxiuanã changed from an active river system into a passive river system since ca. 8000 cal yr BP, as indicated by the change from silty sand to clayey silt deposits, the beginning of pollen and spore accumulation, higher LOI, and lower TiO<sub>2</sub>. The Rio Curuá record shows an increase of *Mauritia* since 7000 cal yr BP, but it is not shown in the LF record. It may be because this river of the LF site is much larger and somewhat deeper. The eustatic Atlantic sea level rise close to modern levels at ca. 8000–7000 cal yr BP, is indicated by the LF and Curuá records and also shown in other available coastal and inland records in northern Brazil (Behling and Costa, 2001). Since ca. 4700 cal yr BP, high values of S of the LF record may indicate the oceanic influence, which may suggest a sea incursion. This inference can correspond to other records in eastern Amazonia. As the Rio Curuá record is from a lake-like ecosystem near the LF study site, it represents the environment on a more regional scale. The Rio

Curuá record shows that the dominant pollen taxa changed from *Mauritia* and Cyperaceae to *Virola* since ca. 5000 cal yr BP (Fig. 4 in Behling and Costa, 2000). Therefore, this change indicates that the environment changed from a shallow lake to an inundated forest, which further suggests a water level rise on a regional scale. The coastal records in eastern Amazonia show the increase of mangroves (Behling, 1996, 2001, 2011; Behling and Costa, 2001), which is the more direct evidence of sea level rise in the mid-Holocene. On the continent, the Peruvian Andes records (e.g., Bird et al., 2011) and lowland records in northern Brazil (e.g. Hermanowski et al., 2015) showed a wetter climate. Combining the above changes with the Atlantic sea level rise, their concurrency may indicate that these changes may be driven by global changes. For example, Bird et al. (2011) suggested that the wetter climate since ca. 5000 cal yr BP is probably caused by changes in precession. Furthermore, the Atlantic sea level rise may be also related to the wetter climate in northern Brazil since ca. 5000 cal yr BP. This is because the flat lowlands in northern Brazil have poorer drainage under a wetter climate causing higher levels of the Atlantic near the coasts along northern Brazil.

Although the macro-charcoal was abundant only in the last 260 years, the changes in the LF record can be further explained from the perspective of human influence from 2600 cal yr BP to the present. This is because the Rio Curuá record shows the high values of micro-charcoal since ca. 2500 cal yr BP, indicating the human activities on the regional scale in the study area (Behling and Costa, 2000). Indicated by the lower and fluctuating values of LOI and organic C content, the LF record was influenced by flooding from 2600 cal yr BP until the present. The flooding is probably caused by soil water loss and soil erosion caused by human activities. In the pollen record of LF, the start of the increase of *Cecropia* during 2600–1800 cal yr BP, the increase of *Banara* during 1800–260 cal yr BP, and the marked increase of *Cecropia* in the last 260 cal yr BP probably reflect first regional and later also the local human influence in the study area.

## 4.6 Summary and Conclusion

To explore the vegetation and environmental changes and the mechanism of the formation of peat and ecosystem dynamics and their influencing factors in eastern Amazonia, we investigated the Lagoa da Fazenda (LF) record from a blocked river channel of Baía de Caxiuanã region. The LF record can be seen as representative of the common setting of the inland bay with many blocked river channels in eastern Amazonia. We studied the vegetation dynamics, peat evolution, organic C accumulation, macro-charcoal, mineral composition, and geochemical composition

based on the multi-proxy analysis of the LF record. The results show that the onset of the peat accumulation and the formation of the local inundated forest at the LF site occurred since 7000 cal yr BP, caused by the indirect influence of the Atlantic sea level rise. During 7000–2600 cal yr BP, peat accumulation was high and the local inundated forest was established with some instabilities, neighbored by *terra firme forest*. The Atlantic sea level further rose since 5000 cal yr BP. From 2600 cal yr BP to the present, the regional study area was influenced by human activities causing soil water loss and soil erosion, which manifests as strong river flooding at the LF site. Influenced by the flooding, peat and C accumulation rates were with more fluctuations during 2600–1800 cal yr BP, became low during 1800–260 cal yr BP, but increased since 260 cal yr BP to the present. The areas of inundated forest became less since 2600 cal yr BP, but a Cyperaceae swamp was formed locally from 1800 cal yr BP to the present. Furthermore, *Banara* increased during 1800–260 cal yr BP, and *Cecropia* became frequent since 260 cal yr BP to the present. Combining the high abundance of *Cecropia* with high values of macro-charcoal, the local LF was strongly influenced by human activities since 260 cal yr BP. The existing large net of small river valleys, which have been formed with larger amounts of peat deposits since 7000 cal yr BP can be seen as an important carbon storage system in eastern Amazonia and should be protected.

## Acknowledgements

This study was supported by the China Scholarship Council (CSC No. 201906190215; for Bowen Wang) and the Brazilian Council for Sciences and Technology (CNPq No. 442871/2018-0 and 305015/2016-8). We thank a lot the editor Claudio Latorre and the reviewers for improving this manuscript.

## References

- Augusto Gomes de Souza, L., 2023. Biodiversity of Fabaceae in the Brazilian Amazon and Its Timber Potential for the Future. *Tropical Forests-Ecology, Diversity and Conservation Status*. IntechOpen.
- Behling, H., 1996. First report on new evidence for the occurrence of *Podocarpus* and possible human presence at the mouth of the Amazon during the Late-glacial., *Vegetation History and Archaeobotany* 5, 241-246.
- Behling, H., 2001. Late Quaternary environmental changes in the Lagoa da Curuca region (eastern Amazonia) and evidence of *Podocarpus* in the Amazon lowland.,

- Vegetation History and Archaeobotany 10, 175-183.
- Behling, H., 2011. Holocene environmental dynamics in coastal, eastern and central Amazonia and the role of the Atlantic sea-level change. *Geographica Helvetica* 66, 208-216.
- Behling, H., Costa, M.L., 2000. Holocene environmental changes from the Rio Curuá record in the Caxiuanã region, eastern Amazon Basin. *Quaternary Research* 53, 369-377.
- Behling, H., Costa, M.L., 2001. Holocene vegetational and coastal environmental changes from the Lago Crispim record in northeastern Pará State, eastern Amazonia. *Review of Palaeobotany and Palynology* 114, 145-155.
- Bird, B.W., Abbott, M.B., Rodbell, D.T., Vuille, M., 2011. Holocene tropical South American hydroclimate revealed from a decadal resolved lake sediment  $\delta^{18}O$  record. *Earth and Planetary Science Letters* 310, 192-202.
- Blaauw, M., Christen, J.A., 2011. Flexible paleoclimate age-depth models using an autoregressive gamma process. *Bayesian Analysis* 6, 457-474.
- Colinvaux, P.A., 1996. Quaternary environmental history and forest diversity in the Neotropics. In: Jackson, J.B.C., Budd, A.F., Coates, A.G. (Eds.), *Evolution and Environment in Tropical America*. University of Chicago Press, Chicago, IL.
- Colinvaux, P., De Oliveira, P.E., Moreno Patiño, J.E., 1999. *Amazon: Pollen Manual and Atlas*. Harwood Academic Publishers, Amsterdam.
- Dellinger, A. S., Kopper, C., Kagerl, K., Schönenberger, J., 2022. Pollination in Melastomataceae: a family-wide update on the little we know and the much that remains to be discovered. *Systematics, evolution, and ecology of Melastomataceae*, pp. 585-607. Cham: Springer International Publishing.
- Díaz, B., Compagnone, R., Suárez, A., 2007. Secondary metabolites from *Podocalyx loranthoides*. *Revista de la Facultad de Farmacia* 70, 28-33.
- Duivenvoorden, J.F., 1995. Tree species composition and rain forest environmental relationships in the middle Caquetá area, Colombia, North-western Amazonia. *Vegetatio* 120, 91-113.
- Duivenvoorden, J.F., Cleef, A.M., 1994. Amazonian savanna vegetation on the sandstone near Araracuara, Colombia. *Phytocoenologia* 24, 197-232.
- Duque, A., Sánchez, M., Cavelier, J., Duivenvoorden, J.F., 2002. Different floristic patterns of woody understorey and canopy plants in Colombian Amazonia. *Journal of Tropical Ecology* 18, 499-525.
- Faegri, K., and Iversen, J., 1989. *Textbook of Pollen Analysis*, fourth ed. Wiley, Chichester, pp.67-89.



- Ferreira, L. V., Almeida, S. S., and Rosário, C. S., 1997. *As áreas de inundação*. In “Caxiuanã” (P. L. B. Lisboa, Coord.), pp. 195–211. Museu Paraense Emílio Goeldi, Belém.
- Gentry, A.H., 1993. A field guide to the families and genera of woody plants of South America (Colombia, Ecuador, Perú). Conservation International, Washington, DC.
- Grimm, E.C., 1987. CONISS: a FORTRAN 77 program for stratigraphically constrained cluster analysis by the method of incremental sum of squares. *Computer & Geosciences* 13, 13-35.
- Gumbrecht, T., Roman-Cuesta, R.M., Verchot, L., Herold, M., Wittmann, F., Householder, E., Herold, N., Murdiyarsa, D., 2017. An expert system model for mapping tropical wetlands and peatlands reveals South America as the largest contributor. *Global Change Biology* 23, 3581–3599.
- Heiri, O., Lotter, A. F., Lemcke, G., 2001. Loss on ignition as a method for estimating organic and carbonate content in sediments: reproducibility and comparability of results. *Journal of paleolimnology* 25, 101-110.
- Hermanowski, B., Da Costa, M. L., Behling, H., 2015. Possible linkages of palaeofires in southeast Amazonia to a changing climate since the Last Glacial Maximum. *Vegetation history and archaeobotany* 24, 279-292.
- Hida, N., Maia, J. G., Hiraoka, M., Shimmi, O., and Mizutani, N., 1997. Notes on annual and daily water level changes at Breves and Caxiuanã, Amazon estuary. In “Caxiuanã” (P. L. B. Lisboa, Coord.), pp. 97–107. Museu Paraense Emílio Goeldi, Belém.
- Hogg, A.G., Hua, Q., Blackwell, P.G., Niu, M., Buck, C.E., Guilderson, T.P., Heaton, T.J., Palmer, J.G., Reimer, P.J., Reimer, R.W., Turney, C.S.M., Zimmerman, S.R.J., 2013. SHCal13 southern hemisphere calibration, 0-50,000 cal BP. *Radiocarbon* 55, 1889–1903.
- Jablonski, 1967. Euphorbiaceae. In B. Maguire (Ed.). *Botany of the Guayana Highland-part IV. Memoirs of the New York Botanical Garden* 17, 80-190.
- Ribeiro, K., Pacheco, F.S., Ferreira, J.W., Sousa-Neto, E.R., Hastie, A., Krieger Filho, G.C., Alvalá, P.C., Forti, M.C., Ometto, J.P., 2021. Tropical peatlands and their contribution to the global carbon cycle and climate change. *Global Change Biology* 27, 489-505.
- Roucoux, K.H., Lawson, I.T., Jones, T.D., Baker, T.R., Honorio Coronado, E.N., Gosling, W.D., L’ähteenoja, O., 2013. Vegetation development in an Amazonian peatland. *Palaeogeography, Palaeoclimatology, Palaeoecology* 374, 242–255.
- Keating, P.L., 2000. Chronically disturbed páramo vegetation at a site in southern

- Ecuador. *Journal of the Torrey Botanical Society* 127, 162-171.
- Kelly, T.J., Lawson, I.T., Roucoux, K.H., Baker, T.R., Jones, T.D., Sanderson, N.K., 2017. The vegetation history of an Amazonian domed peatland. *Palaeogeography, Palaeoclimatology, Palaeoecology* 468, 129–141.
- Kern, D. C., 1996. “Geoquímica e Pedogeogúmica de Sítios Arqueológicos com Terra Preta na Floresta Nacional de Caxiuana (Portel-Pará).” Unpublished Ph.D. dissertation, Universidade Federal do Pará, Pará.
- Kern, D., Costa, M.L. 1997. Composição Química de Solos Antropogênicos Desenvolvidos em Latossolo Amarelo Derivado de Lateritos. *Geociências (UNESP)*. 16: 157-175.
- Lisboa, P. L. B., Silva, A. S. L., and Almeida, S. S., 1997. Florística e estrutura dos Ambientes. In “Caxiuanã” (P. L. B. Lisboa, Coord.), pp. 163–193. Museu Paraense Emílio Goeldi, Belém.
- Marchant, R., Almeida, L., Behling, H., Berrio, J.C., Bush, M., Cleef, A., Duivenvoorden, J., Kappelle, M., De Oliveira, P., Teixeira de Oliveira-Filho, A., Lozano-Garcia, S., Hooghiemstra, H., Ledru, M.-P., Ludlow-Wiechers, B., Markgraf, V., Mancini, V., Paez, M., Prieto, A., Rangel, O., Salgado-Labouriau, M.L., 2002. Distribution and ecology of parent taxa of pollen lodged within the Latin American Pollen Database. *Review of Palaeobotany and Palynology* 121, 1–75.
- Moraes, J. C., Costa, J. P. R., Rocha, E. J. P., and Silva, I. M., 1997. Estudos hidrometeorológicos na Baía do Rio Caxiuanã. In “Caxiuanã” (P. L. B. Lisboa, Coord.), pp. 85–95. Museu Paraense Emílio Goeldi, Belém.
- Nimer, E., 1989. “Climatologia do Brasil.” Fundação Instituto Brasileiro de Geografia e Estatística, Rio de Janeiro.
- Page, S. E., Rieley, J. O., Banks, C. J., 2011. Global and regional importance of the tropical peatland carbon pool. *Global Change Biology* 17, 798–818.
- Pivello, V.R., Shida, C.N., Meirelles, S.T., 1999. Alien grasses in Brazilian savannas: a threat to the biodiversity. *Biodiversity & Conservation* 8, 1281-1294.
- Poinar Jr, G., Steeves, R., 2013. *Virola dominicana* sp. nov.(Myristicaceae) from Dominican amber. *Botany* 91, 530-534.
- Roubik, D.W., Moreno, J.E., 1991. Pollen and Spores of Barro Colorado Island, *Monographs in Systematic Botany*. 36. Missouri Botanical Garden, the United States.
- Somavilla, N. S., Graciano-Ribeiro, D., 2012. Ontogeny and characterization of aerenchymatous tissues of Melastomataceae in the flooded and well-drained soils

- of a Neotropical savanna. *Flora-Morphology, Distribution, Functional Ecology of Plants* 207, 212-222.
- Steeves, R. A. D., 2011. An intrageneric and intraspecific study of morphological and genetic variation in the Neotropical *Compsonura* and *Virola* (Myristicaceae), Doctoral dissertation, University of Guelph.
- Steiner, E., 1983. Pollination of *Mabea occidentalis* (Euphorbiaceae) in Panama. *Syst. Bot* 8, 105-117.
- Stevenson, J., Haberle, S., 2005. Macro Charcoal Analysis: A Modified Technique Used by the Department of Archaeology and Natural History. Australian National University, Canberra
- Swindles, G.T., Morris, P.J., Whitney, B., Galloway, J.M., Gałka, M., Gallego-Sala, A., Macumber, A.L., Mullan, D., Smith, M.W., Amesbury, M.J., Roland, T.P., Sanei, H., Patterson, R.T., Sanderson, N., Parry, L., Charman, D.J., Lopez, O., Valderamma, E., Watson, E.J., Ivanovic, R.F., Valdes, P.J., Turner, T.E., Lahteenoja, O., 2017. Ecosystem state shifts during long-term development of an Amazonian peatland. *Global Change Biology* 24, 738–757.
- Vieira, M. F., de Carvalho-Okano, R. M., 1996. Pollination Biology of *Mabea fistulifera* (Euphorbiaceae) in Southeastern Brazil. *Biotropica* 28, 61–68.
- Wang, B., Hapsari, K. A., Horna, V., Reiner, Z., Behling, H., 2022. Late Holocene peatland palm swamp (*aguajal*) development, carbon deposition and environment changes in the Madre de Dios region, southeastern Peru. *Palaeogeography, Palaeoclimatology, Palaeoecology* 594, 110955.
- Wüst, R.A., Bustin, R.M. and Lavkulich, L.M., 2003. New classification systems for tropical organic-rich deposits based on studies of the Tasek Bera Basin, Malaysia. *Catena* 53, 133-163.
- Xu, J., Morris, P. J., Liu, J., Holden, J., 2018. PEATMAP: Refining estimates of global peatland distribution based on a meta-analysis. *Catena* 160, 134–140.

# Chapter 5 Synthesis

## 5.1 Overview of the Amazonian climate in the Holocene

To understand the role of climate in ecosystem dynamics and peat accumulation in Amazonia, a short introduction to modern and past climate is needed here. The natural climate on a large scale in Amazonia is mainly controlled by the migration of the solar insolation maximum (the so-called caloric equator) and sea surface temperature (SST). The atmospheric circulation caused by thermal contrast (Chapter 1 section 1.1) between the caloric equator and around 30° latitudes in both hemispheres is called Hadley circulation. Influenced by the Coriolis force, north-south surface branches of Hadley circulation form northeast (NE) and southeast (SE) trade winds in the northern and southern hemispheres respectively. The Inter-Tropical Convergence Zone (ITCZ) is the air mass convergence with prolific rainfall at the boundary of NE and SE trade winds, and thus tracks the migration of the band of solar insolation maximum (Vonhof and Kaandorp, 2009).

The migration of solar insolation maximum also drives South America Monsoon System (SAMS) (Vera et al., 2006; Zhou and Lau, 1998; e.g., Fig. 5.1, 5.2). In October of each year (Phase I), as the solar insolation maximum moves from the northern hemisphere to near the equator, the air mass in the lower troposphere (on the surface of the earth) is heated and vertically moves to the upper troposphere, forming a center of lower-level tropospheric convergence on the Amazon basin (Fig. 5.1a). During the latter half of November to the end of December (Phase II), the solar insolation maximum further moves southward as far south as the Southern Tropic (ca. 23.5°S). The heating center during that time is in the east of the central Andes between 16°S to 26°S (Fig. 5.3), close to Gran Chaco in Bolivia. Here, the air mass convergence in the heating center forms a clockwise cyclone in the lower troposphere (Fig. 5.1b), generally called Chaco low. This clockwise direction is driven by the stronger Coriolis force in the higher latitudes. Specifically, as the cycle of a lower latitude is larger than a higher latitude in the southern hemisphere, the running speed of a lower latitude is faster. Thus, the wind blowing from a lower to a higher latitude runs easterly (the earth rotates from west to east) to keep its inertia of faster speed, while the wind blowing from a higher to a lower latitude runs westerly to keep its slower speed. This cyclone brings rainfall to the southern Amazonia (Fig. 5.4a). Concurrently, the eastern part of this clockwise cyclone changes the direction of northeast trade winds forming a strong northwest-to-southeast flow in the lower troposphere (Fig. 5.1b). This low-level flow converging

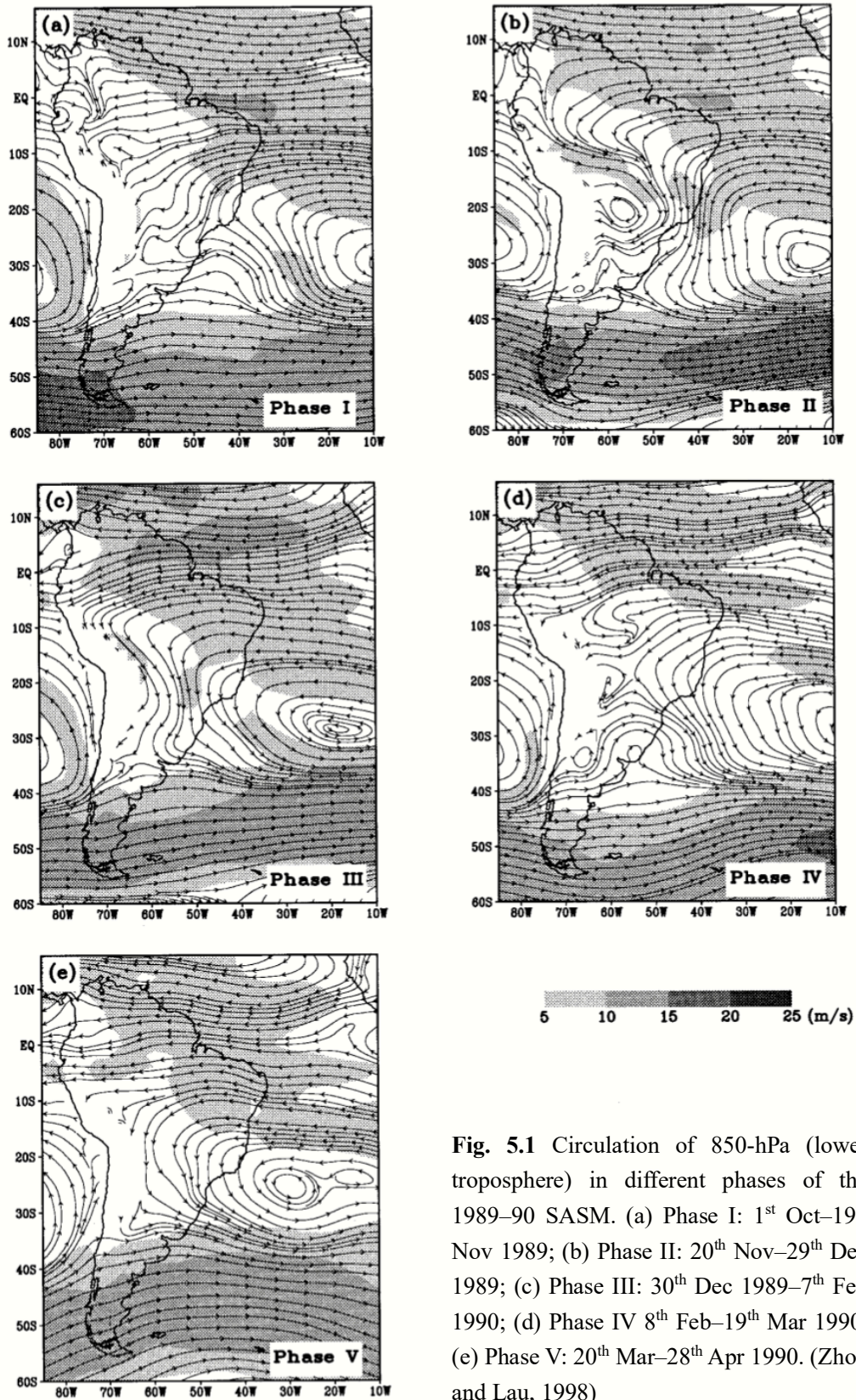
with the western part of the anticlockwise anticyclone on the subtropical Atlantic (probably formed by the lower temperature of the ocean as it has higher specific heat capacity than lands), forms the northwest-to-southeast South Atlantic convergence zone (SACZ), causing severe thunderstorms in southeastern Brazil (Fig. 5.1b; Fig. 5.4a). From the next year January until the beginning of February (Phase III), the solar insolation maximum starts to move northward but is still close to the Southern Tropic. The heating center moves a little northwestward to the Bolivian highlands (Fig. 5.3). It forms an anticlockwise anticyclone in the upper troposphere, called the Bolivian high (Fig. 5.2c). Concurrently, SACZ moves to the southwestward in the lower troposphere (Fig. 5.1c). From early February to the end of April (Phase IV and V), as the solar insolation maximum goes further north, the heating center with heavy precipitation moves northward (Fig. 5.4c and d). It makes the low-level northwest-to-southeast monsoon that is prevailing in Phase II and III firstly break (Fig. 5.1d), then disappear and is replaced by normal easterlies (Fig. 5.1e). It marks that SASM withdraws. SASM in the summer of the southern hemisphere (Phase I to IV) brings over 50% of the total annual precipitation in the monsoon region.

SST also plays an important role in the Amazonia climate, which mainly includes the SSTs of the tropical Atlantic and Pacific Oceans. The influence of the tropical Atlantic SST on the Amazonia climate can be combined with SASM. The colder (warmer) North Atlantic surface can enhance (diminish) the Southeast trade winds by increasing (decreasing) the thermal contrast between the equator and higher latitudes. The SST of the South Atlantic may influence the Amazonia moisture by affecting SACZ. In the Pacific, the El Niño–Southern Oscillation (ENSO) is well-known. ENSO in the aspect of ocean behaves as above-average SST (El Niño) and below-average SST (La Niña) in the eastern tropical Pacific Ocean. ENSO is closely linked with trade winds, which have intense (relaxed) trade winds during La Niña (El Niño), also influenced by random disturbances such as westerly wind bursts and the depth of thermocline (Fedorov and Philander, 2000). The modern data analysis results show that La Niña leads to pronouncedly increasing rainfall along the eastern flanks of the Andes and on the Altiplano-Puna Plateau, also in the Amazon drainage basin but to a lesser extent (Bookhagen and Strecker, 2010). Although not as strong as during La Niña, El Niño also brings more rainfall than non-El Niño period especially in the western flanks of the Andes facing the Pacific, and to a lesser degree in northern Peru, coastal Ecuador, Colombia and most areas of Amazon basin.

Representative records in different regions of the Amazonia and its adjacent areas (Andes and lowlands) during the Holocene mainly show twice SASM intensifications

and/or ITCZ southward migrations: (1) during the Little Ice Age (LIA; ca. 550–130 cal yr BP); (2) since ca. 5000 cal yr BP. During the LIA, the SASM intensification and/or ITCZ southward migration is indicated by: the wetter climate demonstrated by more negative oxygen isotopic ratios ( $\delta^{18}\text{O}$ ) in many records in the southwest (Fig. 5.5 sites 1–4, Fig. 3.5; e.g., Apaéstegui et al., 2014; Bird et al., 2011a; Reuter et al., 2009; Thompson et al., 2013), SACZ southward migration in the southeast (Fig. 5.5 sites 5–10, Fig. 5.8; Novello et al., 2018 and references therein), and drier climate shown by lower Titanium (Ti) in the marine Cariaco record in Venezuela that located north of the equator (Fig. 5.5 site 11; Haug et al., 2001). Not as much evidence as during the LIA, the representative records that are explicitly interpreted as the SASM intensification or ITCZ southward migration since ca. 5000 cal yr BP are only the Andean records that show a wetter climate (e.g., Fig. 5.5 site 3; Bird et al., 2011b and references therein) and the Cariaco record that shows a drier climate in the west of the Amazonia. In the east, only a multi-proxy palaeoecological record shows a wetter climate since ca. 5000 cal yr BP (Fig. 5.5 site 12; Hermanowski et al., 2015 and references therein), which seems consistent with the inference of the SASM intensification. An Atlantic sea level rise in northeastern Amazonia (Fig. 5.5 sites 13–17; Behling, 2011 and references therein) and a shorter periodicity of El Niño (from 15 years to 2–8.5 years) in the Ecuadorian Andes (Fig. 5.5 site 18; Rodbell et al., 1999) were also recorded since ca. 5000 cal yr BP. Partially representative records are shown in Fig. 5.6 to 5.9.

The broadly uniform SASM intensifications and/or ITCZ southward migrations can be considered intense NE trade winds. It can be driven by more thermal contrast between the equator and the northern hemisphere. Cooler SST in the North Atlantic may intensify this process. SASM intensification and/or ITCZ southward migration well-fitted cooler northern hemisphere and lower North Atlantic SST during LIA (Bird et al., 2011a; Vuille et al., 2012) supporting the inference. The underlying driver of the changes in the Holocene may be the earth's orbit forcing. For example, Bird et al. (2011b) thought that SASM intensifications and/or ITCZ southward migrations in the Holocene are probably caused by changes in precession. However, details of how the various components of the earth's orbit changes work on earth's climate are not clear. Here, we provide a possible connection of the observed phenomenon: the earth's orbit changes may cause a cooler northern hemisphere (less solar insolation) and warmer south hemisphere (assuming the total solar radiation earth receives is the same when earth's orbit changes), which leads to SASM intensifications and/or ITCZ southward migrations in Amazonia and its adjacent areas, and South Atlantic level rise when the sea water expands with heat.



**Fig. 5.1** Circulation of 850-hPa (lower troposphere) in different phases of the 1989–90 SASM. (a) Phase I: 1<sup>st</sup> Oct–19<sup>th</sup> Nov 1989; (b) Phase II: 20<sup>th</sup> Nov–29<sup>th</sup> Dec 1989; (c) Phase III: 30<sup>th</sup> Dec 1989–7<sup>th</sup> Feb 1990; (d) Phase IV: 8<sup>th</sup> Feb–19<sup>th</sup> Mar 1990; (e) Phase V: 20<sup>th</sup> Mar–28<sup>th</sup> Apr 1990. (Zhou and Lau, 1998)

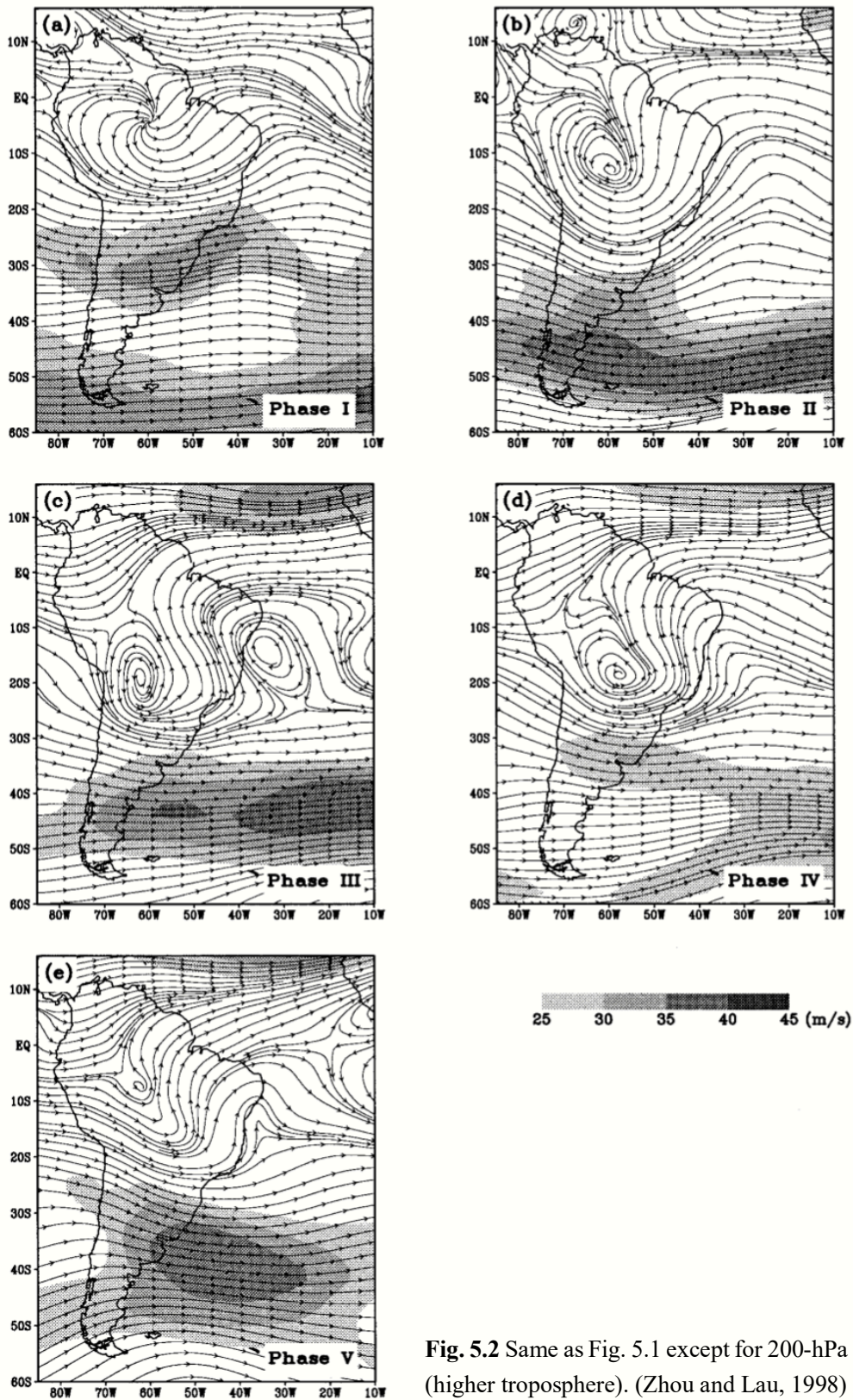
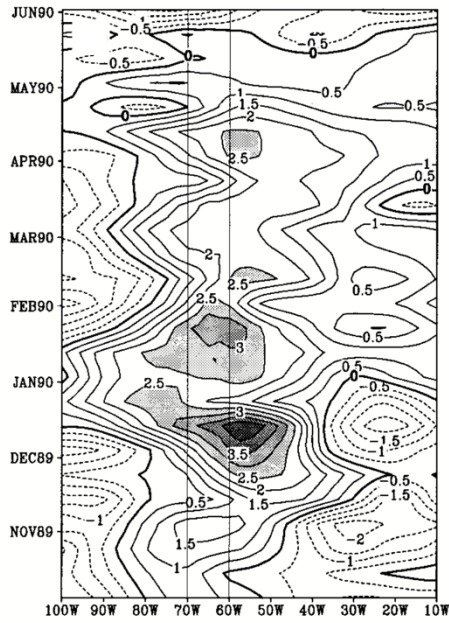
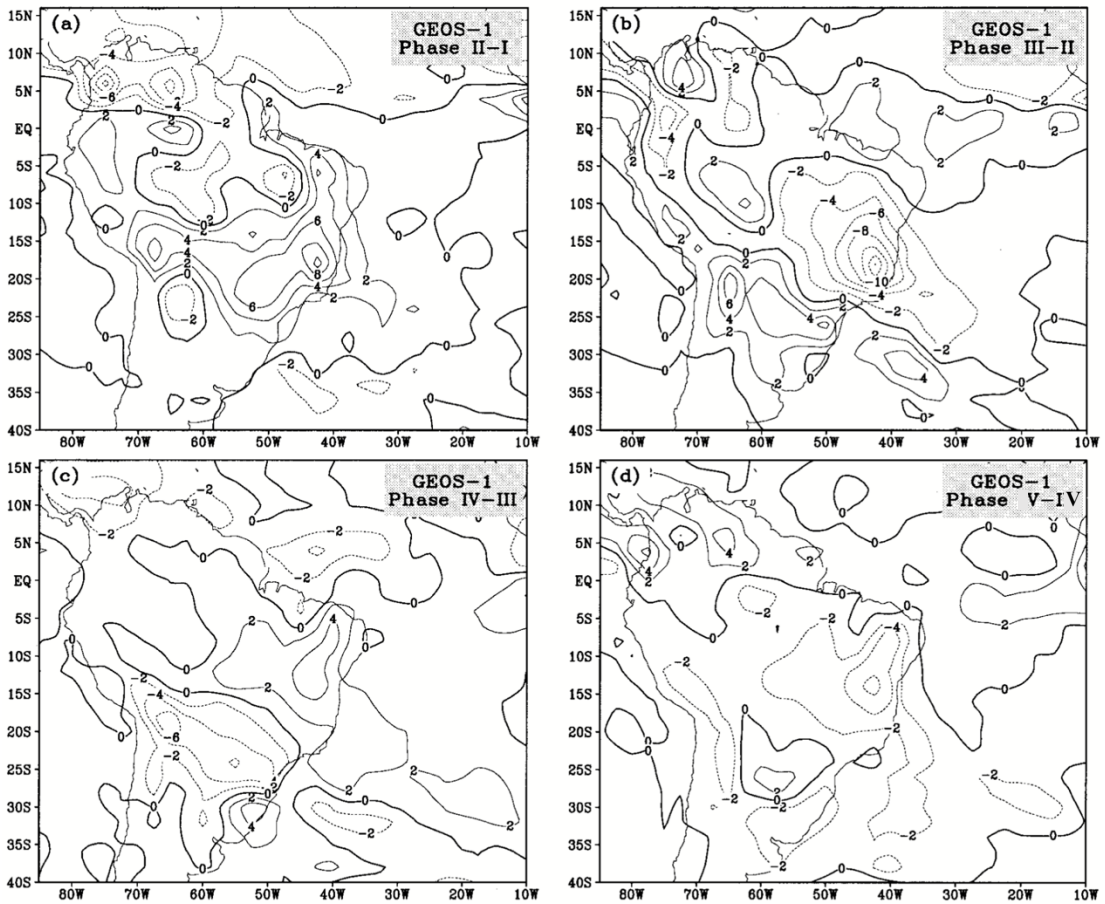


Fig. 5.2 Same as Fig. 5.1 except for 200-hPa (higher troposphere). (Zhou and Lau, 1998)

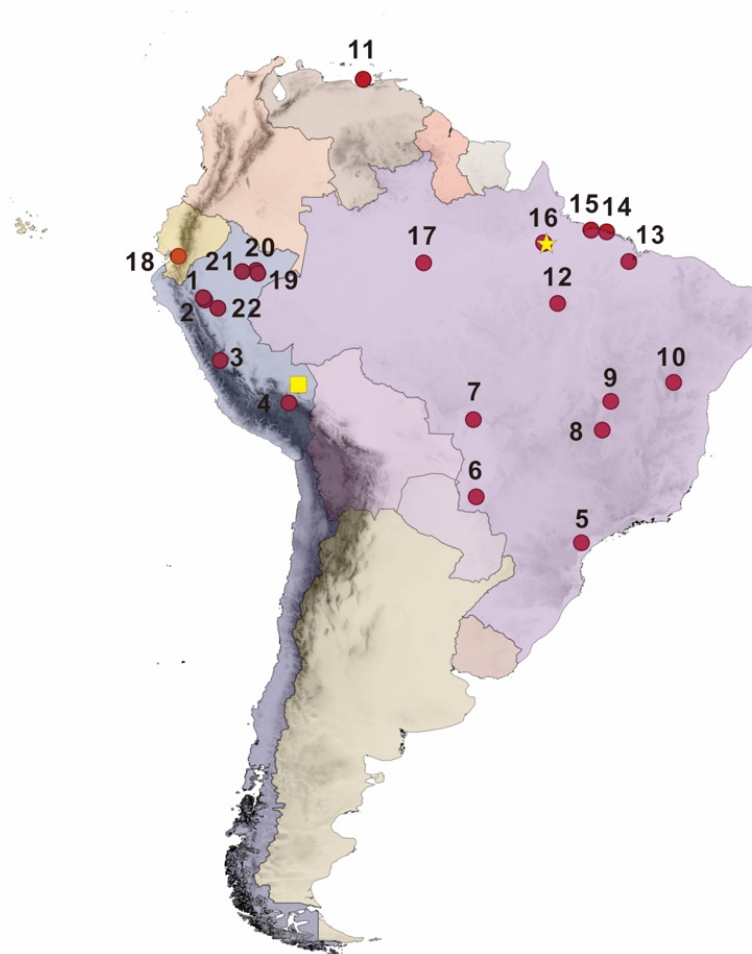




**Fig. 5.3** Time evolution of 200–600-hPa mean and 268–168S averaged temperature (K). The vertical thin lines indicate the east–west boundaries of the central Andes. (Zhou and Lau, 1998)



**Figure. 5.4.** The precipitation difference between each next two phases. Phases are same with Fig. 5.1 and 5.2. (Zhou and Lau, 1998)



**Figure. 5.5** Study sites discussed in the text. Our study area of Madre de Dios (cores of LAA and LAL) is marked by the yellow square. Our study area of Lagoa da Fazenda (LF core) is marked by the yellow star. Red circles 1–21 are study sites used for discussion. Site **1**. Palestina cave (870 m a.s.l, Apaéstegui et al., 2014); **2**. Cascayunga cave (two speleothems connected: CAS-A (930 m a.s.l) and CAS-D (841 m a.s.l), Reuter et al., 2009); **3**. Pumacocha cave (4300 m a.s.l, Bird et al., 2011a, b); **4**. Quelccaya Ice Cap (5670 m a.s.l, Thompson et al., 2013); **5**. Cristal cave (no precise elevation, Taylor, 2010; Vuille et al., 2012); **6**. JAR4+JAR1 in Jaraguá cave (570 m a.s.l, Novello et al., 2018); **7**. ALHO6+CUR4 in Pau d’Alho and Curupira caves (no precise elevation, Novello et al., 2016); **8**. Tamboril cave (no precise elevation, Wortham et al., 2017); **9**. SBE3+SMT5 in Goiás State (631m a.s.l, Novello et al., 2018); **10**. Iraquara caves (no precise elevation, Novello et al., 2012); **11**. Cariaco Basin (drilled at a water depth of 893 m, Haug et al., 2001); **12**. Lagoa da Cachoeira (705 m a.s.l, Hermanowski et al., 2015); **13**. Lago Aquiri (10 m a.s.l, Behling and Costa, 1997); **14**. Braganca Peninsula (includes three records: Campo Salgado, Bosque de Avicennia, and Furo do Chato, 1.9–2.7 m a.s.l, Behling and Costa 1997); **15**. Lago Crispim (1–2 m a.s.l, Behling and Costa, 2001) and Lagoa da Curuça (35m a.s.l, Behling 1996, 2001); **16**. Rio Curuá (3 m a.s.l, Behling and Costa, 2000; Costa et al., 1997); **17**. Lago Calado (23 m a.s.l, Behling et al. 2001); **18**. Laguna Pallcacocha (4060 m a.s.l, Rodbell et al., 1999); **19**. San Jorge (120 m a.s.l, Kelly et al., 2017; Lähteenoja et al., 2009); **20**. Quistococha (no precise elevation, Roucoux et al., 2013; Lähteenoja et al., 2009); **21**. Aucayacu (no precise elevation, Swindles et al., 2017); **22**. Lake Limón (600 m a.s.l, Parsons et al., 2018). Twelve countries in South America are marked by boundary lines and painted in different colors. Shades represent elevation, the darker shades, the higher elevation.

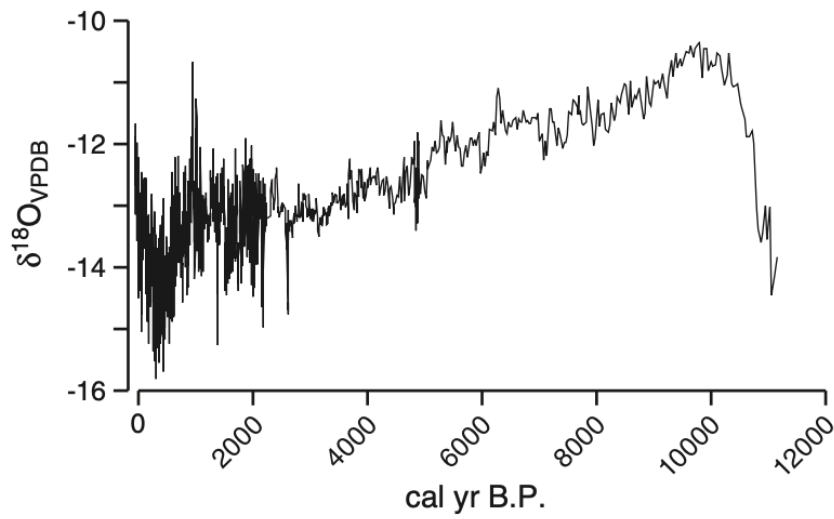


Fig. 5.6  $\delta^{18}\text{O}$  record from Pumacocha (Fig. 5.5 site 3; Bird et al., 2011b).

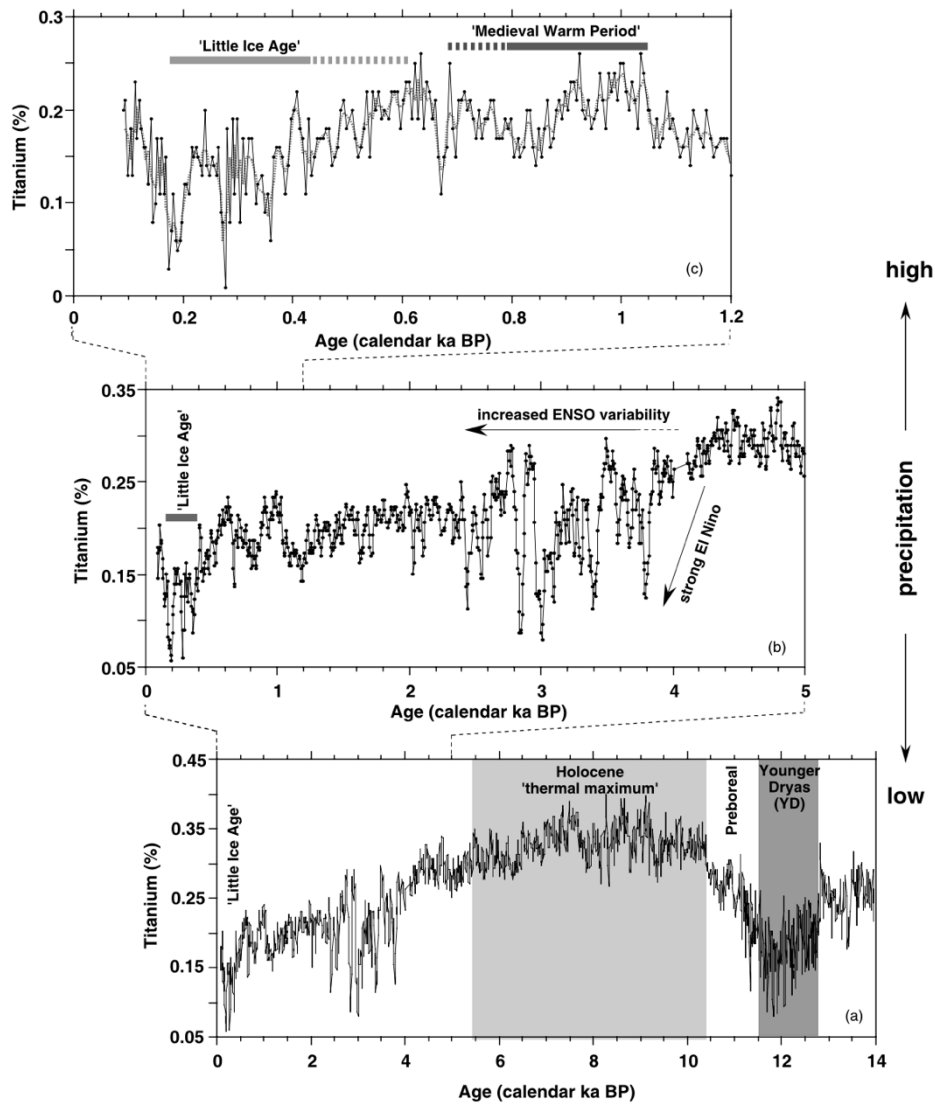
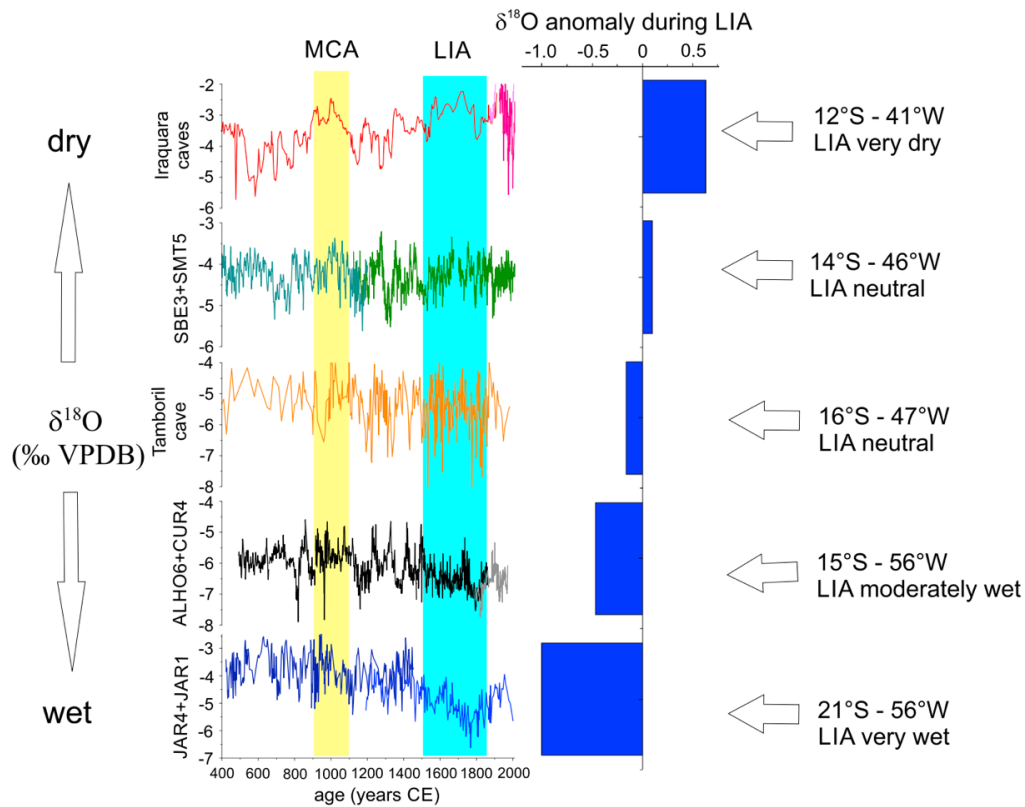
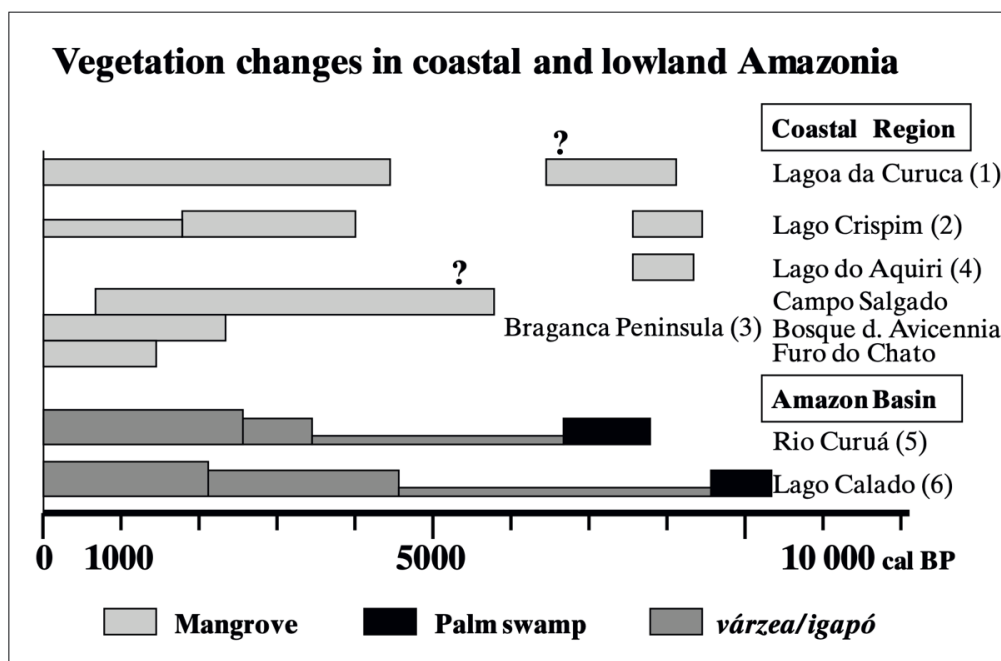


Fig. 5.7 Ti record from Cariaco Basin (Fig. 5.5 site 11; Haug et al., 2001).



**Fig. 5.8** Comparison of the LIA signal in  $\delta^{18}\text{O}$  records from the SACZ region (Fig. 5.5 sites 6–10; Novello et al., 2018)



**Fig.5.9** Vegetational changes in the coasts and lowlands in Amazonia related to sea-level changes in Holocene (Fig. sites 13–17; Behling, 2011).

## 5.2 Peat ecosystems in western Amazonia

### 5.2.1 Summary of the Madre de Dios studies

In the Madre de Dios region, we investigated a peat record called Los Amigos *Aguajal* (LAA) and an oxbow lake record called Los Amigos Lake (LAL) in a *Mauritia* palm swamp (Fig. 5.5, 5.10) by the multiproxy analysis including  $^{14}\text{C}$  radiocarbon dating, pollen, spores, macro-charcoal, Loss-On-Ignition (LOI), organic carbon (C) and X-ray fluorescence (XRF), exploring the development of the peat ecosystem in southwestern Amazonia and its potential influencing factors.

#### A. Study of the peat record (LAA)

The peat record shows vegetation and environmental changes in a local dense *Mauritia* palm swamp. Since ca.1380 cal yr BP, the sediments of the peat record started to accumulate. The lacustrine clay and the dominance of wind-pollinated Moraceae in the pollen record indicate the open-water environment at that time. Since ca.820 cal yr BP, peat with organic C started to form with accumulation rates of  $7.9 \text{ mm yr}^{-1}$  and  $444.5 \text{ g m}^{-2} \text{ yr}^{-1}$  respectively. Concurrently, a local Cyperaceae swamp formed under low-energy flooding events. Since ca.640 cal yr BP, flooding stopped and the local dense *Mauritia* swamp formed. Since ca.520 cal yr BP to the present, peat and organic C accumulation rates decreased but stayed at relatively high levels, which were  $6.2 \text{ mm yr}^{-1}$  and  $288.8 \text{ g m}^{-2} \text{ yr}^{-1}$ , respectively. Since ca.300 cal yr BP, the local dense *Mauritia* swamp became more open with an increase of dwarf *Hedyosmum*.

#### B. Study of the oxbow lake record (LAL)

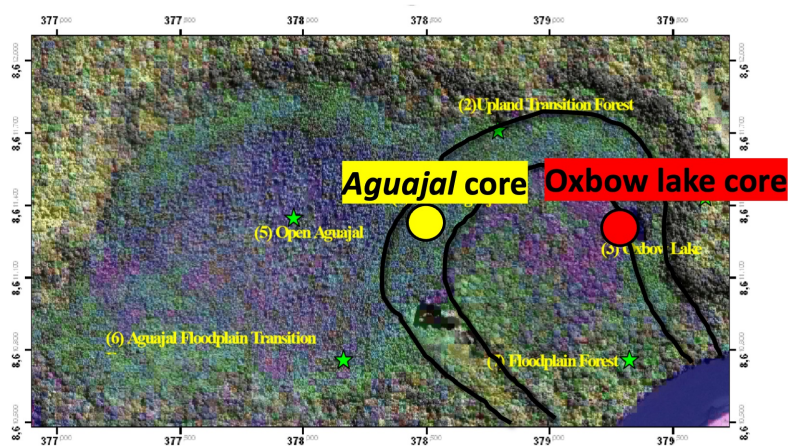
The oxbow lake record was investigated to further explore the vegetation and environmental changes on a more regional scale, which includes solving the questions left from the peat record. The questions are what the initial origin of the studied *Mauritia* palm swamp is, and why peat and organic C accumulation rates decreased since 520 cal yr BP which is out-of-step with the vegetation change.

The studied *Mauritia* palm swamp most likely developed from a cutting off from the Madre de Dios River since ca.1760 cal yr BP, changing from an active to a passive river system. This inference is first suggested by the nice half-circle of the area growing dense *Mauritia* where both records are from (Fig. 5.10), which looks like a cutting off. Then, this inference is evidenced by concurrent changes of different proxies since ca.1760 cal yr BP in the oxbow lake record. The changes include that sediment changed from clay to detritus mud, sediment accumulation rate increased from  $0.36 \text{ mm yr}^{-1}$  to  $1.09 \text{ mm yr}^{-1}$ , values of Loss-on-Ignition (LOI) increased to over 20% indicating the

onset of organic material (OM) accumulation, contents of Titanium (Ti), Silicon (Si) and Kalium (K) which are terrestrial elements decreased indicating less allochthonous detrital and/or clay input.

The decrease in peat and organic C accumulation rates since ca.520 cal yr BP is probably because of a less wet climate by lowering the water table. The less wet climate is suggested by the X-ray fluorescence (XRF) data of the oxbow lake record. As the studied oxbow lake has been a passive river system since ca.1760 cal yr BP, the decrease of Ti, Si, and K since ca.540 cal yr BP is probably caused by less flooding, rainfall, and seepages, which indicates a less wet climate. Concurrently, Calcium (Ca) started to follow changes in terrestrial elements, and ratios of Ca to Ti increased, which together indicate that more Ca (mainly as Calcium Carbonate (CaCO<sub>3</sub>)) was precipitated in the Madre de Dios region and transported by allochthonous inputs. More CaCO<sub>3</sub> precipitation is most likely caused by a less wet climate in the Madre de Dios region (Chapter 3; Haberzettl et al., 2005).

Shown by pollen and spore data of the oxbow lake record, vegetation dynamics on a more regional scale are similar to the local dense *Mauritia* palm swamp. Only the period of Cyperaceae swamp is not recorded. It indicates that Cyperaceae swamp is short or not so common in vegetation succession of *Mauritia* palm swamps in the Madre de Dios region.



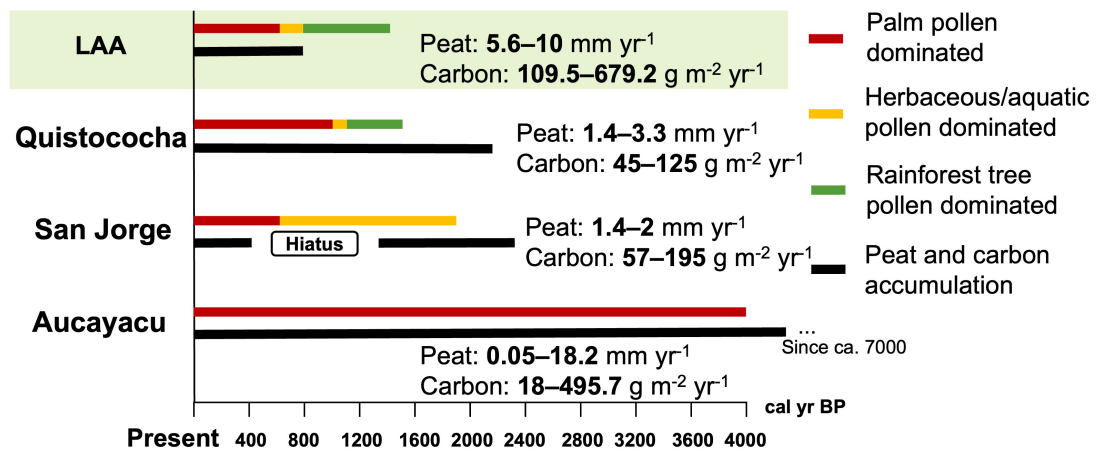
**Fig. 5.10** Both *Mauritia* palm swamp core (LAA, yellow circle) and oxbow lake core (LAL, red circle) are located in a nice half circle which grows dense *Mauritia*.

## 5.2.2 Comparison with other studies in western Amazonia

By comparing with other palaeoecological records of *Mauritia* palm swamps in the western Amazonia, we found that vegetation dynamics, and peat and organic C accumulation rates vary in different study sites (Fig. 5.5 sites 19–21, 5.11). It indicates that the development of peat ecosystems is influenced by local factors in western

Amazonia.

Under the condition of SASM intensification and/or ITCZ southward during LIA (section 5.1), although not as strong as areas in the altiplano, the natural climate of western Amazonia lowlands also should be wetter. It conflicts with the drier climate indicated by the Lake Limón record in northern Peruvian lowlands (Fig. 5.5 site 22, Parsons et al., 2018), and the less wet climate since ca. 540 cal yr BP in our oxbow lake record (the different interpretations of the record were discussed in Chapter 3). This conflict may indicate that the climate in western Amazonia lowlands was driven by non-natural climate factors, such as land surface modifications caused by human activities. Here, we provide a possible interpretation: increased regional human activities cut more rainforests, then less area of rainforests has weaker evapotranspiration which transferred less water vapor into the atmosphere causing less rainfall, concurrently less latent heat absorbed by rainforests causing warmer surface that facilitated a less wet climate. In the Madre de Dios, increased regional human activities since ca. 800 cal yr BP were recorded by Bush et al. (2007). Even if human activities did not directly influence our studied swamp (low macro-charcoal in our oxbow lake record), it also can influence the peat and organic C accumulation rates by affecting the regional climate.



**Fig. 5.11** Comparison of our *Mauritia* palm swamp (*aguajal*) record (LAL) with other *aguajales* in western Amazonia. San Jorge, Quistococha and Aucayacu are the sites of 19, 20, 21 in Fig. 5.5.

## 5.3 Peat ecosystems in eastern Amazonia

### 5.3.1 Summary of the Lagoa da Fazenda study

The Lagoa da Fazenda (LF) peat record (Fig. 5.5) is a representative palaeoecological archive of a net of former small river valleys in eastern Amazonia. LF recorded twice Atlantic sea level rise, since ca. 7000 cal yr BP and since ca. 4700 cal yr BP, respectively.

In local LF, peat and C accumulation (with rates of 0.6–0.67 mm yr<sup>-1</sup> and 25.6–46.7 g m<sup>-2</sup> yr<sup>-1</sup>) and the *Virola*-dominated inundated forest establishment was since 7000 cal yr BP. Peat and C accumulation fluctuated (with a smaller area of the inundated forest and more diverse pollen record) since 2600 cal yr BP, then decreased to a lower level (with Cyperaceae swamp formation and more frequent *Banara*) since 1800 cal yr BP, but started to increase (with Cyperaceae swamp, abundant *Cecropia*, and high macro-charcoal accumulation rate) since 260 cal yr BP to the present. It indicates that the local LF site has been influenced by flooding since ca. 2600 cal yr BP, and by strongly human activities since ca. 260 cal yr BP.

### 5.3.2 Comparison with other studies in eastern Amazonia

As the LF is the first palaeoecological study of a peat ecosystem in northeastern Amazonia, the best palaeoecological study for comparison is the closest lake-like Rio Curuá record (Fig. 5.5 site 16; Behling and Costa, 2000), which represents results on a more regional scale, is the fittest for palaeoecological comparison. Rio Curuá record from the same river net with the LF record (ca. 7 km between them), shows a change from an active to passive river system since ca. 8000 cal yr BP. It is consistent with the inference of the LF record that Atlantic sea level rise blocked the river since ca. 7000 cal yr BP causing the onset of peat and C accumulation. Rio Curuá record also shows a change from a Cyperaceae swamp to *Virola*-dominated inundated forests since ca. 5000 cal yr BP, which indicates a higher water level on a regional scale. This change may be caused by the LF-recorded Atlantic sea level rise since ca. 4700 cal yr BP. Since 2600 cal yr BP, the LF record has been influenced by river flooding. More frequent micro-charcoal in Rio Curuá record since ca. 2500 cal yr BP, indicates more human activities on a regional scale. This brings to mind that more frequent floodings were probably driven by more human activities causing soil water loss and erosion.

On the continental scale, SASM intensification and/or ITCZ southward migration, Atlantic sea level rise (consistent with our LF record), and more frequent El Niño events since ca. 5000 cal yr BP were broadly recorded in northern South America (section 5.1). For example, a wetter climate in northeastern Amazonia since ca. 5000 cal yr BP was recorded (Fig. 5.5 site 12, Hermanowski et al., 2015). These changes may be driven by the changes in the earth's orbit, which redistributed solar insolation on earth causing a cooler northern hemisphere and warmer southern hemisphere (as discussed in the last paragraph of section 5.1).



## 5.4 Summary of peat ecosystems in Amazonia and outlook

The onset of peat ecosystems in Amazonia is needed to provide a stable water-logged environment. It can be caused by Atlantic sea level rise in areas close to the sea, but often by river dynamics such as cutting off or river migration (e.g., increases the water table when rivers come closer) in more inland areas. Regional human activities may indirectly influence the development of peat ecosystems in both southwestern (by changing regional climate) and northeastern (by causing soil erosion) Amazonia, even when both study sites had no human influence locally. The above factors determine the diverse development processes of peat ecosystems in Amazonia. In the future, the peat ecosystems in central and eastern Amazonia need to be further explored. The peat ecosystems in Amazonia also need to be compared with other continents, which can help to understand how peat ecosystems will influence human life on a global scale.

### Reference

- Apaéstegui, J., Cruz, F.W., Sifeddine, A., Espinoza, J.C., Guyot, J.L., Khodri, M., Santini, W., 2014. Hydroclimate variability of the northwestern Amazon basin near the Andean foothills of Peru related to the South American Monsoon System during the last 1600 years. *Climate of the Past* 10, 1967-1981.
- Behling, H., 1996. First report on new evidence for the occurrence of *Podocarpus* and possible human presence at the mouth of the Amazon during the Late-glacial. *Vegetation History and Archaeobotany* 5, 241-246.
- Behling, H., 2001. Late Quaternary environmental changes in the Lagoa da Curuca region (eastern Amazonia) and evidence of *Podocarpus* in the Amazon lowland. *Vegetation History and Archaeobotany* 10, 175-183.
- Behling, H., 2011. Holocene environmental dynamics in coastal, eastern and central Amazonia and the role of the Atlantic sea-level change. *Geographica Helvetica* 66, 208-216.
- Behling, H., Costa, M.L., 1997. Studies on Holocene tropical vegetation, mangrove and coast environments in the state of Maranhão, NE Brazil. *Quaternary of South America and Antarctic Peninsula* 10, 93-118.
- Behling, H., Costa, M.L., 2000. Holocene environmental changes from the Rio Curuá record in the Caxiuanã region, eastern Amazon Basin. *Quaternary Research* 53, 369-377.
- Behling, H., Costa, M.L., 2001. Holocene vegetational and coastal environmental changes from the Lago Crispim record in northeastern Pará State, eastern Amazonia. *Review of Palaeobotany and Palynology* 114, 145-155.
- Behling, H., Keim, G., Irion, G., Junk, W., de Mello, J.N., 2001. Holocene environmental changes in the Central Amazon Basin inferred from Lago Calado (Brazil). *Palaeogeography, Palaeoclimatology, Palaeoecology* 173, 87-101.

- Bird, B.W., Abbott, M.B., Vuille, M., Rodbell, D.T., Stansell, N.D., Rosenmeier, M.F., 2011a. A 2,300-year-long annually resolved record of the South American summer monsoon from the Peruvian Andes. *Proceedings of the National Academy of Sciences* 108, 8583-8588.
- Bird, B.W., Abbott, M.B., Rodbell, D.T., Vuille, M., 2011b. Holocene tropical South American hydroclimate revealed from a decadal resolved lake sediment  $\delta^{18}O$  record. *Earth and Planetary Science Letters* 310, 192-202.
- Bookhagen, B., Strecker, M.R., 2010. Modern Andean rainfall variation during ENSO cycles and its impact on the Amazon drainage basin. *Amazonia, Landscape and Species evolution: A look into the past*, 223-243.
- Bush, M.B., Silman, M.R., Listopad, C.M.C.S., 2007. A regional study of Holocene climate change and human occupation in Peruvian Amazonia. *Journal of Biogeography* 34, 1342-1356.
- Costa, M.L., Moraes, E.L., Behling, H., Melo, J.C.V., Siqueria, N.V.M., Kern, D.C., 1997. Os sedimentos de fundo da Baía de Caxiuanã. Lisboa, P.L.B. Caxiuanã. Belém: Museu Paraense Emílio Goeldi, 121-137.
- Fedorov, A.V., Philander, S.G., 2000. Is El Niño Changing? *Science* 288,1997-2002.
- Haberzettl, T., Fey, M., Lücke, A., Maidana, N., Mayr, C., Ohlendorf, C., Schäbitz, F., Schleser, G.H., Wille, M., Zolitschka, B., 2005. Climatically induced lake level changes during the last two millennia as reflected in sediments of Laguna Potrok Aike, southern Patagonia (Santa Cruz, Argentina). *Journal of Paleolimnology* 33, 283–302.
- Haug, G.H., Hughen, K.A., Sigman, D.M., Peterson, L.C., Rohl, U., 2001. Southward migration of the intertropical convergence zone through the Holocene. *Science* 293, 1304-1308.
- Hermanowski, B., Da Costa, M.L., Behling, H., 2015. Possible linkages of palaeofires in southeast Amazonia to a changing climate since the Last Glacial Maximum. *Vegetation History and Archaeobotany* 24, 279-292.
- Kelly, T.J., Lawson, I.T., Roucoux, K.H., Baker, T.R., Jones, T.D., Sanderson, N.K., 2017. The vegetation history of an Amazonian domed peatland. *Palaeogeography, Palaeoclimatology, Palaeoecology* 468, 129–141.
- Lähteenoja, O., Ruokolainen, K., Schulman, L., Oinonen, M., 2009. Amazonian peatlands: an ignored C sink and potential source. *Global Change Biology* 15, 2311–2320.
- Novello, V.F., Cruz, F.W., Karmann, I., Burns, S.J., Stríkis, N.M., Vuille, M., Cheng, H., Edwards, R.L., Santos, R.V., Frigo, E., Barreto, E.A.S., 2012. Multidecadal climate variability in Brazil's Nordeste during the last 3000 years based on speleothem isotope records. *Geophysical Research Letters* 39, L23706.
- Novello, V. F., Vuille, M., Cruz, F. W., Stríkis, N. M., Saito de Paula, M., Edwards, R. L., et al., 2016. Centennial-scale solar forcing of the South American Monsoon System recorded in stalagmites. *Scientific Reports* 6, 24762.
- Novello, V. F., Cruz, F. W., Moquet, J. S., Vuille, M., De Paula, M. S., Nunes, D., Edwards, R. L., Cheng, H., Karmann, I., Utida, G., Stríkis, N. M., Campos, J. L. P. S., 2018. Two millennia of South Atlantic Convergence Zone variability

- reconstructed from isotopic proxies. *Geophysical Research Letters*, 45, 5045-5051.
- Parsons, L.A., LeRoy, S., Overpeck, J.T., Bush, M., Cárdenes-Sandí, G.M., Saleska, S., 2018. The threat of multi-year drought in western Amazonia. *Water Resources Research* 54, 5890–5904.
- Rodbell, D.T., Seltzer, G.O., Anderson, D.M., Abbott, M.B., Enfield, D.B., Newman, J. H., 1999. An~ 15,000-year record of El Niño-driven alluviation in southwestern Ecuador. *Science* 283, 516-520.
- Reuter, J., Stott, L., Khider, D., Sinha, A., Cheng, H., Edwards, R.L., 2009. A new perspective on the hydroclimate variability in northern South America during the Little Ice Age. *Geophysical Research Letters* 36, L21706.
- Roucoux, K.H., Lawson, I.T., Jones, T.D., Baker, T.R., Honorio Coronado, E.N., Gosling, W.D., L'ähteenoja, O., 2013. Vegetation development in an Amazonian peatland. *Palaeogeography, Palaeoclimatology, Palaeoecology* 374, 242–255.
- Swindles, G.T., Morris, P.J., Whitney, B., Galloway, J.M., Gałka, M., Gallego-Sala, A., Macumber, A.L., Mullan, D., Smith, M.W., Amesbury, M.J., Roland, T.P., Sanei, H., Patterson, R.T., Sanderson, N., Parry, L., Charman, D.J., Lopez, O., Valderamma, E., Watson, E.J., Ivanovic, R.F., Valdes, P.J., Turner, T.E., L'ähteenoja, O., 2017. Ecosystem state shifts during long-term development of an Amazonian peatland. *Global Change Biology* 24, 738–757.
- Taylor, B.L., 2010. A speleothems-based high resolution reconstruction of climate in southeastern Brazil over the past 4,100 years, M.S. thesis, University of Massachusetts.
- Thompson, L.G., Mosley-Thompson, E., Davis, M.E., Zagorodnov, V.S., Howat, I.M., Mikhalenko, V.N., Lin, P.N., 2013. Annually resolved ice core records of tropical climate variability over the past~1800 years. *Science* 340, 945–950.
- Vonhof, H. B., Kaandorp, R. J., 2009. Climate variation in Amazonia during the Neogene and the Quaternary. *Amazonia: landscape and species evolution: a look into the past*, 199-210.
- Vera, C., Higgins, W., Amador, J., Ambrizzi, T., Garreaud, R., Gochis, D., Gutzler, D., Lettenmaier, D., Marengo, J., Mechoso, C.R., Nogues-Paegle, J., Silva Dias, P.L., Zhang, C., 2006. Toward a unified view of the American monsoon systems. *Journal of Climate* 19, 4977-5000.
- Vuille, M., Burns, S.J., Taylor, B.L., Cruz, F.W., Bird, B.W., Abbott, M.B., Kanner, L. C., Cheng, H., Novello, V. F., 2012. A review of the South American monsoon history as recorded in stable isotopic proxies over the past two millennia. *Climate of the Past*, 8, 1309-1321.
- Wortham, B.E., Wong, C.I., Silva, L.C.R., McGee, D., Montañez, I.P., Rasbury, E.T., Cooper, K.M., Sharpf, W.D., Glessner, J.J.G., Santos, R.V., 2017. Assessing response of local moisture conditions in central Brazil to variability in regional monsoon intensity using speleothem <sup>87</sup>Sr/<sup>86</sup>Sr values. *Earth and Planetary Science Letters* 463, 310–322.
- Zhou, J., Lau, K. M., 1998. Does a monsoon climate exist over South America? *Journal of Climate* 11, 1020-1040.

# Acknowledgements

I would like to send my most sincere thanks to my main supervisor Prof. Dr. Hermann Behling. Thanks for all his guidance, teaching and help step by step during my PhD study. It is with his help that I can make such progress in learning scientific methods and thoughts and being a real scientist in paleoecology. He helped me to make such a solid foundation for my future science life.

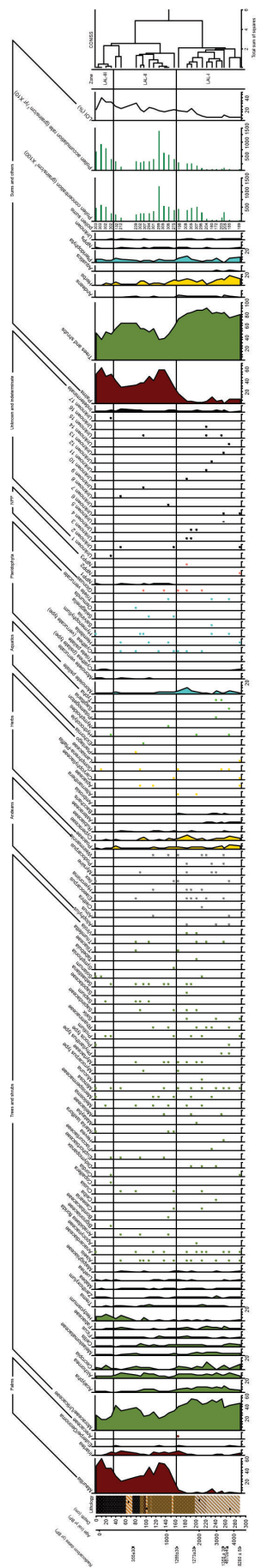
I would like to gratefully thank the China Scholarship Council (CSC No. 201906190215) for supporting my PhD study.

I would like to thank a lot Prof. Dr. Holger Kreft and Dr. Kartika Anggi Hapsari for their always strong support in my PhD study. I also thank our important cooperators Prof. Dr. Marcondes Lima da Costa, Dr. Viviana Horna and Dr. Zimmermann Reiner, and all my colleagues in our department. I learned a lot from all.

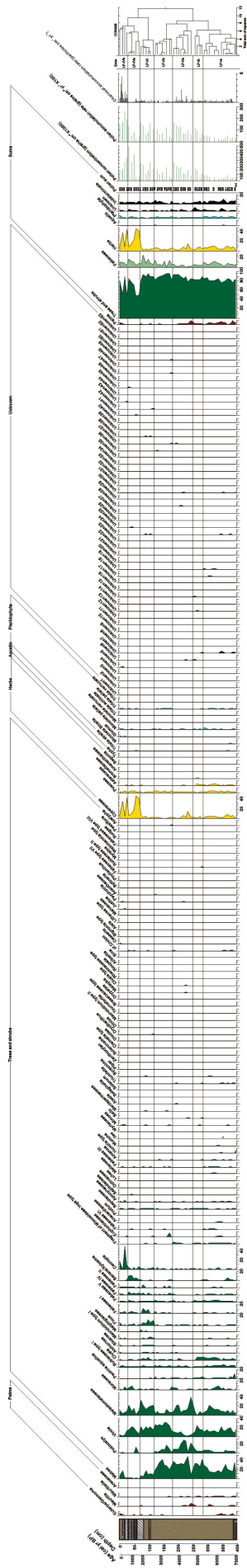
I would like to give all my love and thanks to my dear parents Jincun Wang and Liping Zhu. They always encouraged me to try new things and always be curious about natural phenomenon and regulations. It is their love and strong support that made me to be the person today.

Finally, I would like to thank myself for my persistence and bravery!





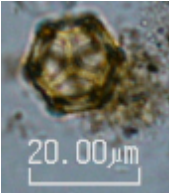
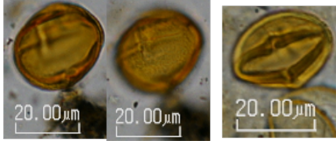
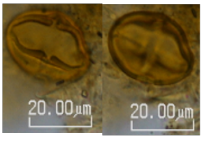
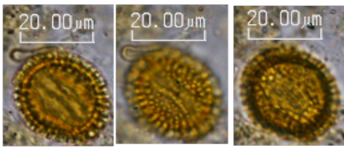
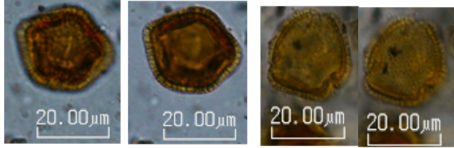
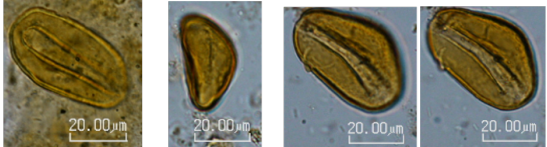
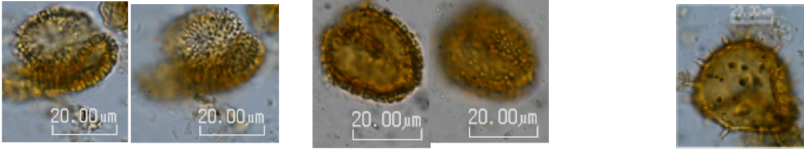
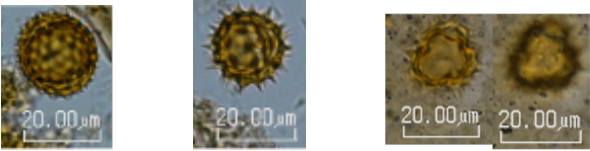

Madre de Dios: Oxbow lake record (LAL)



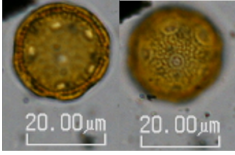
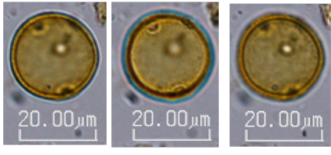
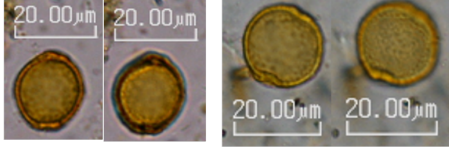
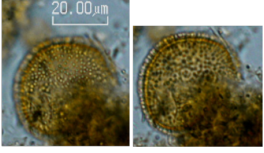
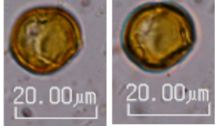

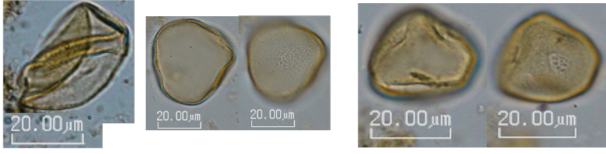


## Lagoa da Fazenda peat (LF) record

# Appendix II

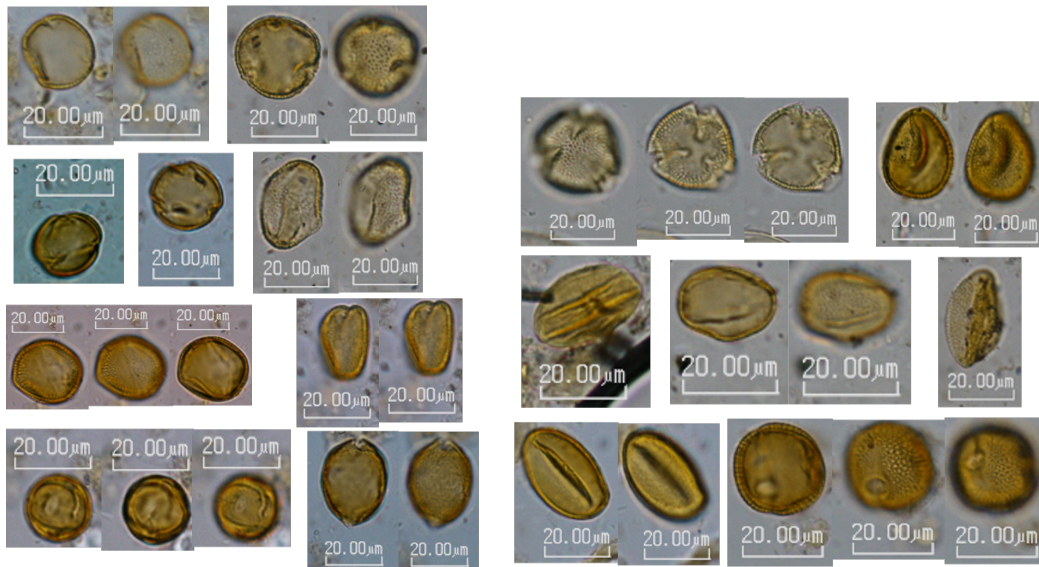
## Photos of important taxa (identified)

<p><b>Amaranthaceae</b></p>  <p><i>Alternanthera</i></p>	<p><b>Anacardiaceae</b></p> 	<p><b>Apiaceae</b></p> 
<p><b>Aquifoliaceae</b></p>  <p><i>Ilex</i></p>	<p><b>Araliaceae</b></p>  <p><i>Didymopanax</i></p>	
<p><b>Areaceae</b></p>  <p><i>Euterpe</i></p>  <p><i>Iriartea</i> <span style="margin-left: 200px;"><i>Mauritia</i></span></p>		
<p><b>Asteraceae</b></p>  <p><i>Ambrosia</i>   <i>Baccharis</i>   Not identified genus</p>		<p><b>Burseraceae</b></p>  <p><i>Protium</i></p>



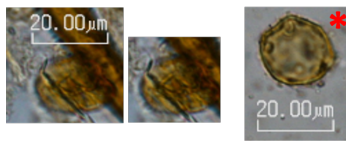
<p><b>Caryophyllaceae</b></p> 	<p><b>Cannabaceae</b></p>  <p><i>Celtis</i></p>  <p><i>Trema</i></p>	
<p><b>Chloranthaceae</b></p>  <p><i>Hedyosmum</i></p>	<p><b>Clethraceae</b></p>  <p><i>Clethra</i></p>	<p><b>Cunoniaceae</b></p>  <p><i>Weinmannia</i></p>
<p><b>Cyperaceae</b></p> 		<p><b>Elaeocarpaceae</b></p>  <p><i>Elaeocarpus</i></p>
<p><b>Euphorbiaceae</b></p>  <p><i>Acalypha</i>      <i>Alchornea</i>      not identified genus      <i>Phyllanthus</i></p> <p><i>Mabea</i>      <i>Sebastiana</i></p>		

**Fabaceae**



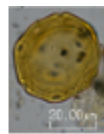
Not identified genus

**Fabaceae**



*Mimosa*

**Juglandaceae**

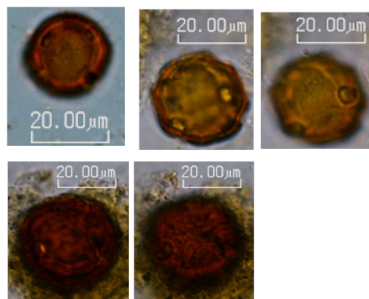


*Juglans*

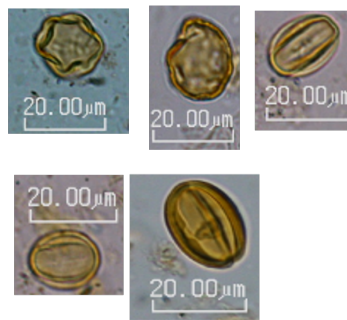
**Loranthaceae**



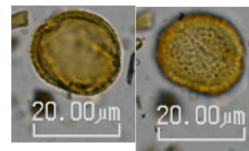
**Malphiaceae**



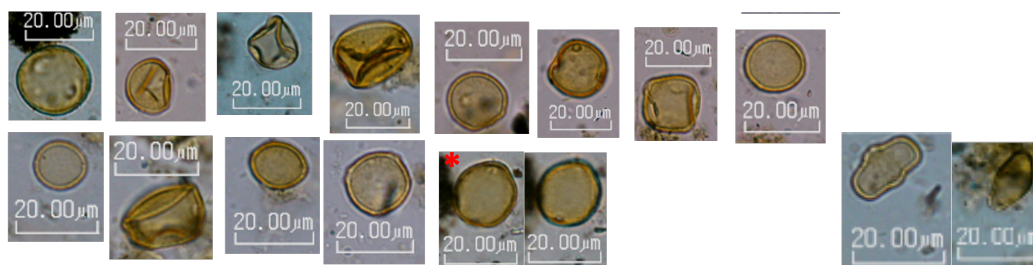
**Melastomataceae**



**Menispermaceae**



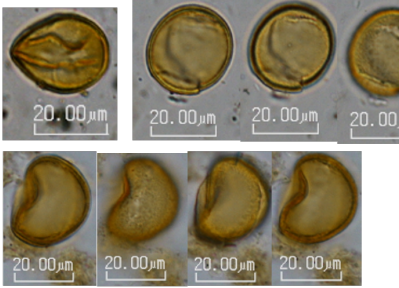
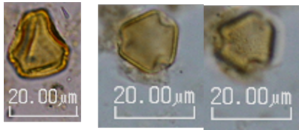
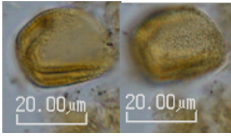
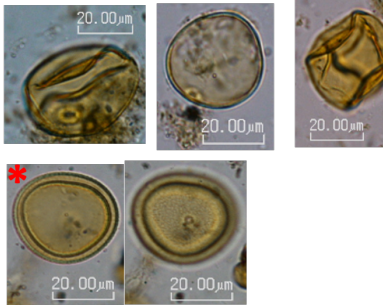
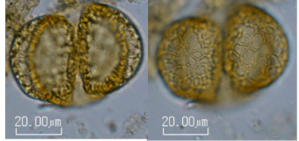
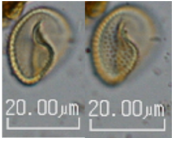

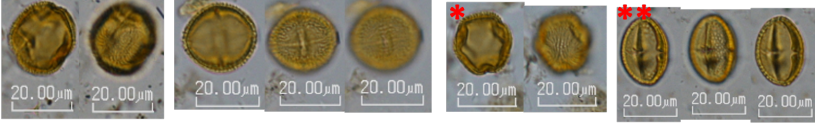
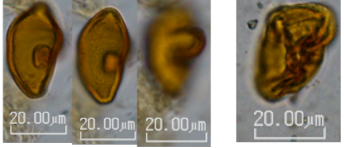

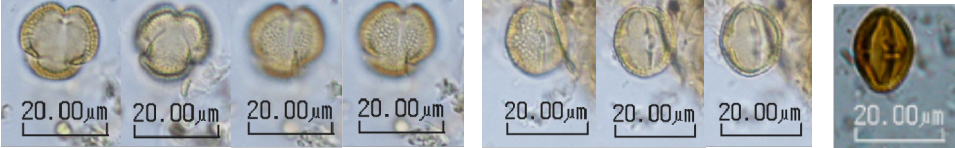
**Moraceae**

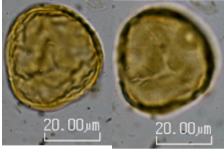
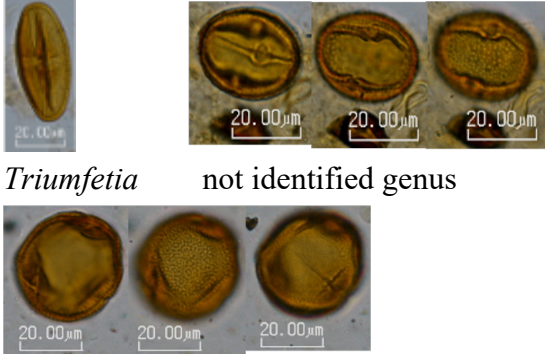
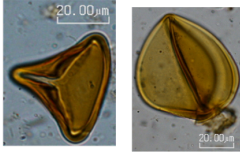
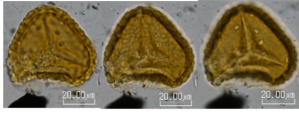
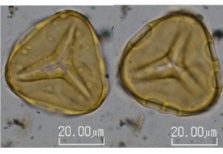

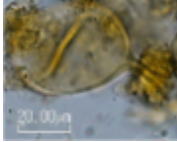

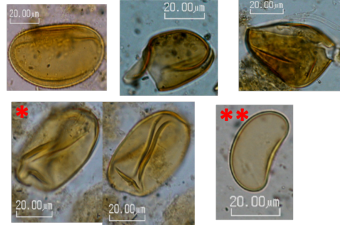
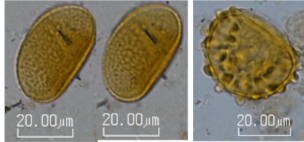
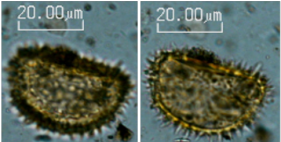
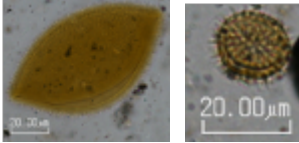
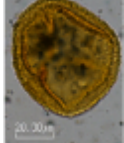
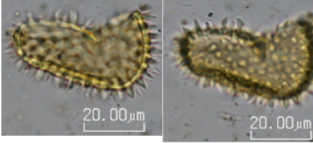


Not identified genus

*Cecropia*

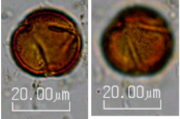
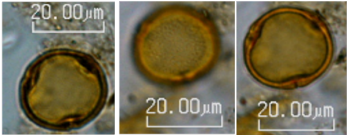
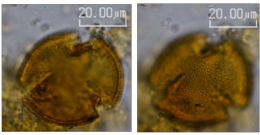
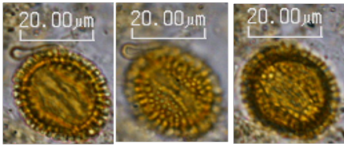
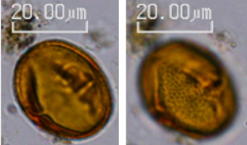
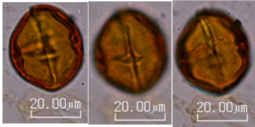
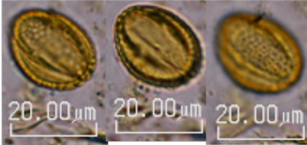
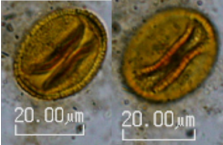
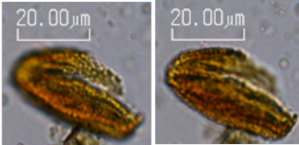


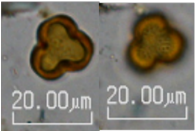
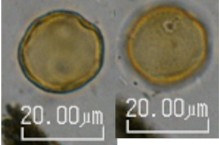




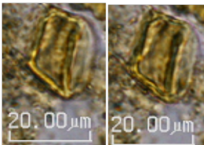
*Ficus*

<p><b>Myrsinaceae</b></p>  <p><i>Myrsine</i></p>	<p><b>Myrtaceae</b></p> 	<p><b>Myristicaceae</b></p>  <p><i>Virola</i></p>
<p><b>Poaceae</b></p> 	<p><b>Podocarpaceae</b></p>  <p><i>Podocarpus</i></p>	<p><b>Potamogetonaceae</b></p>  <p><i>Potamogeton</i></p>
<p><b>Rubiaceae</b></p>  <p><i>Alseis</i></p>	<p><b>Rutaceae</b></p>  <p><i>Zanthoxylan</i></p>	
<p><b>Sapindaceae</b></p>  <p><i>Allophylus</i></p>	<p><b>Sabiaceae</b></p>  <p><i>Meliosma</i></p>	
<p><b>Salicaceae</b></p>  <p><i>Banara</i> <span style="float: right;"><i>Casearia</i></span></p>		
<p><b>Selaginellaceae</b></p>	<p><b>Tiliaceae</b></p>	

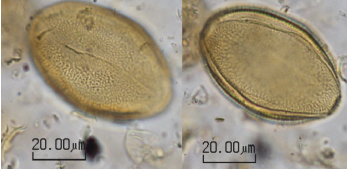
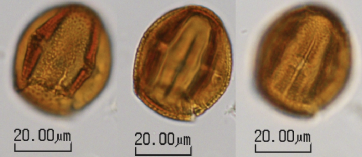
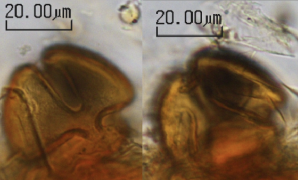
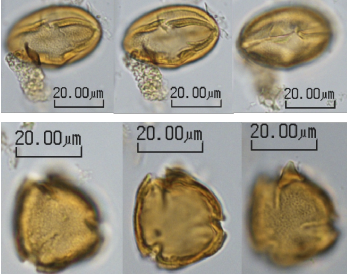

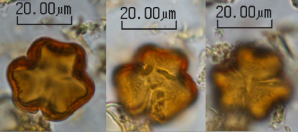
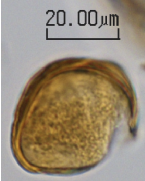
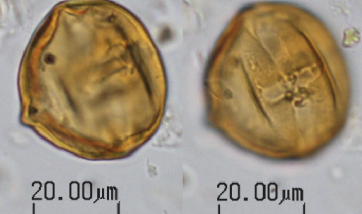
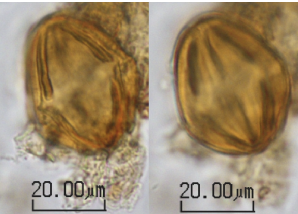

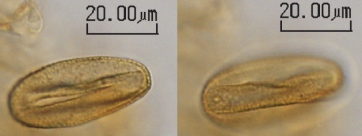
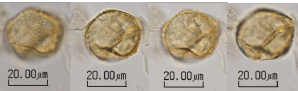
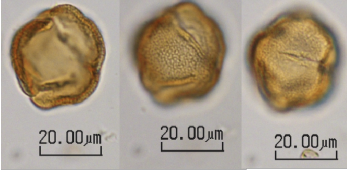
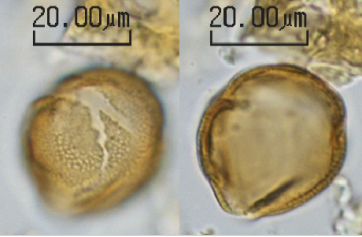
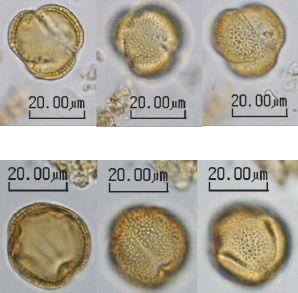
 <p><i>Selaginella</i></p>	 <p><i>Triumphetia</i> not identified genus</p> <p><i>Luhea</i></p>	
<p><b>Cyathea psilate</b></p> 	<p><b>Caythea verrucate</b></p> 	<p><b>Hemitelia</b></p> 
<p><b>Gomphrena-Pfaffia</b></p> 	<p><b>Globus</b></p> 	<p><b>Hyeronima</b></p> 
<p><b>Monolete psilate</b></p> 	<p><b>Monolete verrucate</b></p> 	<p><b>Monolete echinate</b></p> 
<p><b>NPP</b></p>  <p>Type 1      Type 2</p>	<p><b>Trilete verrucate</b></p> 	<p><b>Trilete echinate</b></p> 

## Photos of Unknown types (Madre de Dios)

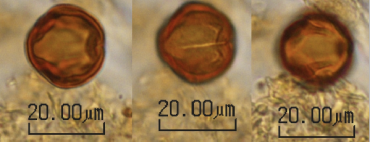
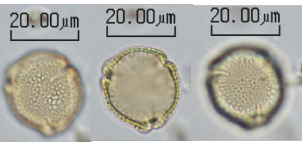
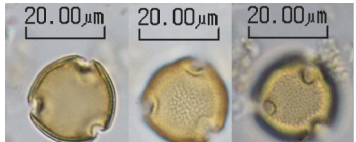
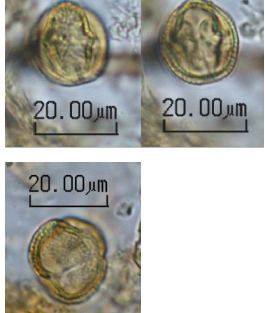

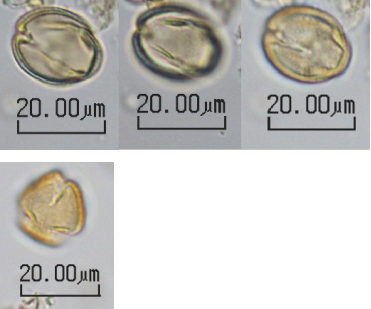
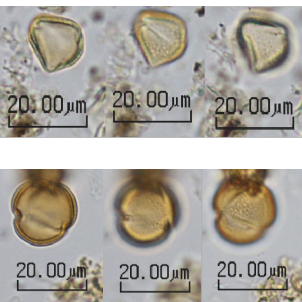
(numbers of unknown types are same in Mauritia palm swam record and oxbow lake record)

<p><b>Unknown 1</b></p> 	<p><b>Unknown 2</b></p> 	<p><b>Unknown 3</b></p> 
<p><b>Unknown 4</b></p>  <p>(Later identified as <i>Ilex</i>)</p>	<p><b>Unknown 5</b></p> 	<p><b>Unknown 6</b></p> 
<p><b>Unknown 7</b></p> 	<p><b>Unknown 8</b></p> 	<p><b>Unknown 9</b></p> 
<p><b>Unknown 10</b></p> 	<p><b>Unknown 11</b></p> 	<p><b>Unknown 12</b></p> 
<p><b>Unknown 13</b></p> 	<p><b>Unknown 14</b></p> 	<p><b>Unknown 15</b></p> 
<p><b>Unknown 16</b></p> 	<p><b>Unknown 17</b></p> 	<p><b>Unknown 18</b></p> 

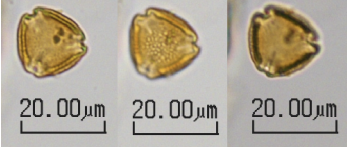

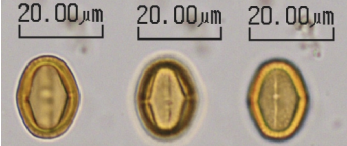
## Photos of Unknown types (Lagoa da Fazenda)

<p><b>Unknown 1</b></p> 	<p><b>Unknown 2</b></p> 	<p><b>Unknown 3</b></p> 
<p><b>Unknown 4</b></p> 	<p><b>Unknown 5</b></p> 	<p><b>Unknown 6</b></p> 
<p><b>Unknown 7</b></p> 	<p><b>Unknown 8</b></p> 	<p><b>Unknown 9</b></p> 
<p><b>Unknown 10</b></p> 	<p><b>Unknown 11</b></p> 	<p><b>Unknown 12</b></p> 
<p><b>Unknown 13</b></p> 	<p><b>Unknown 14</b></p> 	<p><b>Unknown 15</b></p> 

<p><b>Unknown 16</b></p> 	<p><b>Unknown 17</b></p> 	<p><b>Unknown 18</b></p> 
<p><b>Unknown 19</b></p> 	<p><b>Unknown 20</b></p> 	<p><b>Unknown 21</b></p> 
<p><b>Unknown 22</b></p> 	<p><b>Unknown 23</b></p> 	<p><b>Unknown 24</b></p> <p>No photo</p>
<p><b>Unknown 25</b></p> 	<p><b>Unknown 26</b></p> 	<p><b>Unknown 27</b></p> 
<p><b>Unknown 28</b></p> 	<p><b>Unknown 29</b></p> 	<p><b>Unknown 30</b></p> 
<p><b>Unknown 31</b></p>	<p><b>Unknown 32</b></p>	<p><b>Unknown 33</b></p>

		
<p><b>Unknown 34</b></p> 	<p><b>Unknown 35</b></p> 	<p><b>Unknown 36</b></p> 
<p><b>Unknown 37</b></p> 	<p><b>Unknown 38</b></p> 	<p><b>Unknown 39</b></p> 
<p><b>Unknown 40</b></p> 	<p><b>Unknown 41</b></p> 	<p><b>Unknown 42</b></p> 
<p><b>Unknown 43</b></p> 	<p><b>Unknown 44</b></p> 	<p><b>Unknown 45</b></p> 
<p><b>Unknown 46</b></p>	<p><b>Unknown 47</b></p>	<p><b>Unknown 48</b></p>



	
<p><b>Unknown 49</b></p> 	<p><b>Unknown 50–53</b></p> <p>No photos</p>